LANDUSE / LANDCOVER AND CHANGE DETECTION FOR THE IRAQI
PROVINCE OF SULAIMANIAH USING REMOTE SENSING

By

Ardalan A. Faraj
A Thesis
Submitted to the
Graduate Faculty
of
George Mason University
in Partial Fulfillment of
The Requirements for the Degree
of
Master of Science
Geoinformatics and Geospatial Intelligence
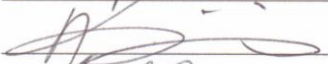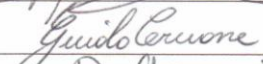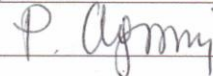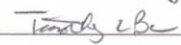
Committee:

_____   Dr.Arie Croitoru, Thesis Director

_____   Dr.Anthony Stefanidis, Committee Member

_____   Dr. Guido Cervone, Committee Member

_____   Dr. Peggy Agouris, Department Chairperson

_____   Dr. Timothy L. Born, Associate Dean for
                                                       Student and Academic Affairs, College of
                                                       Science

_____   Dr. Vikas Chandhoke, Dean, College of
                                                       Science

Date: _____   Spring Semester 2013
                                                       George Mason University
                                                       Fairfax, VA

LAND USE / LANDCOVER AND CHANGE DETECTION FOR THE IRAQI
PROVINCE OF SULAIMANIAH USING REMOTE SENSING

By

Ardalan A. Faraj
A Thesis
Submitted to the
Graduate Faculty
of
George Mason University
in Partial Fulfillment of
The Requirements for the Degree
of
Master of Science
Geoinformatics and Geospatial Intelligence

Committee:

_____   Dr.Arie Croitoru, Thesis Director

_____   Dr.Anthony Stefanidis, Committee Member

_____   Dr. Guido Cervone, Committee Member

_____   Dr. Peggy Agouris, Department Chairperson

_____   Dr. Timothy L. Born, Associate Dean for
                                    Student and Academic Affairs, College of
                                    Science

_____   Dr. Vikas Chandhoke, Dean, College of
                                    Science

Date: 4/30/2013   Spring Semester 2013
                                    George Mason University
                                    Fairfax, VA

Land Use / Land Cover and Change Detection for the Iraqi   Province of Sulaimaniyah in
Using Remote Sensing

A thesis submitted in partial fulfillment of the requirements for the degree of Master of
Science at George Mason University

by

Ardalan Faraj
Master of Science
George Mason University, 2013

Director: Arie Croitoru, Professor
Department of Geography and Geoinformation Science

Spring Semester 2013
George Mason University
Fairfax, VA

DEDICATION

I would like to dedicate this work to my wife, Nazaneen, and my children, Baban and Sasan for enduring the long process that has resulted in this work. Working on a Master's Thesis while working a full time job and trying to spend enough time with your family is a difficult task. I would just like to say thank you all for your patience. Also, I would dedicate this work to my parents, brothers and sisters, as well as to Dr. Jamal Fuad and his wife Kathleen Margaret Fuad.

ACKNOWLEDGEMENTS

TABLE OF CONTENTS

LIST OF TABLES

LIST OF FIGURES

LIST OF EQUATIONS

LIST OF ABBREVIATIONS

Land Use and land Cover..LULC

Land Use and land Cover Change ....LULCC

United State Geological Survey ....USGS

Thematic Map...TM

Enhanced Thematic Mapper Plus ....ETM+

Multispectral Scanner ....MSS

Advanced Very High Resolution Radiometer ....AVHRR

Area of Interest ....AOI

Area of Study ....AOS

Province of Sulaimania ....POS

Normalized Difference Vegetation Index ....NDVI

Normalized Difference Soil Index..NDSI

Normalized Difference Moister Index..NDMI

Tasseled Cap Transformation index ....TCT

Classification and Regression Trees..CART

Cross-Correlation Analysis...CCA

Near Infrared ....NIR

Far Infrared ....FIR

ABSTRACT

LAND USE / LAND COVER AND CHANGE DETECTION FOR THE IRAQI
PROVINCE OF SULAIMANIYAH IN USING REMOTE SENSING

Ardalan Faraj, M.S.

George Mason University, 2013

Thesis Director: Dr. Arie Croitoru

Over the last several years the Iraqi Province of Sulaimania has gone through

significant changes. The purpose of this study is to highlight and understand major

changes in land-use and land-cover change (LULCC) relates to the growing population

and increased economic activity in the Province of Sulaimania, in northern Iraq between

1998 and 2010. Land use and land cover change (LULCC) can be driven by both natural

and anthropogenic drivers, and these LULCC changes can impact the availability of

products and services for the human population in the area, and can have deleterious

effect on the region's fauna and flora, as well as the environmental and ecological

systems. Despite its rapid growth and increasing importance, LULCC studies in this tend

to be limited and outdated. To address this issue, this work utilized a time-series

of Landsat 5 Thematic Mapper (TM) and Landsat7 Enhanced Thematic Mapper Plus

(ETM+) satellite imagery data, covering the time frame between 1998, and 2010. Change

detection in land-use/land-cover was carried out using a workflow consisting of establishing the LULC classification scheme, image data acquisition, scene processing, data analysis, post-processing, and validation. In particular, classification and Regression Tree (CART) have been utilized to perform image classification based on the 1998 image, and Cross-Correlation Analysis (CCA) was used to identify changes between image pairs. Validation was carried out using a random stratified process by classes, and by comparing the results against Rapid Eye image date from 2011.

Introduction

1.1 Chapter overview

This chapter covers a brief introduction of   Landuse-Landcover and Landuse-Landcover Change (LULC\ LULCC), location and background of the area of study (AOS), political stability and population record of the AOS, rainfall history of the AOS, geology of the area of study (AOS), research questions and objective, and thesis organization.

1.2 Introduction of Landuse – Landcover and Landuse-Landcover Change:

Issues of land use and land cover have become increasingly important as problems of uncontrolled development, deteriorating environmental quality, loss of prime agricultural lands, destruction of important wetlands, and loss of fish and wildlife habitat continue to worsen (http://www.ncrs.fs.fed.us/). To better understand the impact of land use change on global ecosystems, the factors affecting land use must be further examined. Growing human population exert increasing pressure on the landscape as demands multiply for resources such as food, water, shelter, and fuel. These social and

economic factors often dictate how land is used regionally. Land use practices generally develop over a long period under different environmental, political, demographic, and social conditions. These conditions often vary yet have a direct impact on land use and land cover (Ojima, et. al., 1994).

Land use and land cover dynamics are widespread, accelerating, and are significant processes driven by human actions but also producing changes that impact humans (Campbell, 2007). Land use data are crucial to analyzing environmental processes and problems and to maintaining or improving living conditions and standards (http://www.ncrs.fs.fed.us/).

Modern society depends upon accurate land- use data for both scientific and administrative purposes; it is forms an essential component of local and regional economic planning, to assure that various activities are positioned on the landscape in a rational manner (Campbell, 2007). For example, accurate knowledge of land-use patterns permits planning to avoid placing residential housing adjacent to heavy industry, or floodplains. In another context, land-use is an important component of climatic and hydrologic modeling, to estimates the runoff of rainfall from varied surfaces into stream systems.

It is important to recognize a difference between land use and land cover; land use refers to how and for what purposes the human use the lands in another words land use

can be defined as how land is utilized. Examples of land use include creating parks, golf courses, urban areas, and athletic fields. Land cover refers to natural features of the surface of earth, such as vegetation cover, which may or may not been modified by humans (Richardson and Al-Tahir, 2009). A change in land use and land cover (LULC) may limit the availability of products and services for human populations and can have a profound impact on a region's fauna and flora, as well as on environmental and ecological health.

The vast majority of land use and land cover data are acquired through interpretation of aerial photography and other similar imagery. Remotely sensed data provide the comprehensive detail needed to effectively study land use patterns. In this study remotely sensed data were used because they lend themselves to accurate land cover and land use analysis. Land cover information can be visually interpreted using evidence from aerial images, and specific objects can be seen in the context of their neighboring features (Campbell, 2007).

In addition, according to Wilkie and Finn (1996), by utilizing geospatial technologies and techniques, researchers can monitor changes in land use and land cover and map areas for specific research and analysis. To study the dynamics of land use and land cover change (LULCC), researchers can use spatial distribution and patterns of LULCC classes to test remotely sensed data, which is the primary focus of this research.

The area of study (AOS) selected for this research is in part, due to the anthropogenic modifications and conversions have occurred to the landscape as a result of economic and population growth and development that have affected land use and land cover in the rural areas, small cities, and in particular the city of Sulaimaniaya, especially after 2003. Understanding Land Use/Land Cover changes that have occurred in recent years in the Province of Sulaimaniyah is of interest since this province has enjoyed a political stability that is unique to the region, therefore allowing insight into the impact of such political conditions on Land Use/Land Cover changes.

1.3 Location and background of Area of Study

The Province of Sulaimaniyah (AOS) shares an internal border with Erbil Province on the north; Kirkuk Province on the west; Salah al-Din Province on the southwest; and Dylah Province on the south (Figure 1), (IAU, 2011). It is located in the northeast of Iraq on the border with Iran; its topography becomes increasingly mountainous towards the eastern border (Figure 2). The weather in the summer is rather warm, with temperatures ranging from 15 C (60 F) to 35 C (95 F) and sometimes reaching 40 C (104 F). In the winter, there is a significant amount of snow; temperatures are dense and dry in the summer and windy in the winter. Its area is 17,023 square kilometers. Since 1991, the Province of Sulaimaniya has been part of the Kurdistan Regional Government (KRG) under the rule of the Kurds. The border between the POS and Iran is monitored by Iraqi Kurdish authorities and the Iranian government. There are two international gateways (ports of entry) between Sulaimaniya province and Iran. The

first one is called Parwizkhan which is located in the eastern side of the city of Kalar, and the second one is Bashmakh which is located in the northern side of the City of Penjwen. In addition, there are several secondary border crossing points between the two sides. Namely, they are: 1- Pishta in Garmyan area, 2- Shapal, Syranband, Gokhlan, and Hoshayry in the northeast side of the city of Pengwen, 3- Choman, Mashan, Marwe, and Awakurte in Sharbazher area, 4- Kele and Qindol in Qaladze area. Besides these entire official border crossing points, there are many illegal pathways and passageways between the two sides which are used by smugglers from both nations for all kinds of trades, especially, in the rigid mountainous areas. Before 2003, the high mountainous areas near the cities of Tawela and Byara had been used by the terrorist group of Ansar al Sunna. But in 2003, Kurds, with the support of the US army, controlled these two areas completely.

1.4 Political Stability and Population Record

The province had been affected by different wars in the past namely, long-term central government war against Kurds from early 60s until 1990, Iraq –Iran war from 1980 to 1988, and both first and second Gulf War in 1991 and 2003. Political consistency in Kurdistan regional Government (KRG) area began in 1991 and stabilized after 2003, when the regime of Saddam Hussein fell after Operation Iraqi Freedom. The region became an area of interest for the nations in the area as well as some other nations around the world. The economy grew, and the population rose after 1991. The population of the province in 1997 (Table 1) was 1,362,739 and 1,878,764 9 (Table 2) in 2011

5

(COSIT 1997, 2011). In conjunction with economic growth and population increase,

anthropogenic factors may have had a role in land change in that area.

1.5 Rainfall History of the AOS

The area of study is affected by dry seasons (drought).The highest records of

rain fall from 1980 to 2010 were found in 1991 which was 1547.2 mm, and 1992 which

1007.5 mm (Figure 3, and Appendix 2/ Table 14) . After this period the rain fall declined

frequently until the year of 2002 which reached only 929.5 mm; however this record is

still lower from the record of the year 1992 (Diary Ali, 2008). According to Salahlding,

(2007) the mean annual rainfall in Sharazoor-Piramagroon basin, one of the most

important hydrogeologically basins of the Iraqi Kurdistan Region, was 741mm during the

period of 1980/1981-2005/2006.

1.6 Geology of AOS:

Iraq can be considered as a large anticline (or anticlinorium) which has NW-SE

trend and contains many small folds (syncline and anticlines). The northeastern limb of

this anticline has suffered from recumbence and then thrusting over the southwestern

limb. Because of colliding of Arabian and Iranian plates Iraq is divided tectonically to

the Western desert, Mesopotamian (Unfolded Zone), Low, High, Imbricated and Thrust

Zones from southwest toward northwest (Figure 4, Figure 5). The tectonics of AOS is

divided to four zones: first one is a Thrust Zone on the north east border along with the

Iranian border, second zone is Imbricated zone which is dominates a small segment of

the AOS , and then High Folded zone , and the last zone is Low Folded zone (Kamal

,2009). The AOS is mostly dominated by the High and Low Folded Zones.

Alluvium sediment and soil cover most of Iraq including Province of Sulaimaniya

(Kamal, 2009). These are all loose sediments that deposited by running water which

include:

(1) Alluvial fan deposits (boulder, gravel, and sand silt and clay deposits. The boulder

and gravel are generally: (A) angular (Figure 6.), (B) Badly sorted,

(C)Mineralogically immature, and D- they have fan shape (Figure, 7).

(2) River bed deposits: they consist of sorted, rounded and mature boulder gravel and

sand

(3) Flood plain sediments: they are fine detritus sediments that deposited during very

large flooding (Figure 8).

Figure 1 Administration Boundary of the AOS (IAU, 2011)
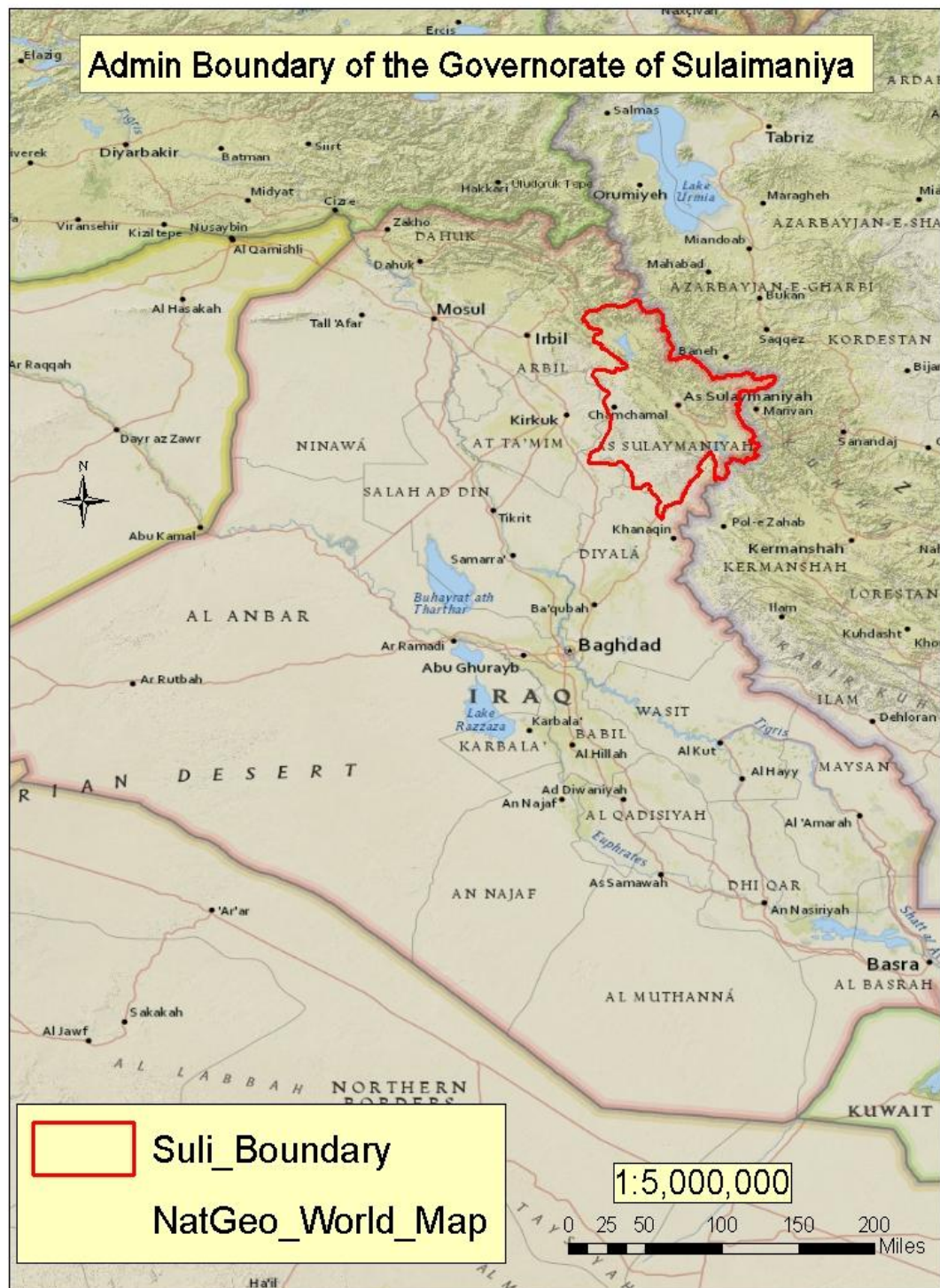
Figure 2 The Administration boundary of Iraq and Province of Sulaimanyia (National Geographic and Esri)
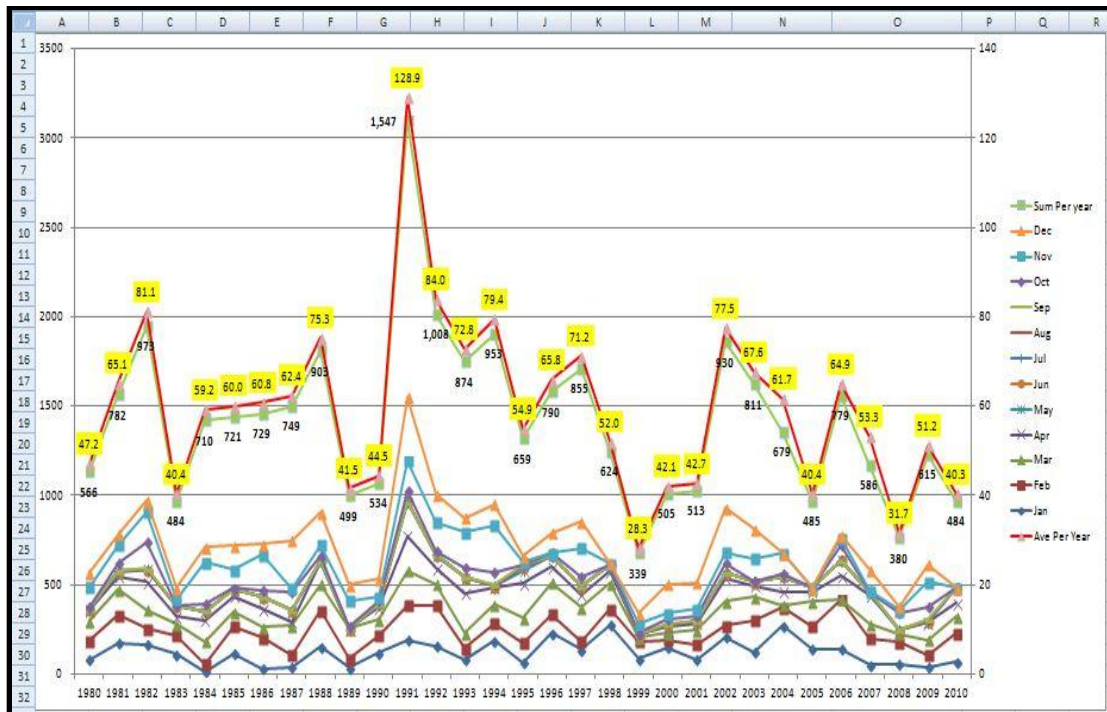
Figure 3 Rainfall records of the AOS from 1980-2010. The two top lines: first (red line) is represents average per a year and the second one (green line) is represents sum per a year, the others on bottom are represent each month per year (Source: UVS/COS/DoG)
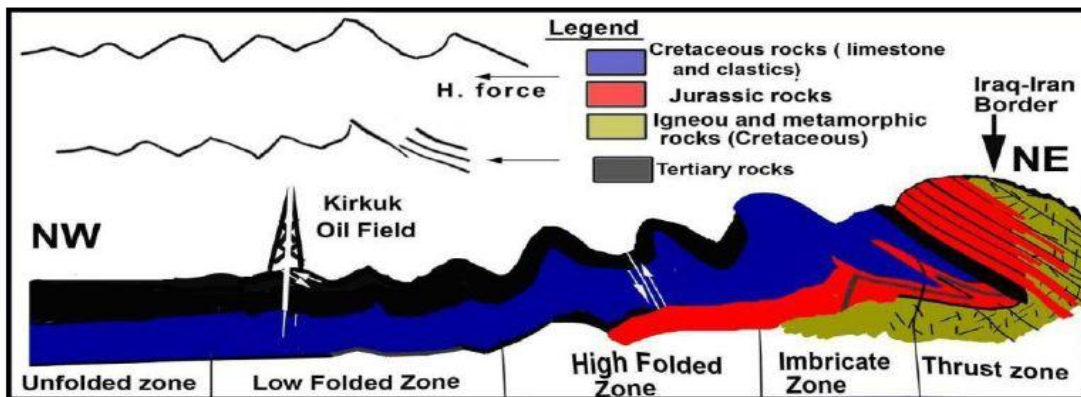
Figure 4 Tectonic subdivision of Iraq (Kamal, 2009)
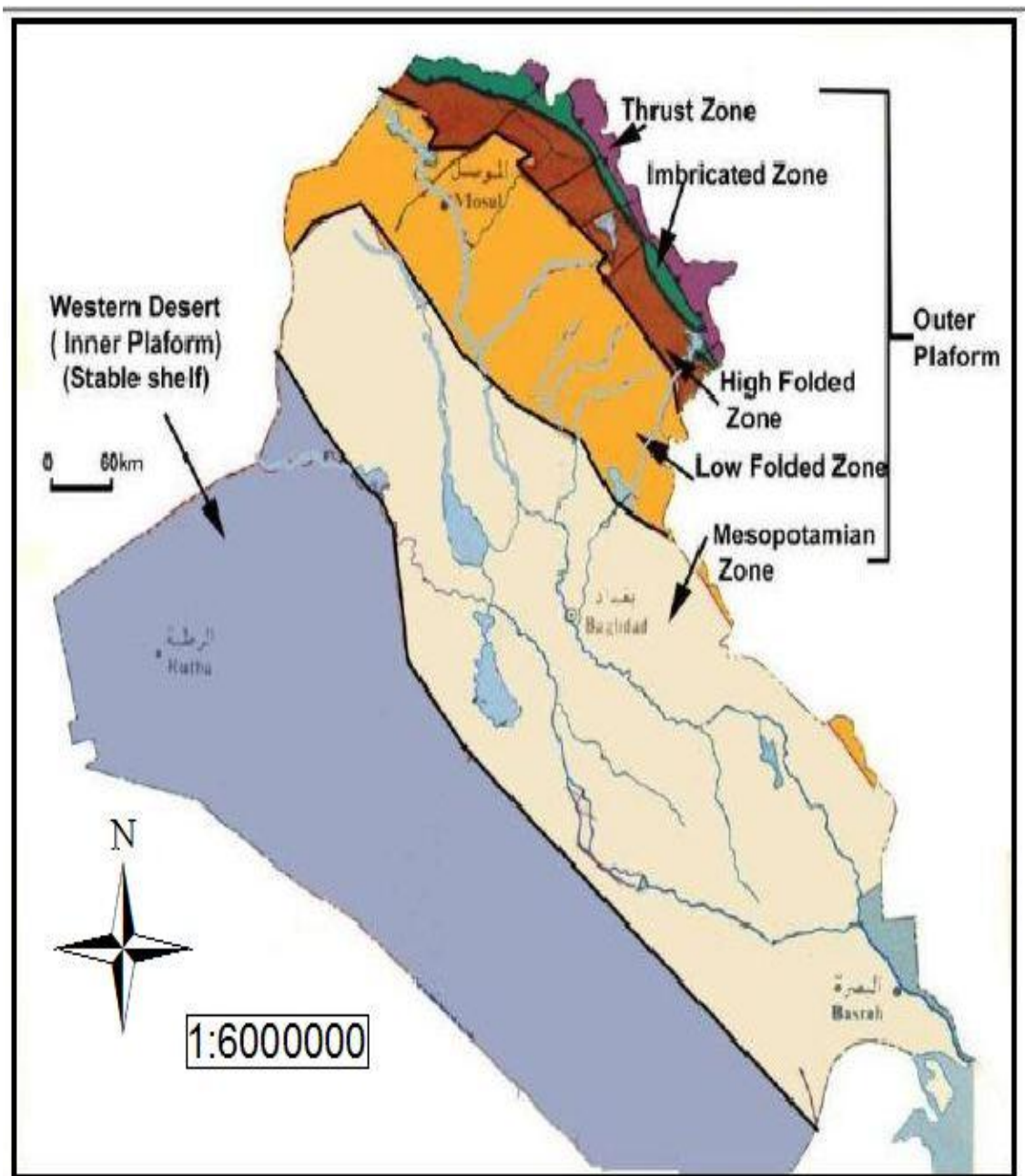
Figure 5 Iraq map shows the most accurate tectonic subdivision of Iraq (Kamal, 2009).

Figure 6 Deposit of alluvium fan at west of Sulaimaniaya city underlain by flood plain clay (Kamal, 2009).
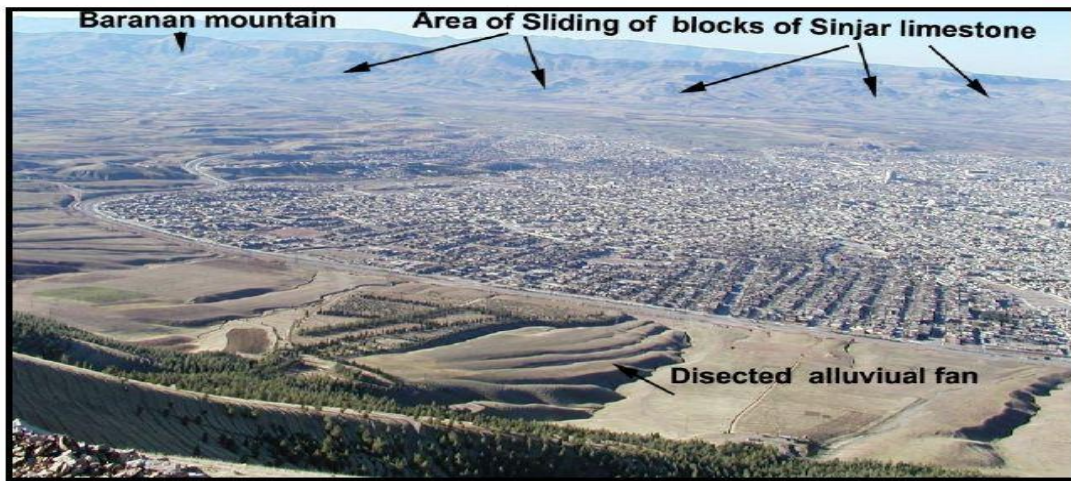
Figure 7 Northeastern of Sulaimaniya city (pediment of Goizha Mountain) shows proximal part of several alluvial fans (Ali, 2007). Background: Baranan Mountain which contains area of sliding of blocks of Sinjar Formation on Kolosh Formation (Kamal, 2009).

Figure 8 Riverbed deposits in braided river near Darbandikhan town which is mostly consist of gravel and sand (Kamal, 2009)

1.7 Research Questions and Objectives

The overarching objective of this study is to highlight and understand the nature of Land Use/Land Cover (LULC) and to understand major Land Use/Land Cover Changes (LULCC) related to the growing population and economy in the province of Sulaimaniyah, Northern Iraq after 1998, which leaded to rapid expansion of urban areas. Increasing urban areas within the cities for example city of Sulaimaniyah is increasing additional demand on natural resources thereby causing LULCC. Knowledge of LULC and LULCC is important for the economy planning of the region.

To the best of my knowledge, systematic LULC and LULCC studies have not been performed for this area. To address this gap, I conducted a systematic study of LULC and LULCC in the Province of Sulaimaniya between 1998 and 2010. To achieve this goal, I utilized in my work three primary data sources: (a) land cover type for that area, for which data are not available; (b) economic indicators, for which data are available at limited reliability; and (c) census data, for which data are available and accessible. Based on this data, the research questions and the objectives of this study are as follows:

1.7.1 Research questions:

- What tools or methods are needed to better characterize historic and current land use and land cover attributes and dynamics?

- How can geospatial methods be used to characterize land use and land cover changes in the POS?

- What are the most accurate LULC classes in AOS?

- What are the primary drivers of land-use and land-cover change in AOS between 1998 and 2010?

1.7.2 Research Objectives

- Classify the LULC of the Area Of Study (AOS).

- Introduce and identify LULC Schema.

- Explore and evaluate the potential and performance of remote sensing data and remote sensing methods for the understanding the impact of different factors on LULC.

- Understand the nature of LULCC.

- Identify the factors that caused the change

- To detect, delineate, and map areas that have experienced land use and land cover change, specifically, the reurbanization in the AOS over the 12 years from 1998-2010.

A secondary objective of this study is to evaluate the level of accuracy of remote sensing data for classifying LULC in the AOS. In particular, I plan to determine how accurate remote sensing techniques are given the causes of the changes in the area between 1998 and 2010. It is hoped that this study will provide information for decision

makers and development practitioners about the magnitude and dimensions of long term

land use and land cover changes, their drivers, impacts and community mitigating

strategies in the study areas and surrounding.

Table 1 Population of Iraq in 1997 (COSIT 1997)

توزيع السكان حسب المحافظات والجنس والبيئة حسب نتائج تعداد 1997

POPULATION DISTRIBUTION BY GOVERNORATES, GENDER AND SOCIAL ORIGIN ACCORDING TO THE 1997 CENSUS RESULTS

Table (2/5)										جدول (2/5)
	مجموع Total			ريف Rural			حضر Urban			
Governorate	مجموع Total	آناث Female	ذكور Male	مجموع Total	آناث Female	ذكور Male	مجموع Total	آناث Female	ذكور Male	المحافظة
Ninevah	2042852	1019009	1023843	778133	391664	386469	1264719	627345	637374	نينوى
Kirkuk	753171	380755	372416	222245	114148	108097	530926	266607	264319	كركوك
Diala	1135223	570348	564875	656320	332287	324033	478903	238061	240842	ديالى
Al-Anbar	1023736	510899	512837	484449	243668	240781	539287	267231	272056	الانبار
Baghdad	5423964	2701869	2722095	572616	289323	283293	4851348	2412546	2438802	بغداد
Babylon	1181751	594294	587457	616095	311489	304606	565656	282805	282851	بابل
Kerbala	594235	300309	293926	201865	101935	99930	392370	198374	193996	كربلاء
Wasit	783614	398150	385464	366936	188133	178803	416678	210017	206661	واسط
Salah A-Deen	904432	456795	447637	497358	252691	244667	407074	204104	202970	صلاح الدين
Al-Najaf	775042	391791	383251	233124	117838	115286	541918	273953	267965	النجف
Al-Qadisiya	751331	381206	370125	353563	179990	173573	397768	201216	196552	القادسية
Al-Muthanna	436825	224841	211984	240956	125311	115645	195869	99530	96339	المثنى
Thi Qar	1184796	604757	580039	484502	247484	237018	700294	357273	343021	ذي قار
Maysan	637126	325943	311183	215973	111334	104639	421153	214609	206544	ميسان
Basrah	1556445	787007	769438	314632	161227	153405	1241813	625780	616033	البصرة
*Kurdistan Region:										*اقليم كردستان:
Duhouk	402970	195843	207127	102354	49744	52610	300616	146099	154517	دهوك
Erbil	1095992	544708	551284	247694	123104	124590	848298	421604	426694	اربيل
AL-Sulaimaniya	1362739	670468	692271	388381	191084	197297	974358	479384	494974	السليمانية
Total	22046244	11058992	10987252	6977196	3532454	3444742	15069048	7526538	7542510	المجموع

* Estimted population in 1997 according to 1987 census results

تقديرات السكان لعام 1997 حسب نتائج تعداد 1987

Table 2Iraqi population in 2011(COSIT 2011)

تقديرات السكان حسب المحافظات والبيئة لسنة 2011
ESTIMATED POPULATION BY GOVERNORATES, SOCIAL ORIGIN FOR THE YEAR 2011

Table (2/8) B   جدول (2/8) ب

Governorate	Total مجموع	Rural ريف	Urban حضر	المحافظة
	مجموع Total	مجموع Total	مجموع Total	
Ninevah	3270422	1282561	1987861	نينوى
Kirkuk	1395614	395481	1000132	كركوك
Diala	1443173	751231	691942	ديالى
Al-Anbar	1561407	805015	756392	الانبار
Baghdad	7055196	905481	6149715	بغداد
Babylon	1820673	961701	858972	بابل
Kerbala	1066567	357395	709172	كربلاء
Wasit	1210591	509348	701243	واسط
Salah AL- Deen	1408174	785660	622515	صلاح الدين
Al-Najaf	1285484	371876	913607	النجف
Al-Qadisiya	1134313	493981	640332	القادسية
Al-Muthanna	719069	404570	314499	المثنى
Thi Qar	1836181	681002	1155178	ذي قار
maysan	971448	268177	703271	ميسان
Basrah	2531997	507703	2024295	البصرة
Total	28710310	9481182	19229129	مجموع 15 محافظة
Kurdistan Province:				محافظات اقليم كردستان:
Erbil	1612692	271565	1341127	اربيل
Duhouk	1128745	300759	827986	دهوك
AL-Sulaimaniya	1878764	283236	1595528	السليمانية
Total	4620202	855560	3764642	مجموع محافظات الاقليم
Grand total	33330512	10336741	22993771	المجموع الكلي للعراق

1.8 Thesis Organization

Complete presentation of the thesis includes five separate but connected chapters including this introductory chapter. Chapter one gives an introduction and background, location and rain fall records of AOS, geology of the AOS, objectives of the study and the thesis Organization. Chapter two introduces the study in the context definition of LULC and LULCC, existing literature on land use and cover change and its drivers and impact. Along with the major procedures and software required. It also includes a review of several studies done in the areas along with important findings and knowledge gaps that call for further research, which further guides us to formulate the purpose of the study and the research questions. In this chapter the remote sensing methodology of

classification, change detection and validation are reviewed. Chapter three describes the

sources and type of data and imagery which been used for the classification, change

detection and validation of the result. Chapter four presents the classification, change

detection and validation of the result. Finally, chapter five presents the result as well as

an evaluation of the study and potential impact.

CHAPTER TWO

Literature review

2.1 Chapter overview

This study is conducted to examine the use of remote sensing methods for assessing the LULC and LULC of AOS, as well as to identify the factors of the change. This review summarizes the fundamentals, components and history LULC, LULCC, remote sensing technology, previous study of the AOS. In addition, covers review of the sensors which produced the images of the AOS, LULC schema, classification methods (CART), change detection method (CCA), vegetation indices, and validation which they been used and invoked to conduct this study.

2.2 Land cover and Land use (LULC)

Land use and land cover are discrete but interrelated concepts. Land use involves the way people work the land and use its resources. For example, agriculture, grazing, mining, logging, and urban development are all modes of land use. Land cover involves the physical features of the land, such as crops, trees, pasture, roads, wetlands, and urban structures (CAST, 1999; Zubair and Ayodeji, 2004). Originally, the idea of land cover encompassed only the vegetation of the area. However, it was later broadened to include

man-made structures such as edifices and roads, as well as characteristics of the natural

environment, such as surface water, groundwater, biodiversity, and soil (Meyer, 1995).

Land use and land cover are not only driven by human action but also produce

changes that impact people (Agarwal et al., 2002). They can alter the availability of

different biophysical resources, such as soil, vegetation, water, animal feed, and so on.

Consequently, land use and land cover changes can lead to decreased availability of

certain products and services for people, livestock, and agricultural production, as well as

damage to the environment.

In addition, land use describes use of the land surface by human (Campbell,

2007). Normally, land use is defined in an economic context, so we may think of land as

it used for agricultural, residential, commercial, and other purpose; however, Campbell

(2007) considers land cover as visible features of the Earth's surface including vegetation

cover, natural and as modified by humans, its structures, transportation, and

communication.

2.3 Land cover and Land use Change (LULCC)

Land use affects land cover, and changes in land cover affect land use. However,

changes in land cover due to land use do not necessarily imply a degradation of the land,

although many land use patterns, driven by a variety of social causes, can result in land

cover changes that affect biodiversity, water and radiation budgets, trace gas emissions and other processes that cumulatively affect the global climate and biosphere. Land cover can be altered by natural events such as weather, flooding, fire, climate fluctuations, and ecosystem dynamics. Today, land cover is altered principally by agriculture and livestock raising, forest harvesting and management, and urban and suburban construction and development (Jensen, 2005)

Most land cover change can be associated with two broad change types: systemic and cumulative. Systemic change operates directly on the biochemical flows that sustain the biosphere. Depending on its magnitude, systemic change can lead to global changes. Cumulative change is the most common type of human-induced environmental change. Cumulative changes are geographically limited but if repeated sufficiently, become global in magnitude. Changes in landscape, cropland, grasslands, wetlands, or human settlements are examples of cumulative change (CAST 1999).

2.4 Remote Sensing and LULC

Remote Sensing is the science and art of obtaining information about an object, area, or phenomenon through the analysis of data acquired by a device that is not in contact with object, area, or phenomenon under investigation (Lillesand and Kiefer, 1987; CAST, 1999).

The term of remote sensing has been defined many times and from cursory look at these definitions, it is easy to identify a centurial concept: gathering of information at a distance (Campbell, 2007). The term of remote sensing goes back to early 1960s by the staff of the Office of Naval Research Geography Branch (Jensen 2007).

Analysts developed spectral signatures based upon the detected energy's measurement and position in the electromagnetic spectrum. By utilizing the developed spectral signatures in mulitspectral classification and thematic mapping, the analyst can generate new data for analysis (CAST, 1999). In order to classify the LULC of the AOS, multispectral images with different bands can be used. In this research the spectreal signatures of each band have been considered during collection of training sample, classification, change detection, and validation.

The term *resolution* is commonly used to describe remotely sensed imagery. CAST (1999) and Campbell (2007) outlined four types of resolution that must be considered when remotely sensed data are used: spatial, spectral, radiometric, and temporal. Spatial resolution is the minimum size of terrain features that can be distinguished from the background in an image or from other closely spaced features. Spectral resolution refers to the electromagnetic wavelength intervals that a sensor or sensor band can read or record. Radiometric resolution refers to the dynamic range, or number of possible data values, in each band. Temporal resolution is a measure of how often a given sensor system obtains imagery from a particular area (i.e., how often an

area can be revisited). For example, the temporal resolution of satellites is typically fixed, which allows for more regular viewings. The resolution of all imagery used for this study, are detailed in chapter 3.

2.5 Previous studies of the AOS:

In the past, several studies have explored this area, including a study by the United Nation (UN). According to the results of this study, the AOS has been classified as approximately 50% of crop / grass/wood, 20% dry land crop/pasture, 15% scrub, 10% water, 5% other classes of irrigated crop, and urban development (Figure9). These percentages are my visual interpretation of the map. Errors with this study occur within the misclassifying of most barren and grass areas in the south west of the AOS; furthermore, the urban area is not mapped.
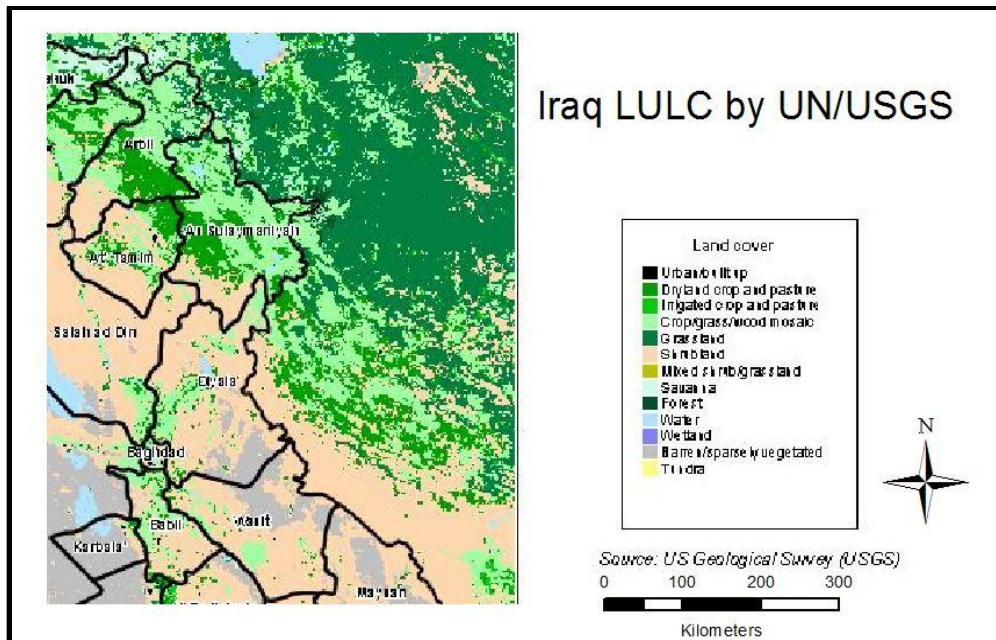
Figure 9 LULC classification of Iraq by the UN

A second study was done by the Global Land Cover Facility (GLCF), which is housed at the University of Maryland (UMD). The GLCF has developed and distributed land cover data with an emphasis on determining where, how much and why land cover changes around the world. In this study, AVHRR images are used for LULC classification, the time frame of the images is between 1981 to 1994 (Figure 10). Again, the main issue with this classification is the lack of urban space; in addition, more open shrub land is seen around the lake of Dokan on northwest of the AOS, for this area should be mostly crop land (AG) in different stages of growth. The dominant LULC class along the Iranian border should be deciduous trees and scrubs. Also, grass lands (range land) and barren regions should appear as minor classes within this area.
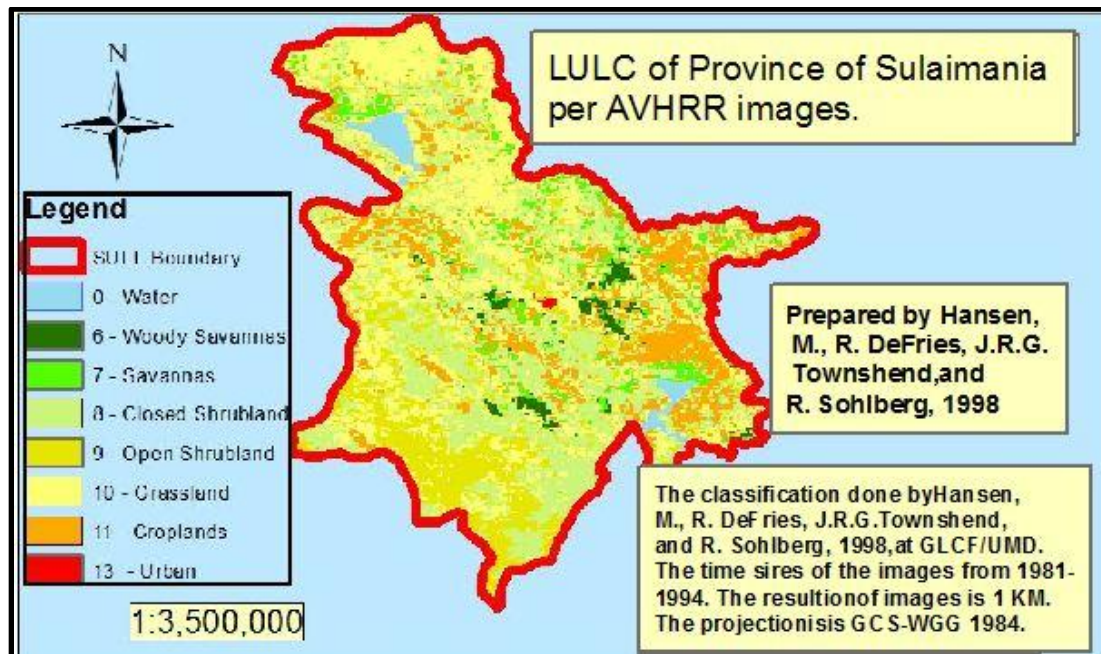
Figure 10 LULC map of AOS from 1981 to1984 (GLCF/UMD Hansen et al., 1998)

Another LULC study done by International Geosphere and Biosphere Program
(IGBP) in 2002 engages the conventional supervised maximum likelihood classification
approach based on the Regional Land Cover Ground Truth (RLCGT) database; here, the
temporal coverage from 2000-01-01 to 2000-11-30 and MODIS images resolution of 1
KM have been used. In these results, the dominant LULC class was herbaceous with
sparse scrub, and the water class is under-identified, for one of the major lakes has not

25

been mapped, only a few small urban area had been mapped, and a deciduous forest was
not mapped (Figure, 11).
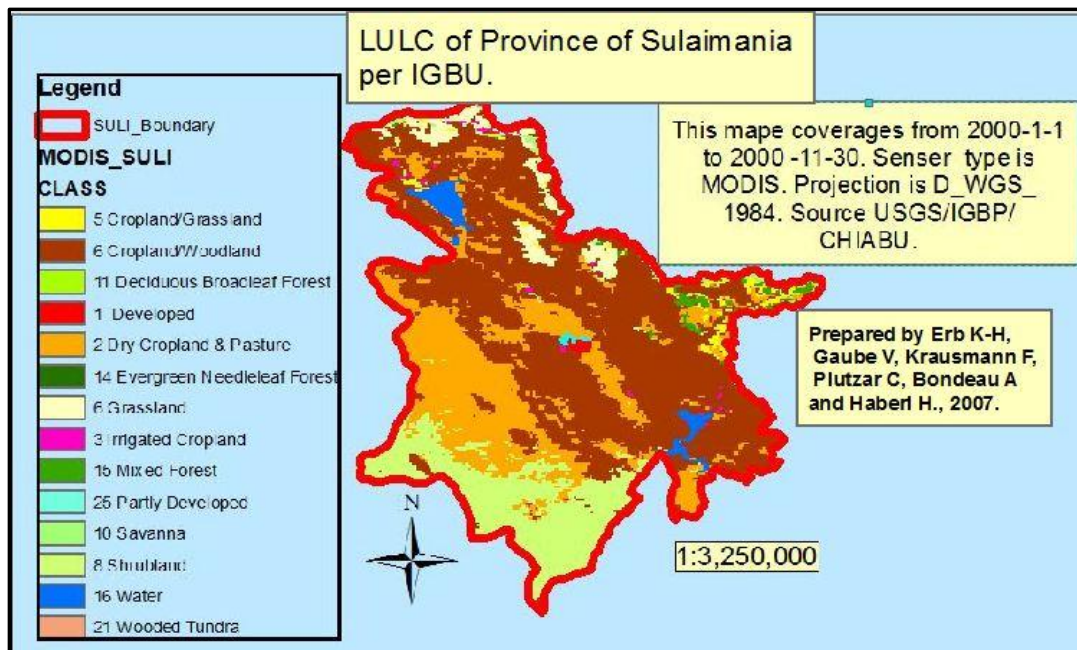
To the best of my knowledge, systematic LULC and LULCC studies have not
been performed for this area. Most of the studies which have been done so far
demonstrate errors due to weaknesses of Ground Truth (GT), and other errors are due to
human interpretation and analysis. Other errors may occur due to seasonal changes; for
example, parts of the area around Lake Dokan in UMD are classified as open shrub land

and wooded grassland; this area is currently dominated by agricultural (AG), and this may be a result of changes from wooded grassland to AG land. The southwest of the AOS had been classified incorrectly in both of the above studies; the UN study had classified this area as shrub land, and the UMD had classified it as open shrub land; however, this area should be mostly barren and grass lands. The misclassification may possibly be due to the incorrect GT of those areas.

In the summery, there is a gap in the type of LULC classes in this area as a result of poor GT and personal interpretation. Thus, for conducting any studies such as change detection, there must first be an area classification done much more accurately than those that had been previously conducted by any other RS studies. Therefore, in this study, and attempt is made to classify the AOS first based on Thematic Mapper (TM) images from 1997 and then on detection in LULCC between the images of 1997 and 2011 through several essential and efficient steps: namely, identifying the LULC classification scheme, image data acquisition, scene processing, data analysis, other remote-sensing processing, and validation.

2.6 LULC Classification scheme

Due to different data from different sensors, a multilevel land use and land cover classification system has been developed (Table 3). Different agencies within various governmental levels collect data about landuse and land cover. However, for the most part, they have worked independently and without coordination. Due to the variety of

data obtained from many different sensors, a multilevel land use and land cover

classification system has been developed (see Table 3). The land use and land cover

classification scheme used in this study is the USGS classification system, which was

developed by Anderson (1976), (see Table 4). Only the I and II levels of Anderson

schema been invoked in this study which is satisfies the three major attributes of the

classification process as outlined by Greg (1965): (a) It gives names to categories by

simply using accepted terminology, (b) it enables information to be transmitted, and (c) it

allows inductive generalizations to be made.

Table 3Classification level and data type (Anderson, 1976).

Classification level	Typical data characteristics
I...........................	LANDSAT (formery ERTS) type of data.
II.........................	High-altitude data at 40,000 ft (12,400 m) or above (less than 1:80,000 scale).
III.........................	Medium-altitude data taken between 10,000 and 40,000 ft (3,100 and 12,400 in)(1:20,000 to 1:80,000 scale).
IV.........................	Low-altitude data taken below 10,000 ft (3,100 m) (more than 1:20,000 scale).

Also, according to Campbell (2007) this system has many advantages over the previous systems. Whereas previous systems did not consider the unique advantages of aerial imagery as a source of land-use and land-cover data, the USGS system was specifically prepared for use with aerial photography and related imagery.

Table 4USGS /LULC classification scheme(Anderson et al., 1976; Jensen, 2005 and Campbell, 2007)

Land use and land cover classification system for use with remote sensor data

Level I	Level II
1 Urban or Built-up Land	11 Residential.
	12 Commercial and Services.
	13 Industrial.
	14 Transportation, Communications, and Utilities.
	15 Industrial and Commercial Complexes.
	16 Mixed Urban or Built-up Land.
	17 Other Urban or Built-up Land.
2 Agricultural Land	21 Cropland and Pasture.
	22 Orchards, Groves, Vineyards, Nurseries, and Ornamental
	23 Horticultural Areas.
	24 Confined Feeding Operations.
	Other Agricultural Land.
3 Rangeland	31 Herbaceous Rangeland.
	32 Shrub and Brush Rangeland.
	33 Mixed Rangeland.
4 Forest Land	41 Deciduous Forest Land.
	42 Evergreen Forest Land.
	43 Mixed Forest Land.
5 Water	51 Streams and Canals.
	52 Lakes.
	53 Reservoirs.
	54 Bays and Estuaries.
6 Wetland	61 Forested Wetland.
	62 Nonforested Wetland.
7 Barren Land	71 Dry Salt Flats.
	72 Beaches.
	73 Sandy Areas other than Beaches.
	74 Bare Exposed Rock.
	75 Strip Mines. Quarries, and Gravel Pits.
	76 Transitional Areas.
	77 Mixed Barren Land.
8 Tundra	81 Shrub and Brush Tundra.
	82 Herbaceous Tundra.
	83 Bare Ground Tundra.
	84 Wet Tundra.
	85 Mixed Tundra.
9 Perennial Snow or Ice	91 Perennial Snowfields.
	92 Glaciers.

2.7 CART

Classification and Regression Tree analysis (CART) is a special method of creating decision rules to distinguish between clusters of observations and determine the class of new observations. A particular feature of CART is that decision rules are represented via binary trees that are why it can be easy to apply these rules in practice (Breiman et al., 1984; Seguin and Guray, 2005).

It is a classification method which uses Binary Recursive partitioning to divide the independent variables into two parts by using regression and the dependent variable to determine the best possible split. Regression tree classification is a recursive and iterative algorithm that requires 2 types of inputs:

- A dependent variable (Training Data in this study)
- More than one independent variables (the image bands ,NDVI, NDSI, NDMI, TCT, in this study)

CART is non-parametric data mining approach that allows any number of independent variables to be of any data type, e.g. DEMs, ancillary datasets, imagery, binary masks. This is a significant advantage of CART .Above producers promote CART for been a powerful and flexible classification tool. In particular:

- It can be applied to any data structure through the appropriate formulation of a set of questions.

- The final classification has a simple form which can be compactly stored and that efficiently classifies new data.

- It makes powerful use of conditional in information in handling non-homogeneous relationships.

- It dose automatic stepwise variable selection and complexity reduction.

- It gives, with no additional effort, not only a classification, but also an estimate of the misclassification probability for the object (Breiman et al., 1984).

Due to these advantages, CART approaches to ecological analysis and land cover mapping have become more widespread in recent years (Michaelson *et al*., 1987). An example of the use of for LULC studies is the work of Villarreal et al. (2011). The aim of this study was involved to map the area of Santa Cruz Watershed in Arizona, United States, and northern Sonora, Mexico by creating a series of land-cover maps at decadal intervals (1979, 1989, 1999, and 2009) using Landsat Multispectral Scanner and Thematic Mapper data. The *See5* software used to develop the CART models and the *NLCD* Mapping Tool to classify the spatial data in ERDAS Imagine (www.rulequest.com/see5).

2.8 Cross-Correlation Analysis (CCA)

CCA was developed by Greg Koeln (2000) and later copyrighted by Earth Satellite Corp., which became MDA Information Systems LLC. CCA uses classes (zones) from one date and imagery from another date (Figuer, 12). Z-Score values are calculated for each image pixel within the class zones to determine likelihood of change. The primary strength of CCA is that it can be used to compare geospatial dataset of any season or format. It can be used to identify changes that have occurred in a previously mapped area.

CCA involves two steps: first, a thematic map is overlaid upon a recent multispectral image. Class boundaries from the older thematic map separate image pixels into different class zones . Then the "expected" class average spectral response and standard deviation are calculated for each pixel falling within a particular class zone(Kolen and Jeana, 2000).The Z- statistic is used to describe how close pixel's response is to the expected spectral response of its corresponding class value in land-cover map (Jensen, 2005). A multivariate Z statistic can be defined as follows (Eq. 1):

Equation 1 (Kolen, 2000):

$$Z = \sum_{i=1}^{n} \left(\frac{Observed_i - Expected_i}{Std.Dev._i} \right)^2$$

Where:

Z is the measure of the distance in n-dimensional space from the norm

i is the attribute index

n is the number of attributes

Observed$_i$ is the observed value of the attribute with index i,

Expected$_i$ is the expected or mean value of the attribute with index i,

Std.Dev.$_i$ is the standard deviation of the attribute with index i,

The power and uniqueness of CCA lies in its ability to accurately detect change between images not necessarily acquired under similar conditions. Whether the recent multispectral image was acquired in a hotter, colder, wetter or drier year, CCA will use former class boundaries to derive new class signatures that take current image conditions into consideration (Kolen, 2000)
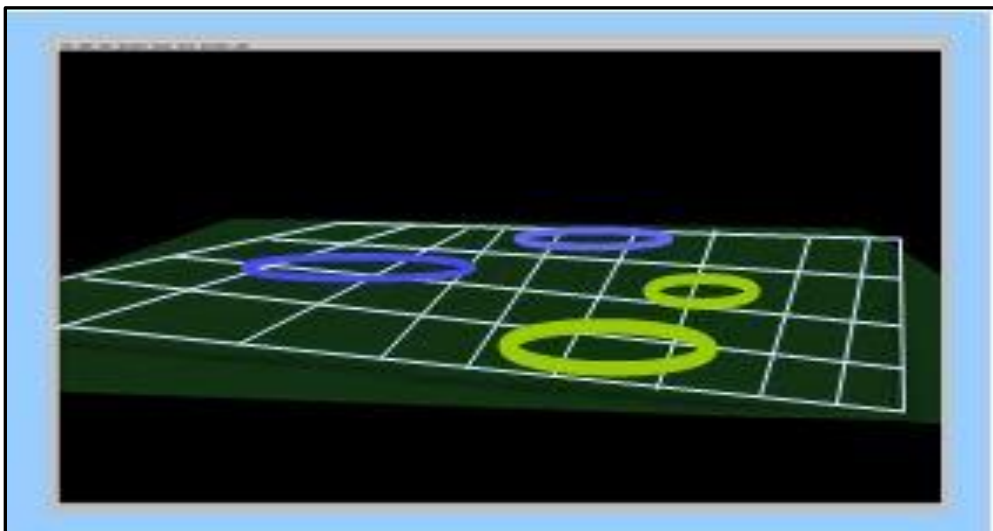
Figure 12 Class Zones created by   overlay a Thematic Map onto a Recent Multispectral Image (Kolen, 2000)

2.9 Validation

The data derived from remotely sensed imagery are becoming progressively more important for environmental models at the local, regional and global scales. Every LULC contains some degree of error. It's important to understand the accuracy of the LULC product by doing a validation study. The thematic information derived from the remote-sensed data must be accurate because decisions are made throughout the world using this information. Unfortunately, the thematic information contains errors. Recognizing the source of these errors is very important and should be minimized as much as possible. The sources of these errors are many; it is possible that errors are introduced during the imagery collection, during preprocessing, or during information extraction, data conversion, or error assessment (Figure 13).

There are different steps and methods by which improve accuracy assessment (Table 5), (Jensen 2005, 495-513). My chosen method use sample polygons within my classified product. The sample size will be based on multinomial distribution, and the sample distribution will be based on stratified random sampling. This is usually done by a random process stratified by classes and validated against reference data such as Rapid Eye or Google Earth (Campbell 2007, 392-403).
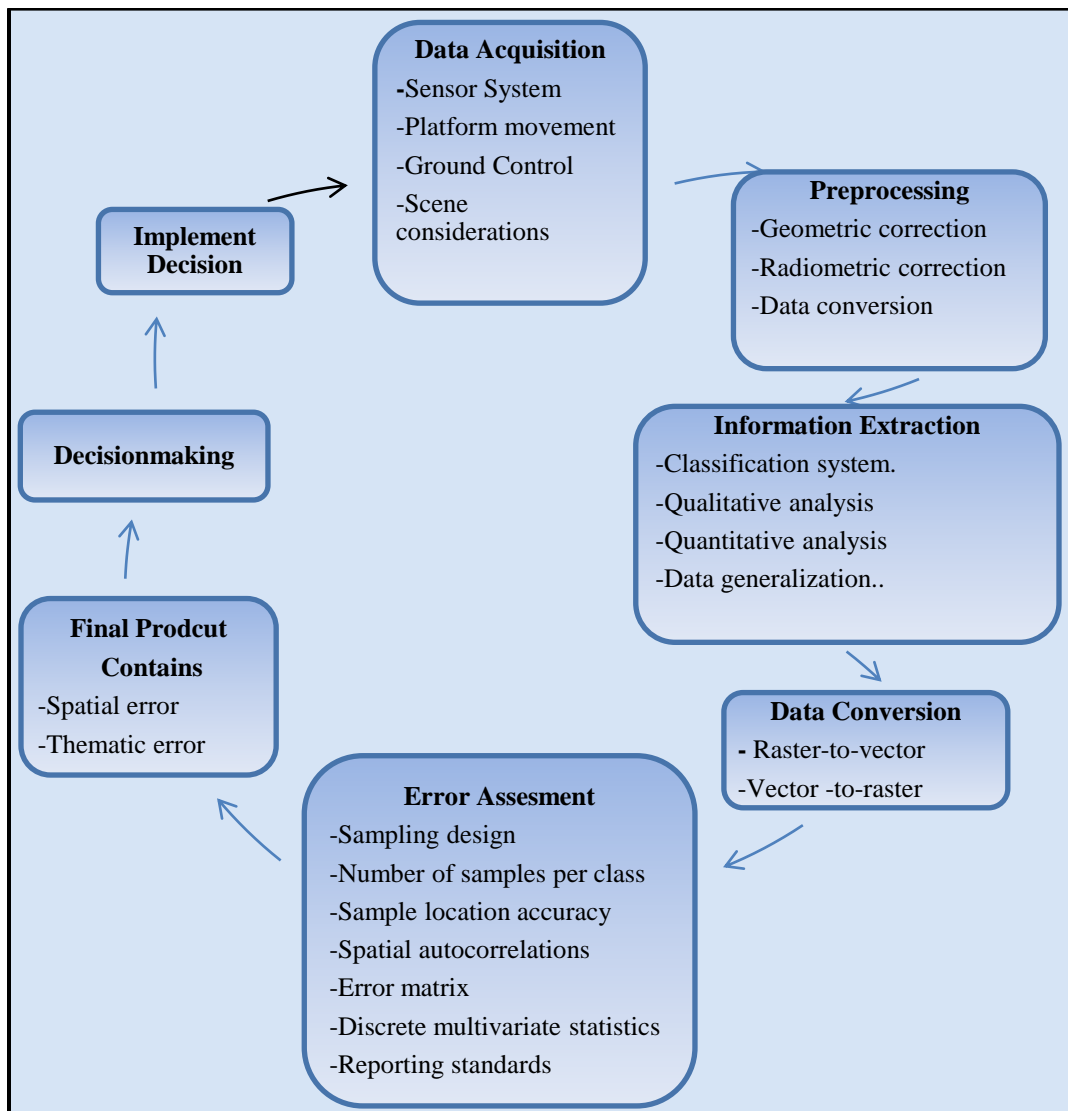
Figure 13 Sources of errors in remote sensing-derived information (Jensen 2005, 495-513)

Table 5 General steps to assess the accuracy of thematic information derived from remotely sensed data (Jensen, 2005)

State the nature of the thematic accuracy assessment problem.
* State what the accuracy assessment is expected to accomplish.
* Identify classes of interest (discrete or continuous).
* Specify the sampling frame within the sampling design:
    - *area* frame (the geographic region of interest)
    - *list* frame (consisting of points or areal sampling units)

Select method(s) of thematic accuracy assessment.
* Confidence-building assessment:
    - Qualitative
* Statistical measurement:
    - Model-based inference (concerned with image processing methodolog
    - Design-based statistical inference of thematic information

Compute total number of observations required in the sample.
* Observations per class.

Select sampling design (scheme).
* Random.
* Systematic.
* Stratified random.
* Stratified systematic unaligned sample.
* Cluster sampling.

Obtain ground reference data at observation locations using a response design.
* Evaluation protocol.
* Labeling protocol.

Error matrix creation and analysis.
* Creation:
    - Ground reference test information (columns)
    - Remote sensing classification (rows)
* Univariate statistical analysis:
    - Producer's accuracy
    - User's accruacy
    - Overall accuracy
* Multivariate statistical analysis:
    - Kappa coefficient of agreement; coñditional Kappa
    - Fuzzy

Accept or reject previously stated hypothesis.

Distribute results if accuracy is acceptable.
* Accuracy assessment report.
* Digital products.
* Analog (hard-copy) products.
* Image and map lineage report.

CHAPTER THREE

Data Source

3.1 Chapter Overview

In my approach, I used remote sensing data and remote sensing techniques because remote sensing data for land use/land cover and its changes are key to many varied applications such as environment, forestry, hydrology, agriculture, and geology. Methods for monitoring change range from intensive field sampling with plot inventories, to broad analysis of remotely sensed data, which has been verified to be more cost effective for large regions, to small site assessment and analysis. Additionally, commercial satellites are now providing a large amount of remotely sensed data at a range of spatial, spectral, and temporal resolutions from which natural and manmade features (that are most important for detecting LULCC) could be detected.

An example of the approximate coverage extent of a Landsat TM scene can be seen in figure 14. It requires 3 separate Landsat Scenes tiled together in order to cover the entire AOS. The study area considered for this project, Province of Sulaimaniya shown in red, is entirely contained in the Landsat scene Path/Row 168/35, Path/Row 168/36, Path/Row 169/35 and, Path/Row 169/36 (Figure 14)
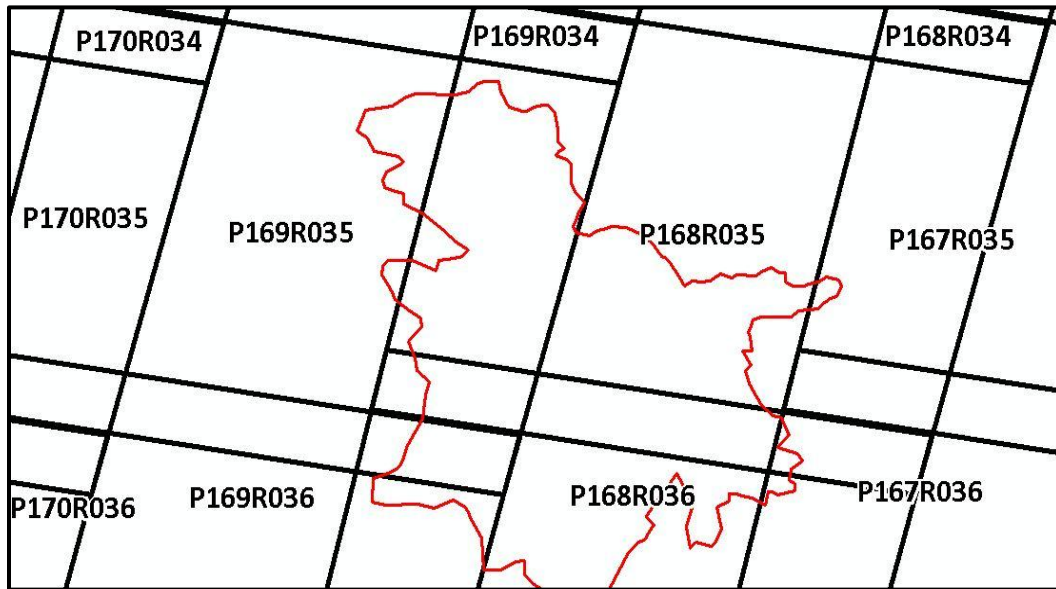
Figure 14 LANDSAT TM World Reference System (WRS Path/Row coverage of Province of Sulaimaniaya.

To address my research goals, I used a time-series of Landsat 5 Thematic Mapper (TM) and Landsat7 Enhanced Thematic Mapper Plus (ETM+) satellite imageries data covering the time frame between 1998 (Figure 15), and 2010 (Figure 16). The applications and software that I used to perform the data analysis are ERDAS imagine (version 11) and ArcGIS (version 11). In addition, I have used Rapid Eye imagery (Figure 17), Google Earth, ESRI Imagery, and Bing Maps (Aerial) for validation of my results.

3.2 LANDSAT

Landsat5 TM has been monitoring the globe since it was launched in 1984 March, and the images of TM widely used in LULC, chance detection, forest health, water quality management (Qingsheng Gaohuna, 2010, p1). Therefore many techniques for TM images been developed which helps in analyzes an example is TCT.

3.2.1 Landsat 5 TM

Landsat thematic mapper has been used for the study. In general Landsat 4, 5 are carrying both MSS and TM sensors. In my instance, landsat 5 TM has been used which its resolution 30m and has 6 bands. Some characteristics and applications of this sensor, namely, Band 1 is blue-green 0.45-0.52 μm useful for analyze and identify bathometry, mapping of coastal waters, Chlorophyll absorption, distinguish between coniferous and deciduous vegetation, penetration of clear water. Band 2 is green, 0.52-0.60 μm, this band records green radiation reflected from healthy vegetation, assess plant vigor, records reflectance from turbid water. Band 3 is red, 0.63-0.69 μm, functional for Chlorophyll II absorption. Band 4 is near infrared, 0.76-0.90 μm, this band is indicator of plant cell structure biomass, plant vigor and delineation of shoreline. Band 5 is Mid-infrared, 1.55-1.75 μm, and it is indicative of vegetation moister and soil moister mapping, differentiating snow from clouds, and penetration of thin clouds. Band 6, is far infrared,

10.4-12.5 µm and only this band has 120m resolution; this band is valuable for analyze vegetation stress, soil moister, brightness temperature, and some other applications.

3.2.2 Landsat 7 ETM+

Landsat 7 and Enhanced Thematic Mapper Plus, this is a current active landsat which is carrying ETM+ sensor and it is placed in orbit in April 1999. The Landsat ETM+ which I used in my study is covering only a small segment of my AOS on the North West and it been used for change detection part. It has 6 bands, 30m resolution for all bands expect band 6 which has resolution of 60 meter. The spectral ranges of the band are, band 1 is 0.45-515µm, band 2 is 0.525-0.605µm, band 3 is 0.630 -0.69µm, band 4 is 0.75-0.90 µm, band5 is 1.55-1.75 µm, band 6 is 10.4-12.5 µm. The only issue with Landsat7 is a scan line issue that has been observed since May 2003, which affects the classification.

3.3 RAPIDEYE

The RapidEye images which used for validation is Ortho Product (Level 3A) which offers the highest level of processing available. Radiometric, sensor and geometric corrections have been applied to the data. The product accuracy depends on the quality of the ground control and DEMs used. It is high resolution image and some of the characteristics of this sensor, namely, 5m pixel spacing , bit depth is 16 bits , and the spectral bands are Blue:430-510nm , Green:520-590nm,Red:630-685nm, Red Edge:690-

730, NIR:760-850nm. The tile size is 25KM (5000 line) by 25KM (5000 columns) and

250 Mbytes per Tile for 5 bands at 5 pixel spacing. Only 2 tiles were available for the

AOS which covers the city of Sulaimaniyah and area around, namely, 3855416_2011-11-

26_RE2_3A_140527 and 3855516_2011-11-26_RE2_3A_140527 (Figure 17).
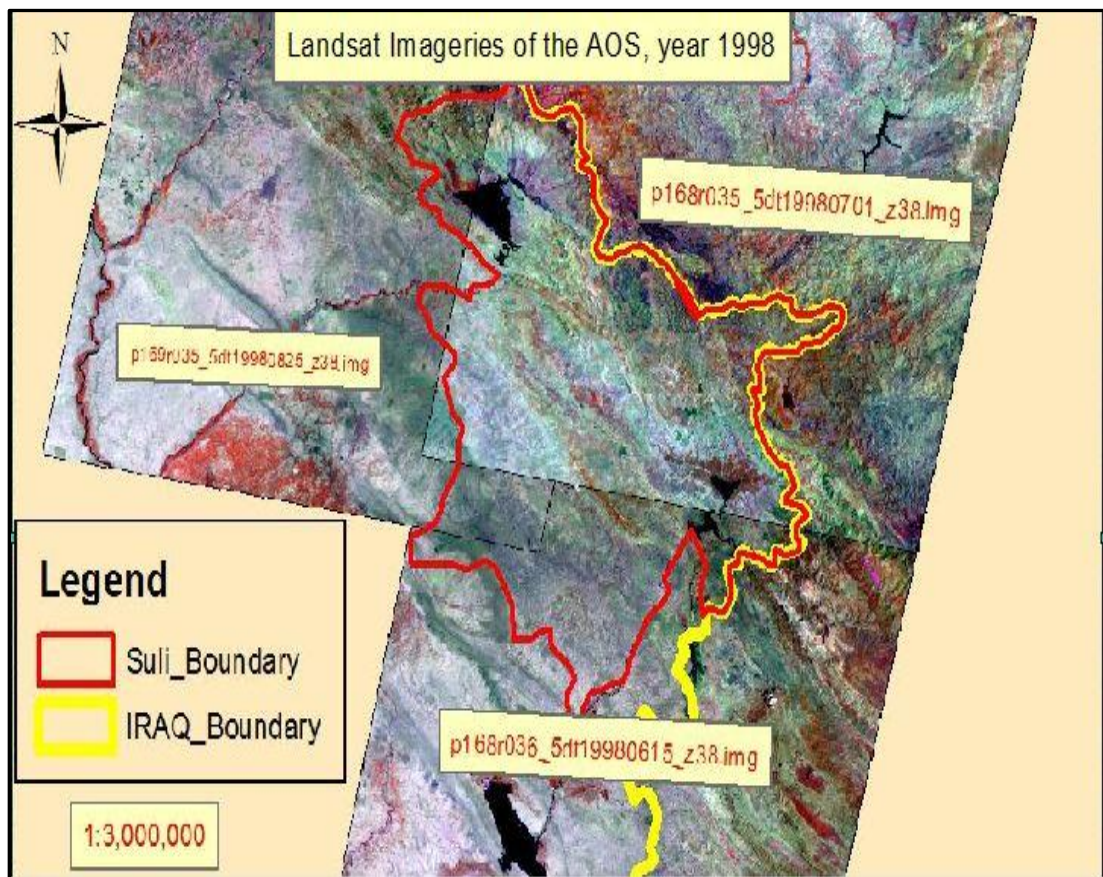
Figure 15 Landsat Imageries of 1998.
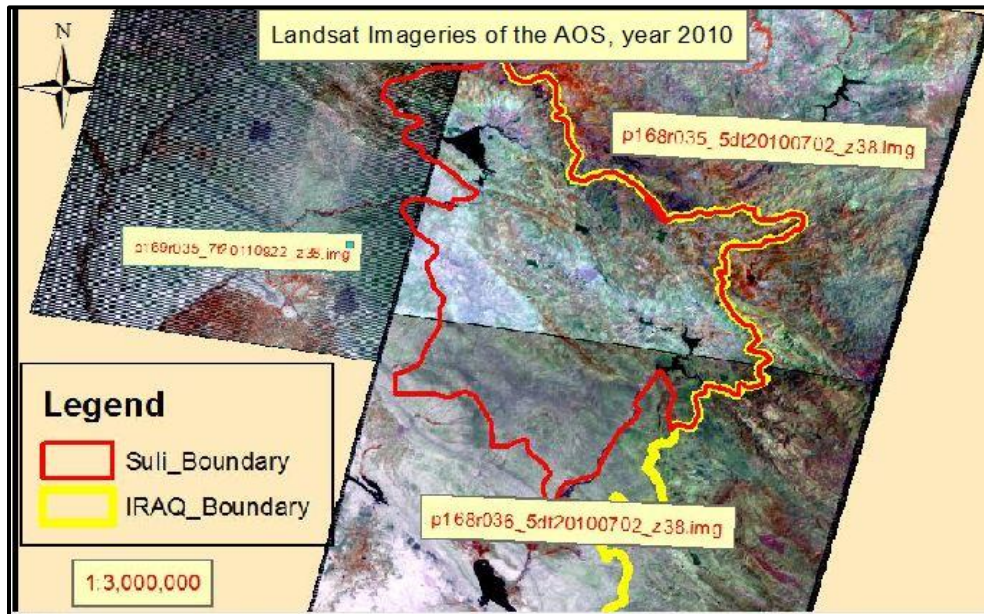
Figure 16. Landsat Imagery of 2010
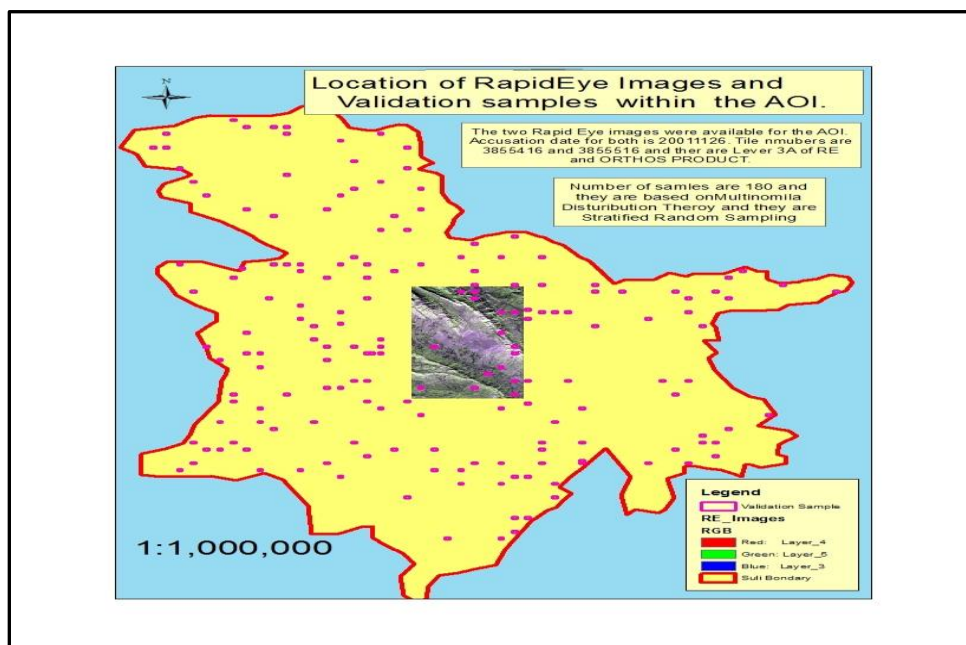
Figure 17 Location of Rapid Eye image and validation sample within the AOS.

CHAPTER FOUR

Research Methodology

4.1 Chapter Overview

This research addresses land LULC and LULCC over a 12 year period of study, 1998 to 2010, in AOS, Iraq. The dynamics of LULC classes, LULCC, and the spatial distribution and patterns are the primary focus of this study.

The image processing techniques employed in this study were applied using ERDAS imagine 2011. All final maps were produced in ArcMap. To analyze the data and to conduct the study several essential and efficient steps are required, namely: image data acquisition, image processing, image classification, other remote sensing processing, and validation. All above steps are shown in Figure 18.
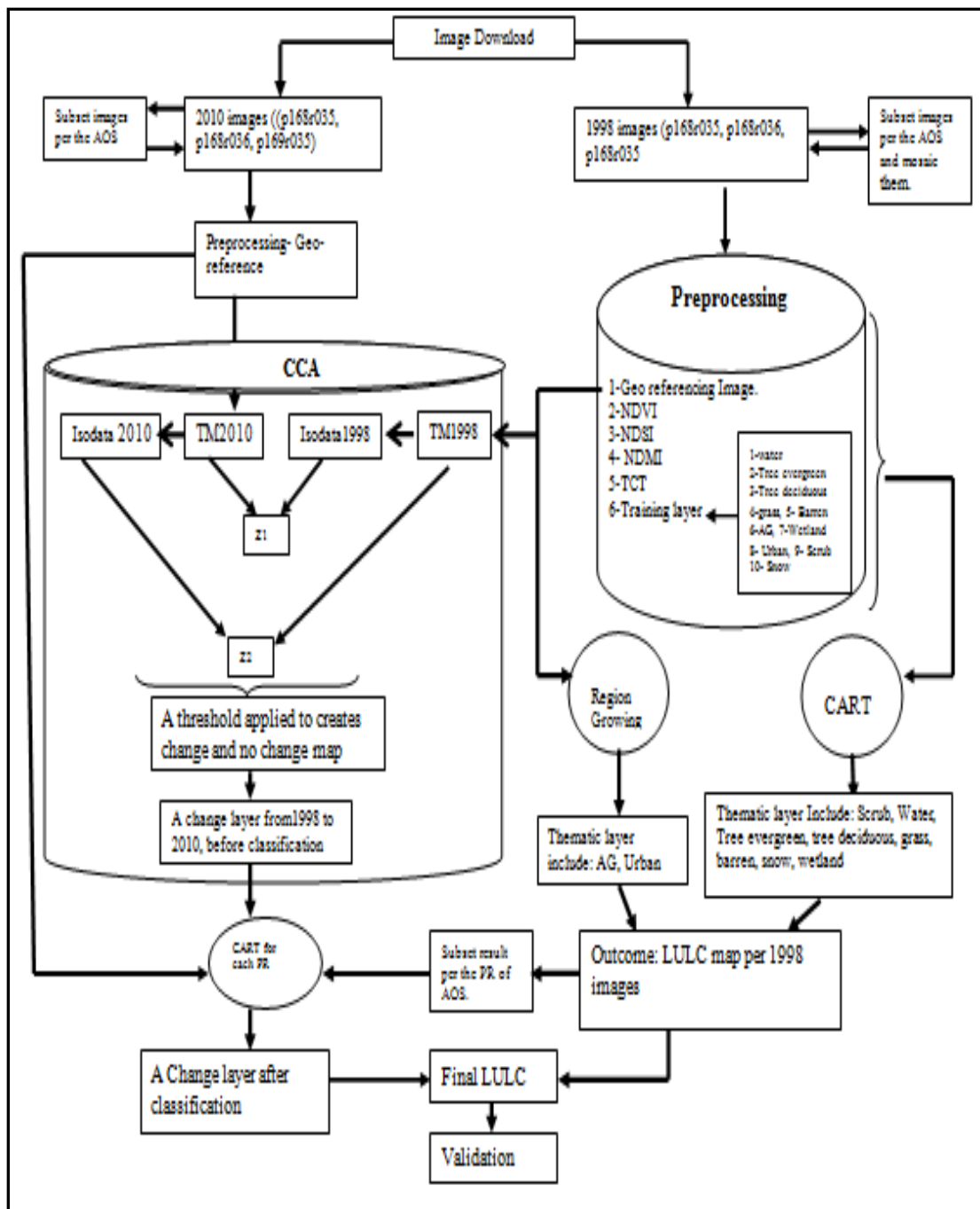
Figure 18 Workflow which explains all work steps in this paper.

4.2 Image Data Acquisition

The images of the study area have been downloaded from the USGS website (http://earthexplorer.usgs.gov/); the images must have a low amount of cloud and no scan line as much as possible. In this research only one image has scan lines, it covers only a small portion of North West of my AOI and it used for the change detection portion. In this image the scan lines appear as long line that can affect the classification process. However, these areas can fill with accurate class based on the closest class or feature around them or based on the open courses data such as GE or other high resolution images. The area of study is covered by three imageries for each year 1998 and 2010, (Table 6), (USGS).

Table 6 Landsat images which used for LULC and LULCC

Scene No.	Satellite Sensor	WRS Path\Row	Date	USGS format of date and PR
1	Landsat 5TM	P168R035	19980701	p168r035_5dt19980701_z38
2	Landsat 5TM	P168R036	19980615	p168r036_5dt19980615_z38
3	Landsat 5TM	P169R035	19980825	p169r035_5dt19980825_z38
4	Landsat 5TM	P168R035	20100702	p168r035_5dt20100702_z38
5	Landsat 5TM	P168R036	20100702	p168r036_5dt20100702_z38
6	Landsat 7 ETM +	P169R035	20100722	p169r035_7t20100722_z38

In this study it is assumed that changes detected in LULC are the result of changes occuring on the ground changes and are not changes due to changees in sensor charcectiestic.

4.3 Image Preprocessing

Preprocessing satellite images prior to image classification and change detection is important because of radiometric and geometric errors. Preprocessing commonly comprises a number of sequential operations, including atmospheric correction or normalization, image registration, geometric correction, and masking. Also, preprocessing involves combining the single band images to a six band image (i.e. combining all the bands together). In addition, in this study the preprocessing include generating and organizing the data layers that are required for classification and change detection, namely, NDMI which is helps to identify the degree of moister and moister areas within the AOS (Figure 19), NDSI which helps to identify the soil within AOS (Figure 20), NDVI which is helps to identify the vegetation area (Figure 21), TCT (Figure 22), (Campbell, ,2007, p.478-477) , and a training layer. These indices are included to help CART develop the classification schema. The training layer is an empty layer which will be used during the training data collection for the CART classification.
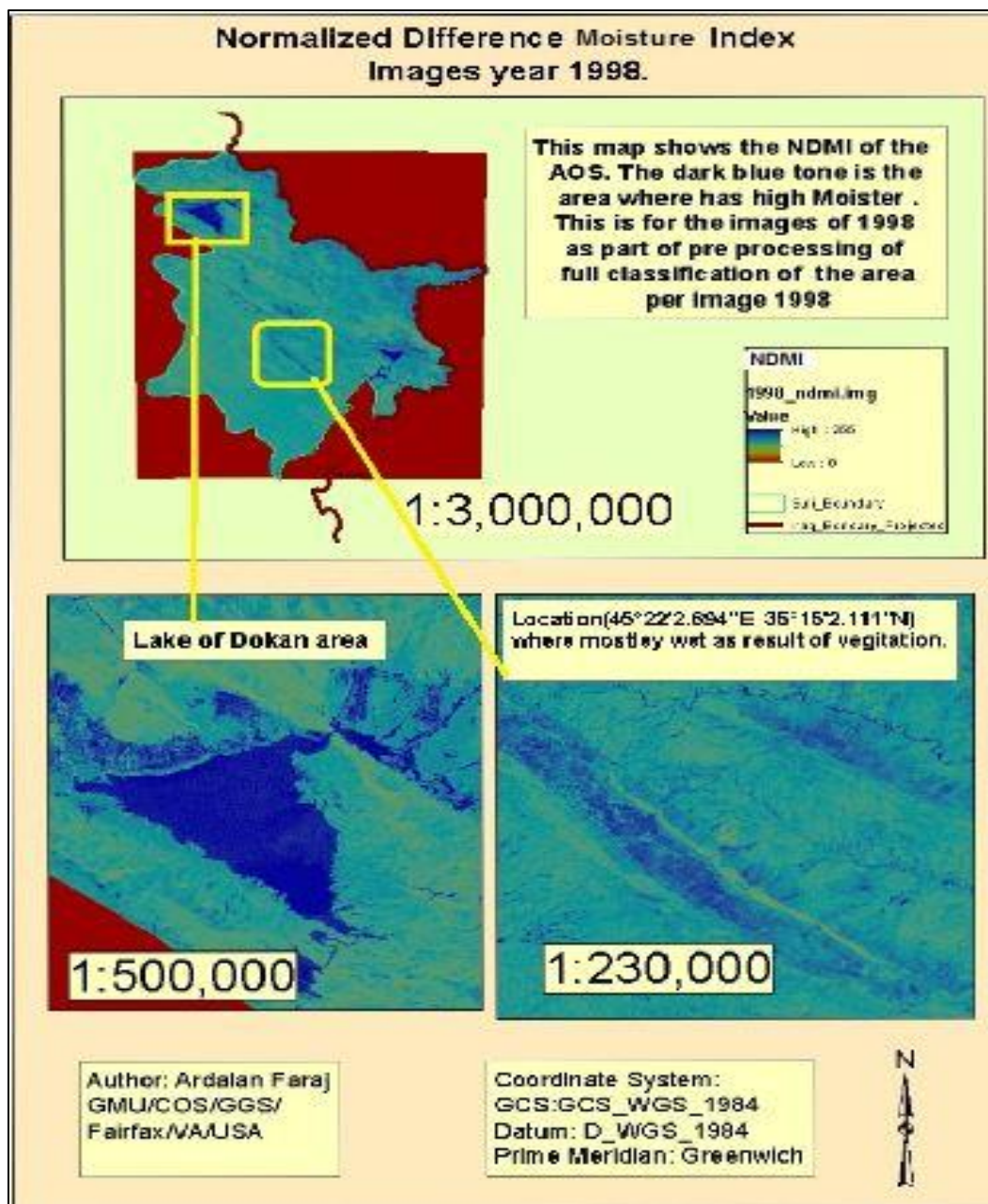
Figure19 NDMI layer based on image 1998.
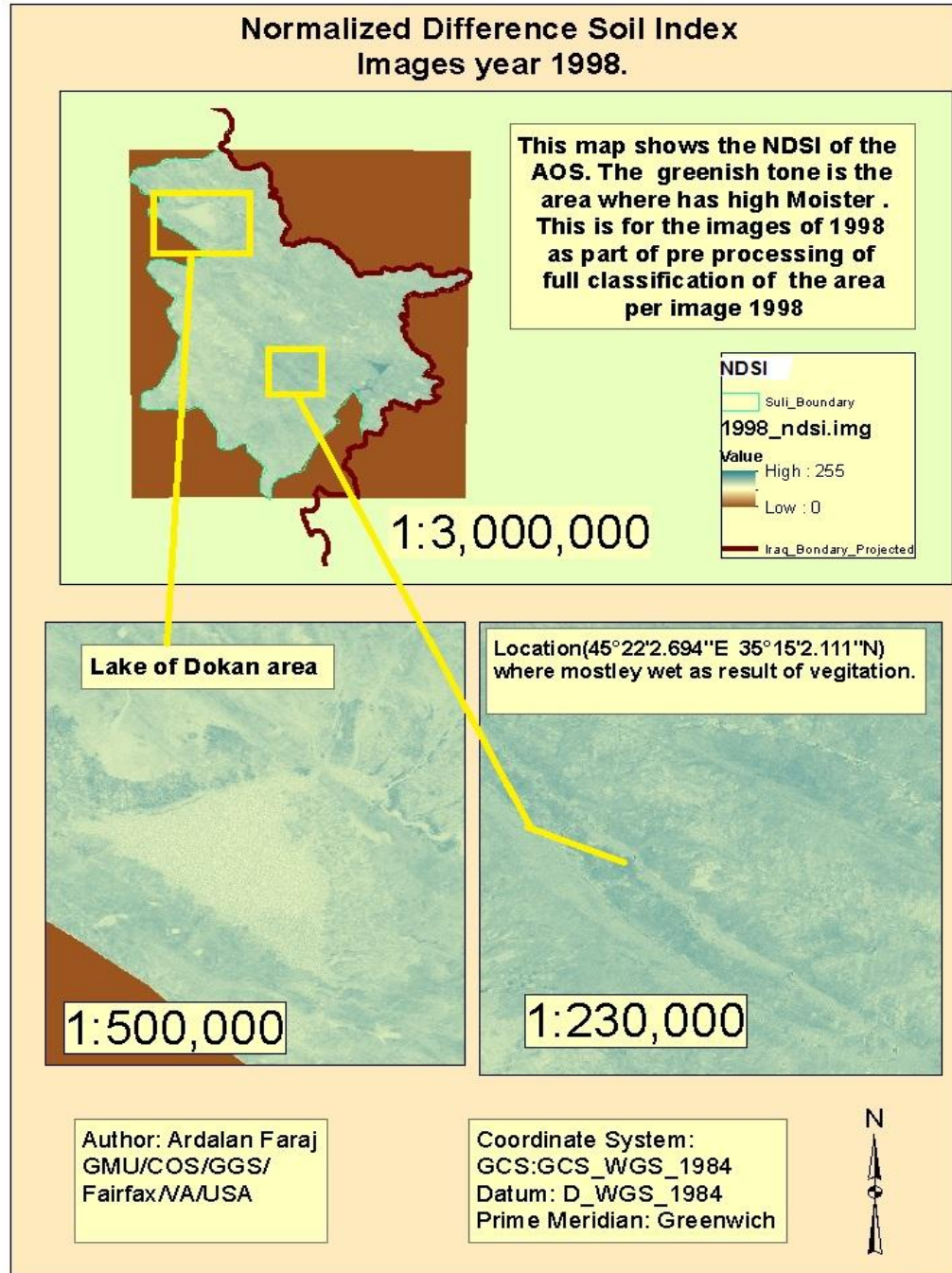
Figure 20 NDSI layer based on image 1998.
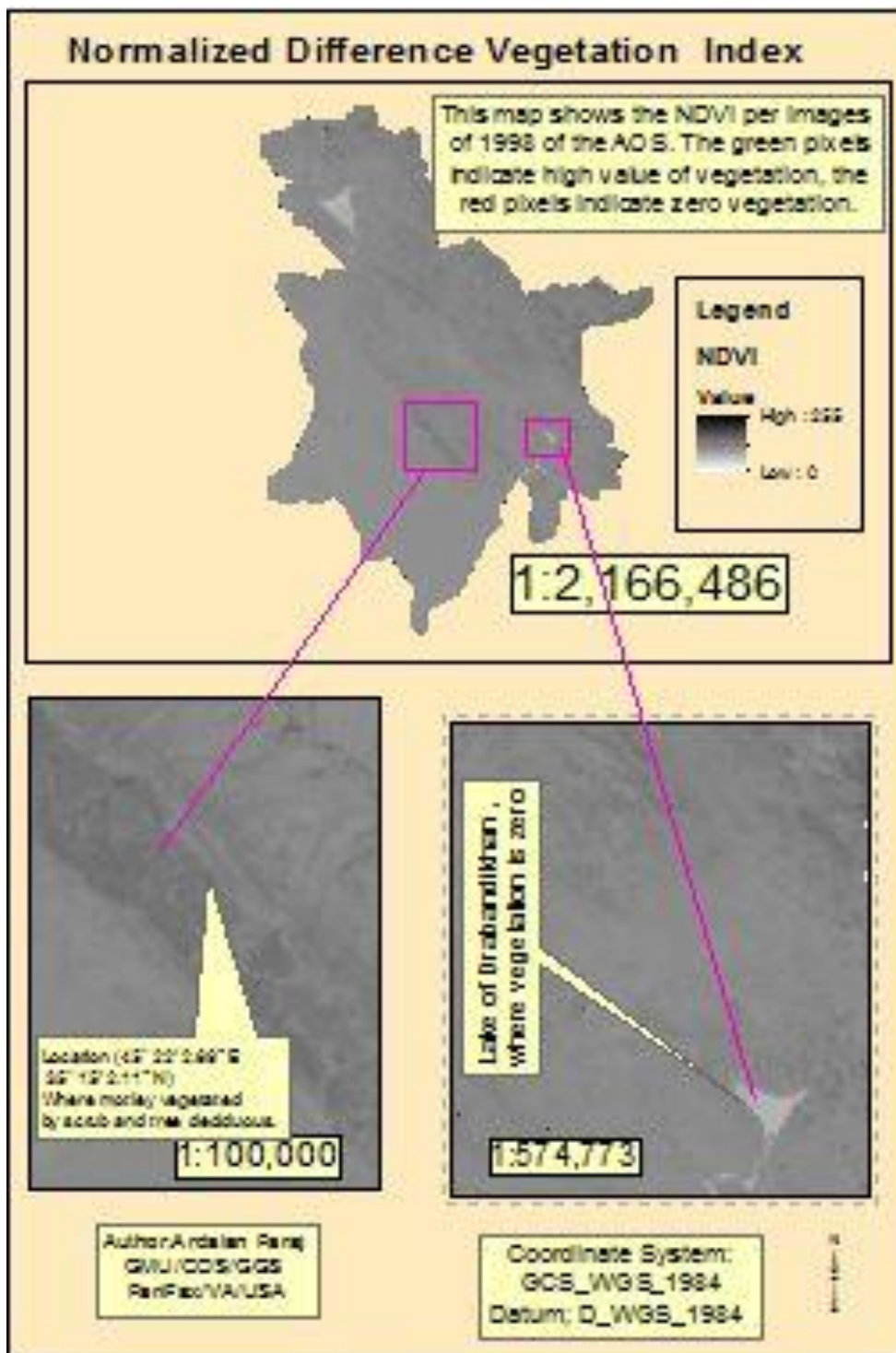
Figure 21 NDVI layer based on image 1998
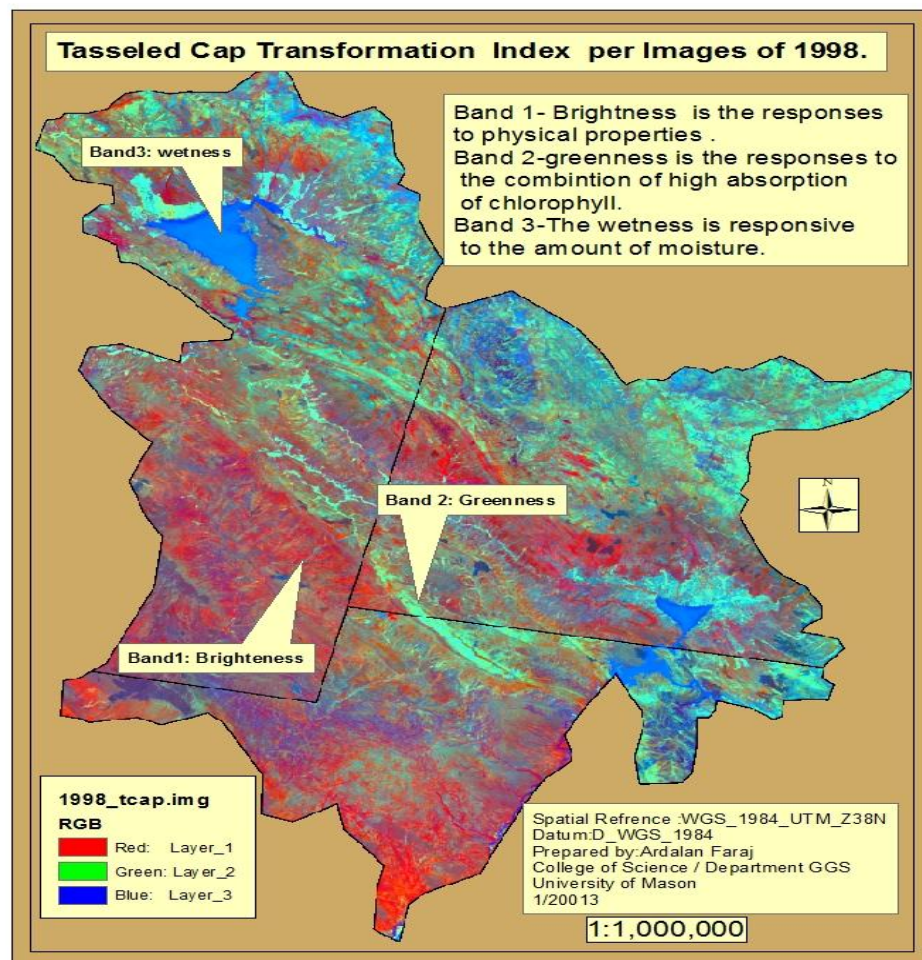
Figure 22 TCT based on image1998 and image 1998.

4.4 Image Classification

The objective of image classification is to assign labels to unknown pixels. The image classification process includes several key pointes, namely are: ground truth and classification schema, extraction training sample (TS), and classification method. USGS LULC schema has been utilized to identify LULC categories, stratify ratio and average per class been considered to extract the training data, also CART and Region Growing was deployed to perform image classification (based on the 1998 imagery). Before beginning to collect training data, it is important to verify that the images correctly georeferenced.

4.4.1 Ground Truth and Classification Schema

Ground truth data are very important in order to identify most accurate land class and create a training sample. In this study open source data such as Google Earth and previous studies, my geological and geographical familiarities with the area, USGS LULC system (Campbell, 2007, p.559-81 ; Anderson, 1976, p.2-22) have been employed to identify the most accurate land classes within the area of study. Per that scheme the land use and land cover categories of focus were: urban, barren, herbaceous /rangeland/ Grass land, shrub / scrub, tree deciduous, evergreen, and agricultural/ crop, water, wetland, and snow. All LULC classes within AOS are fall in the Level I of Anderson classification. However, I considered Level II classification for Forest (Evergreen forest and Deciduous Forest) and for Shrub / scrub. In addition, the definition of the classes

been considered during class selection for example some other classification call grass

land as Range land as , but in fact both definition are close(Table 7).

4.4.2. Collecting Training Sample (Data) and Signature Generation

This include collection data training within the empty training layer which has

been created in preprocessing step and this empty layer must load into ERDAS and the

actual images must load in different viewer of ERDAS, then link both viewers together. I

have scanned the scenes in order to get familiar with possible of the land cover class with

in my study area .After all necessary layers for this step, I collected training data as small

and consistently polygons using AOI tool. I considered stratify ratio and average per class

of the collection for each class. More specifically if a class dominates 50 % of the AOS

then the training samples should be at least 50 % of this class within the AOS samples.

During collecting the training samples I considered only 8 classes namely: grass, barren,

deciduous tree, evergreen tree, wetland, water , snow and scrub ; also excluded AG and

urban , the reason will explain in section (4.4.3.1), therefore the total number of TS are

80 samples and 40 among these are grass and barren and the other 40 from the other

classes.

Table 7 Class name and the description of all classes within the AOS

Class Name	Description \Definition\Property
Evergreen Forest	Trees > 3 meters in height, >25% intermixture with evergreen species that seasonality not lose leaves. Includes both broadleaf and needle leaf species.
Tree Deciduous	Trees > 3 meters in height, <25% intermixture with evergreen species that seasonality lose leaves. Includes Deciduous in the wetland environment.
Scrub\Shrub	Woody vegetation <3 meter in height, with at least 10% ground cover. Includes wetland with woody vegetations < 3 meters in heights.
Grass\herbaceous\Range Land	Upland herbaceous grasses, >10% ground cover, but tree shrub cover is < 10%; including pasture lands.
Barren	Land exposed soil, sand, rocks and has < 10% vegetated cover. Land with minimum ability to support vegetation.
Urban	Developed areas at least have 60 meters wide, land covered by buildings and other man-made structure.
Water	Ocean, seas, lakes, reservoirs, and rivers; it can be fresh or salt water.
Agricultural\Corp	Cultivated crop land, lands covered with temporary followed by harvest and bare soil period.
Wetland\herbaceous	Areas where the water table is at or near the surface for a substantial portion of growing season; vegetated wetland consist of herbaceous.
Ice\Snow	Land areas covered permanently or nearly permanently with ice or snow.

4.4.2.1 Water TS:

Water sample were collected water sample with in Lake Dokan and Lake Darbandikhan, also water pixels were verified by their spectral which the reflection curve goes down in band 3,4,5 from band 1 to 6 and it is dark in tone in landsat (Figure 23).
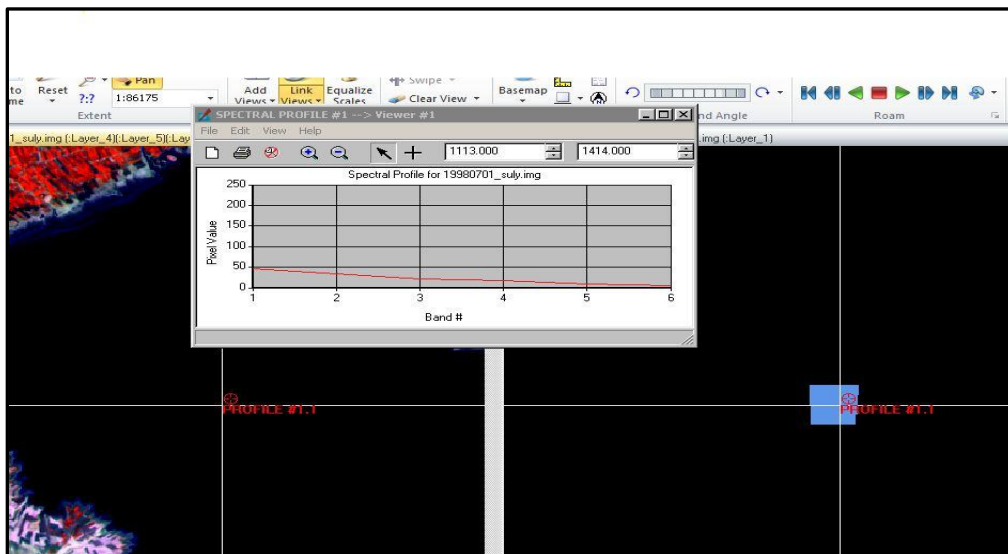
Figure 23Training data of water (left the TS, left image, top SP).

4.4.2.2 Grass /Herbaceous /Rangeland TS

The tone of the grass is white bright in band 3,4,5 , andsmooth in texture; the SP should has high reflection due to high albedo in grass. It has high reflection to all bands from 1 to 5 and its reflection very high in band 4-5, also very birth in tone (Figure 24).
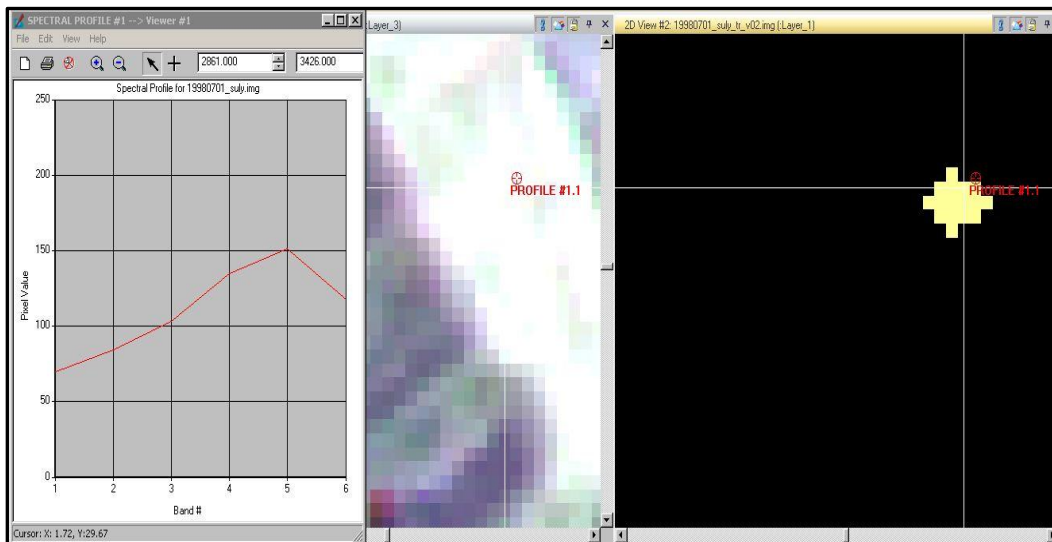
Figure 24 Grass /Herbaceous /Rangeland TS; right is TS, middle is image, left is SP.

4.4.2.3 Barren TS

The barren TS appears as different tones in different locations within the AOS = green or white (Figure 25), with SP that is not too high and medium reflection.
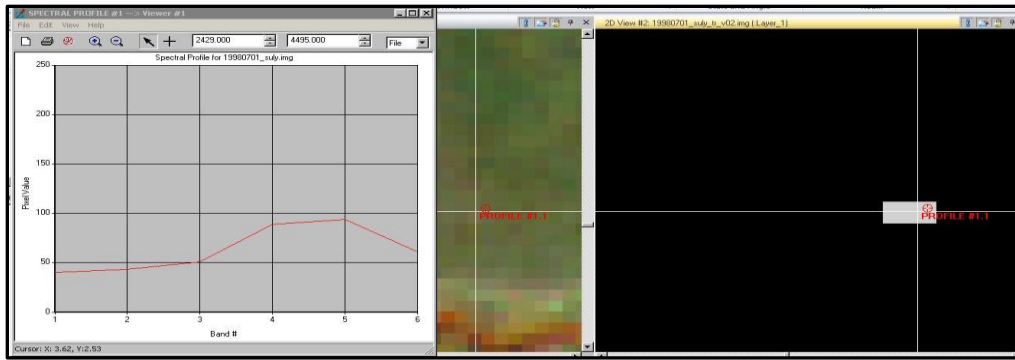
Figure 25 Barren TD (right is TS, center image, left is SP)

4.4.2.4 AG / Crop TS

The AG TS appears as different tones depending on the growth of the AG, in

some area appears as light gray pinkish, in some area as smooth orange, also appears as

very dark blue (Figure 26, center). The manmade shape of AG and crop is a great

evidence of the AG area. Also, the SP of all AG tones is has reflection to bands 1 to 5.

Red SP represents the high growth of AG, olive SP is for the AG which is in medium

stage of growth and visible as dark blue and light green SP is for the light gray pinkish

which in early stage of growth (Figure 26 left).
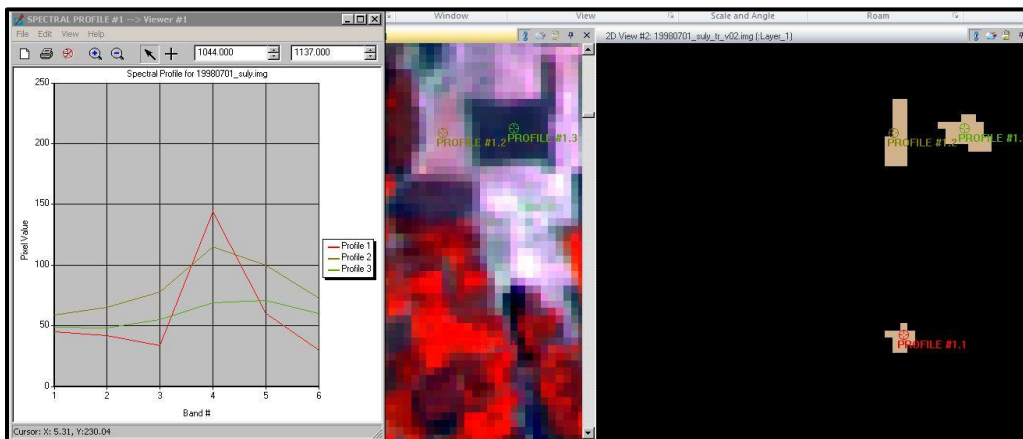
Figure 26 AG TD (right is 3 TS, center 3 different tone of AG, left is 3 SP).

4.4.2.5 Scrub TS

      The scrub within the AOS appears as light orange with texture, and dark green with texture and also it has high reflection (Figure27 center). It has reflection to band 4 and 5 (Figure, 27 left).
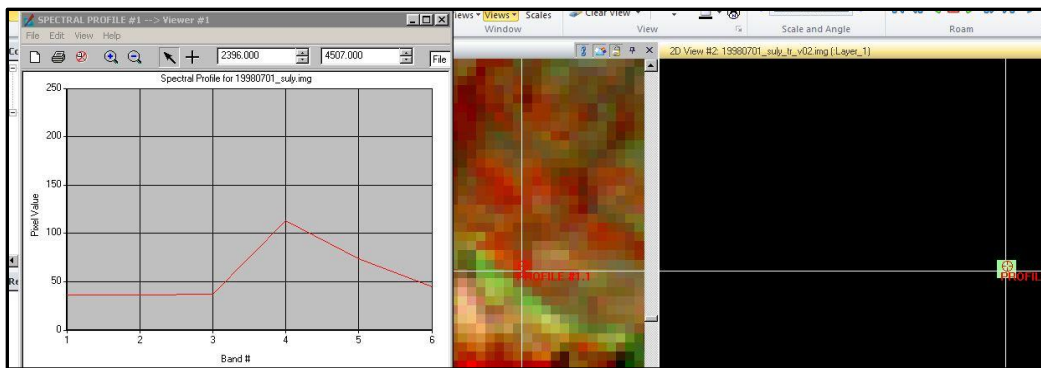
Figure 27 Scrub TD (right is TS, center is image, left is SP)

4.4.2.6 Tree Deciduous   TS:

      The tree deciduous   is appears as dark orange and bright orange with texture with high reflection of SP (Figure 28)
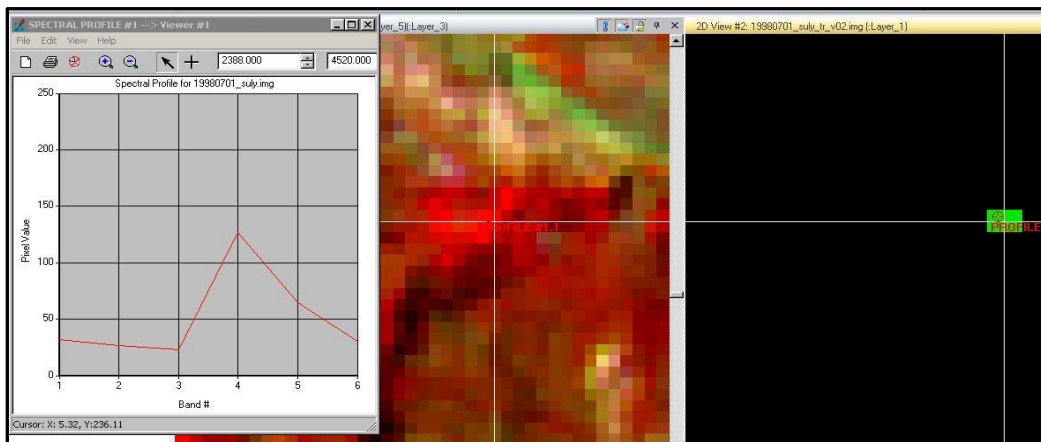
Figure 28 Tree Deciduous (right TS, center is image, and left SP)

4.4.2.7 Evergreen   TS:

The evergreen areas as dark purple in this area, there is not a lot evergreen in the
AOS (Figure 29, center) also has reflection to band 3 and 4. The location of this training
point is Mountains of Goizha north of city of Sulaimaniya.
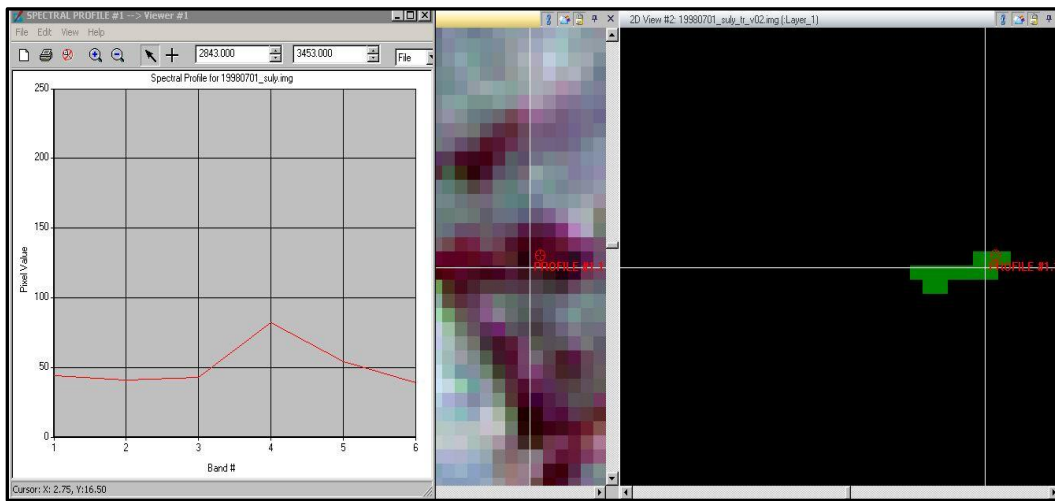
Figure 29Evergreen TD (right is TS center is image, left is SP)

4.4.2.8 Urban TS:

The urban is appear as light purple in band 3, 4, 5 (Figure 30, center) and in some
area appears as gray with geometry shape, The SP is lightly high in band 3 (Figure 30,
left)
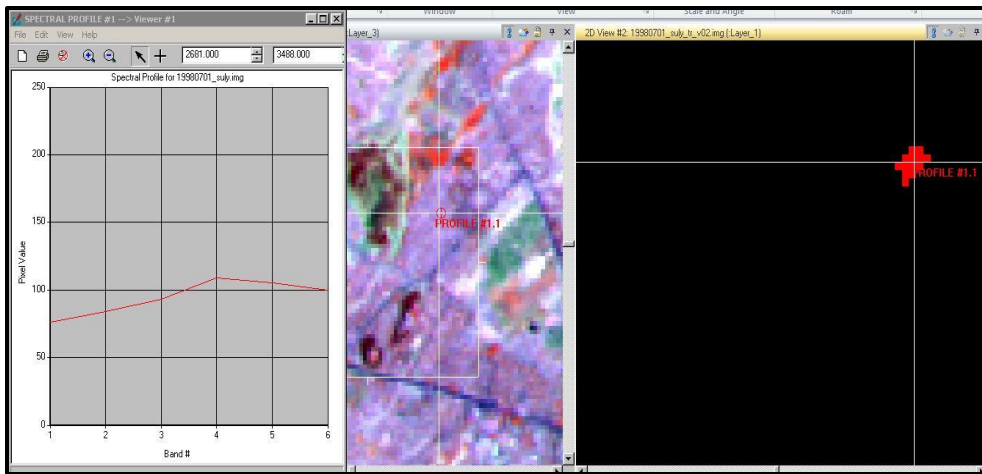
Figure 30 TDs of Urban (right TS, center is image, left SP).

4.4.2.9 Wetland:

The wetland is appear as light blue in band 3, 4, 5 , mostly they appears along the

stream bed (Figure 30, left) , The SP is low in band 3(Figure 30, top center).
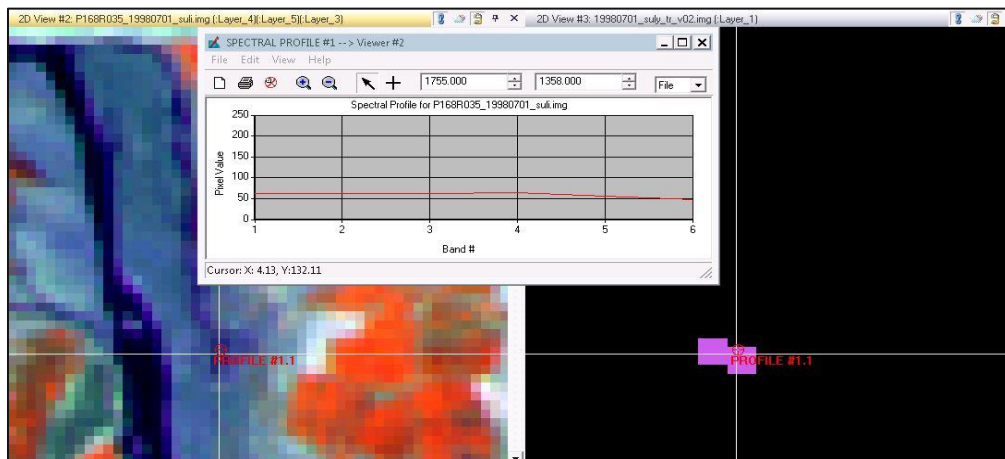
Figure 31 TD of wetland east of lake of Dokan (left is 1998 image, top center is SP

4.4.2.10 Snow:

Snow mostly appears in the winter season; however, there were some permanent snow segments in the 1998 and 2010 images, on high mountains of Qandil, locate in the northeast of AOS in summer time. In the spectral profile of snow it was noted that the snow has slight reflection to bands from (1, 2, 3, 4) as result of the ground and has absorption features to band (4, 5), and not any refraction and absorption from after band 6 (Figuer32).
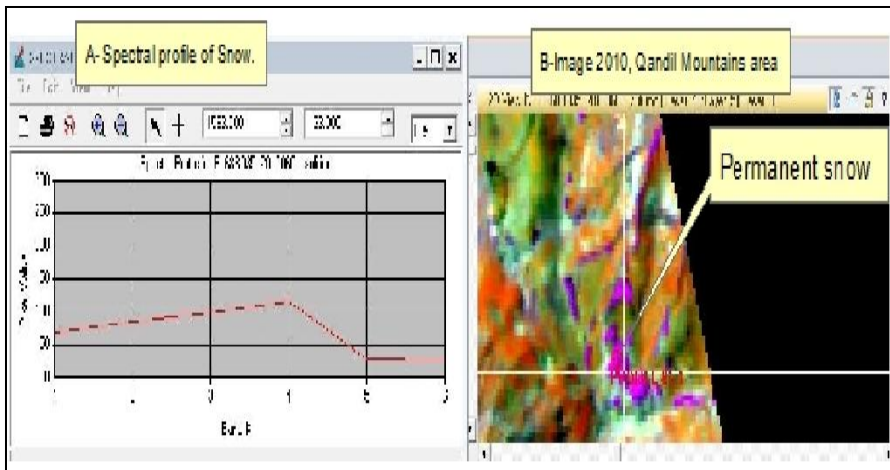
Figure 32 SP profile of snow

4.4.3 CART Analysis and Region Growing

CART and Region Growing were used to develop the LULC map of the AOS. Only urban, and agricultural extracted by Region Growing. These two classes lead to misclassification in CART, and for this reason they were excluded from the CART analysis.

4.4.3.1 CART Analysis

Two variables are needed to run CART; independent variables which have been created in preprocessing step (6-band image of 1998, NDVI, NDMI, NDSI, TCT), and dependent variables which is the training layer containing the TS which been created during preprocessing. Urban and AG are two classes which may lead CART to misclassification due to similarity of urban pixels and barren pixels, as well as due to the similarity between AG pixels and deciduous tree pixels ; consequently, CART has been run twice in order to evaluate its outcome. First, CART was run with TS of the classes

61

(barren, grass, tree deciduous, water, evergreen, wetland, snow, scrub, AG, and Urban).

Then, it was run excluding AG and urban from the training layer.

The CART analysis includes 3 steps:

- Using ERDAS, all necessary data (independent variables and dependent variables) were loaded and NLCD Sampling Tool was run using the following options (Figure 33). After running the tool three files created, namely: 19980701_sulyclip_cart.names which contains filenames and locations of all dependent and independent variables, and whether they are continuous or thematic, and the range of values, 19980701_suly_clip_cart.data which contains all the values for each variable at the geographic location of the dependent variable, and 19980701_suly_clip_cart.test which has values only for points to be used for calculating validation statistics.
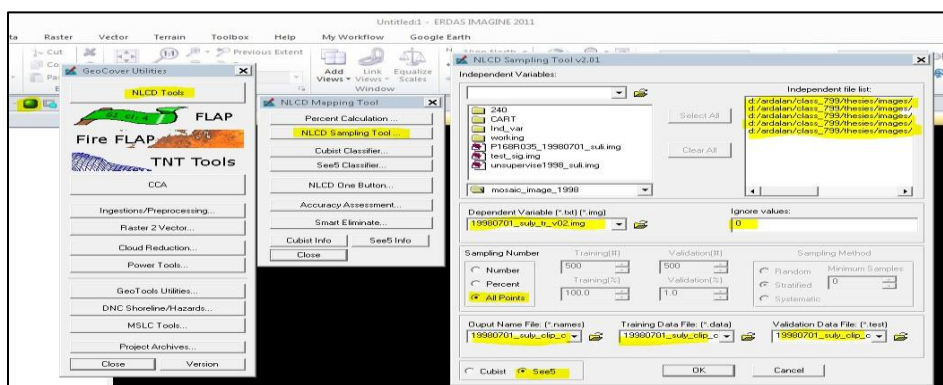
Figure 33 ERDAS 2011 shows steps of using CART

- In the second step the See5 software was run. In this step the data file 19980701_suly_clip_cart.data (which been created in step 1) was used to construct a classifier. The See5 tool was run using the following options (Figure 34). See5 was invoked and a decision tree was constricted (see Appendix 1). Figure 35 shows one the decision tree as the result of the classification process.

- In the third step the See5 Classifier from ERDAS 11 (Figure 33) was used. Here the input was the clip_cart.names, which was created in step one, a default tree, and the mask layer was checked. The mask input is the original training layer, which was created in preprocessing and contains TS. The output was suly_v01. As was stated earlier, CART was run twice, first with all TS and then excluding AG and urban, thus two results obtained from CART (Figure 36, Figure 37).
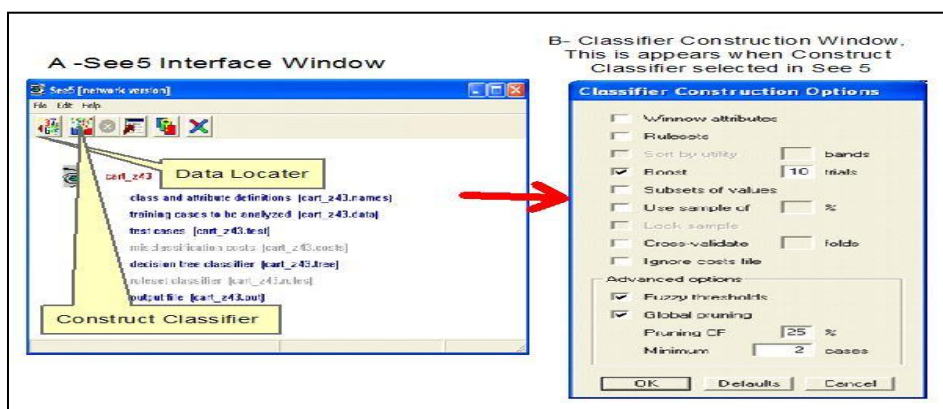
Figure 34 See5 Interface

Figure 35 Explanation of trail 0 of the decision tree; rectangles represent bands and the circles are represent LULC classes after the CART made its decision based on the independent variable and depend variable. Also, See5 classifier uses gain ratio criterion to select splitting attributes (http://www.rulequest.com).
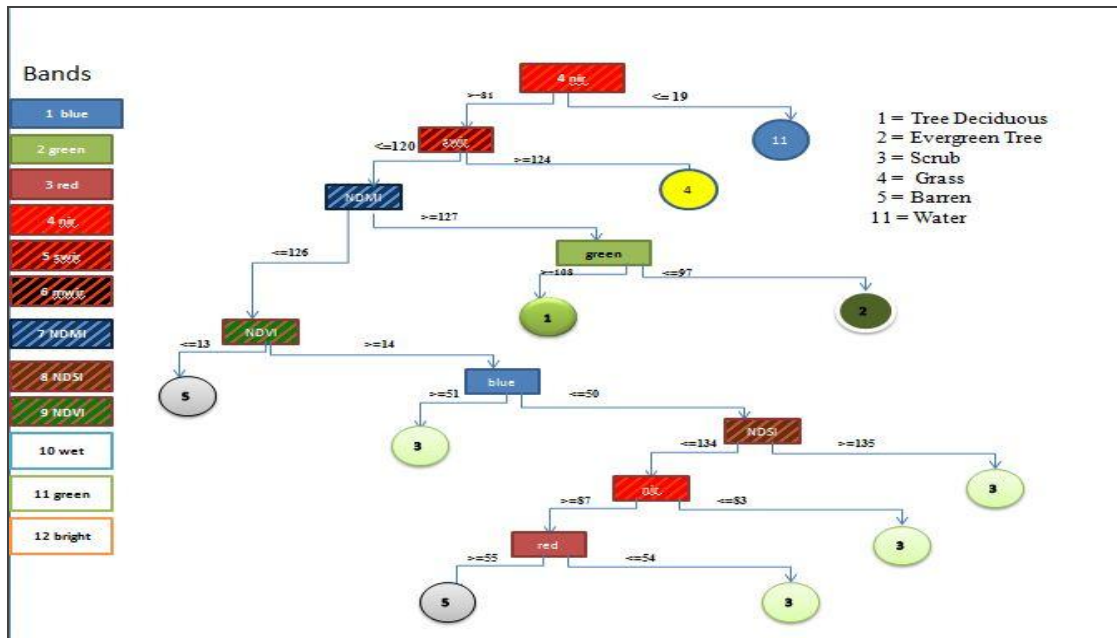
A comparison of the CART classification outcomes with original 1998 image reveals some significant issues. The outcome with AG and Urban contain some misclassifications, for example a stream bed classified as urban instead of barren or wetland (Figure 38 C), also some other pixels from other segments of the image were classified as urban while they were barren. Other errors include misclassification of urban, the main roads and some pixels over the city of Sulaimanyia been called AG instead of Urban and Barren (Figure 39 C). Some of them not AG but they are vegetated such as grass land and scrub. For these reason, the outcome which included AG and Urban not been used for the LULC classification of this study.
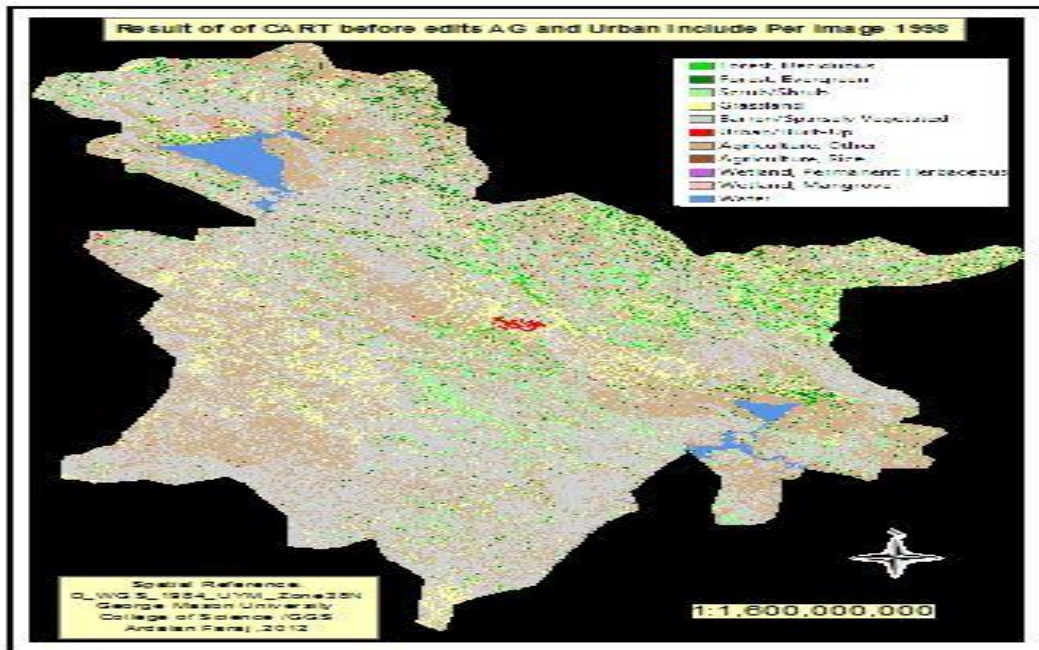
Figure 36 Outcome of CART including AG and Urban; this result has not been used, for LULC, as result of misclassification.
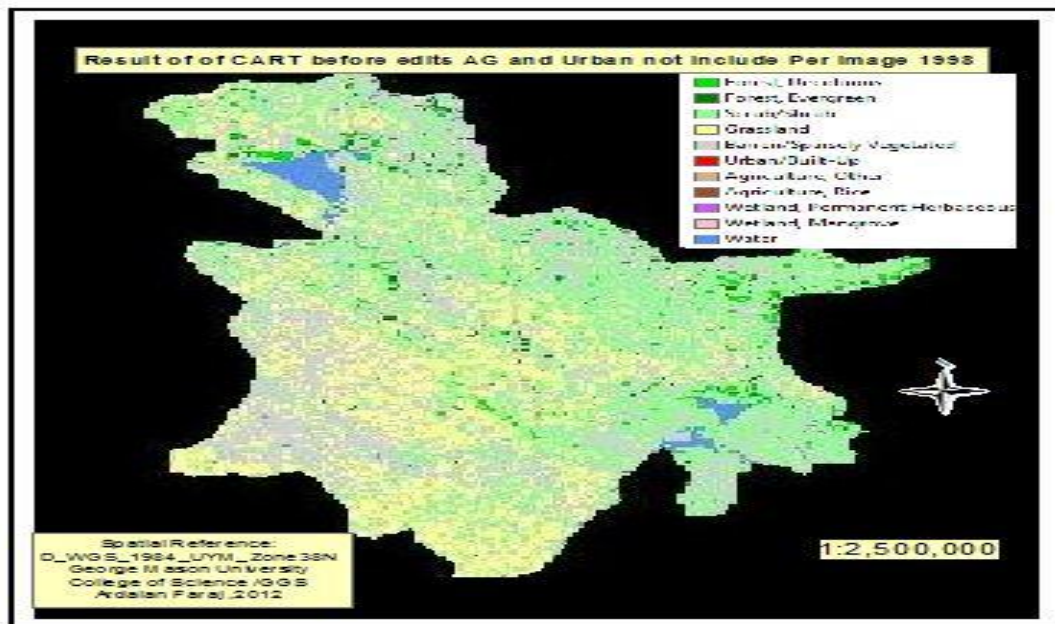
Figure 37 CART outcome, AG and Urban not include. This result selected for LULC of the area.
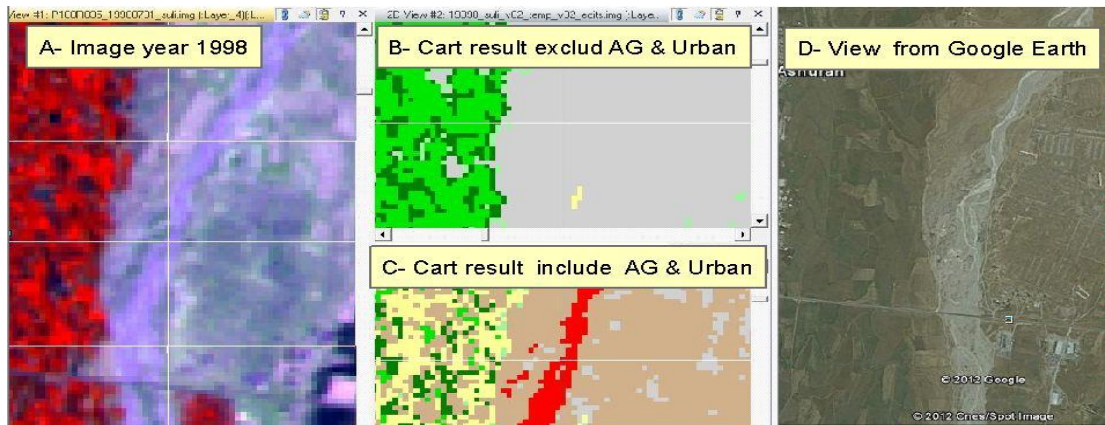
Figure 38 example of misclassification. A- is image of 1998, B- Is CART outcome excluded AG and Urban, C- Is CART result included Urban and AG, D- is Google Earth view for same spot used for verification
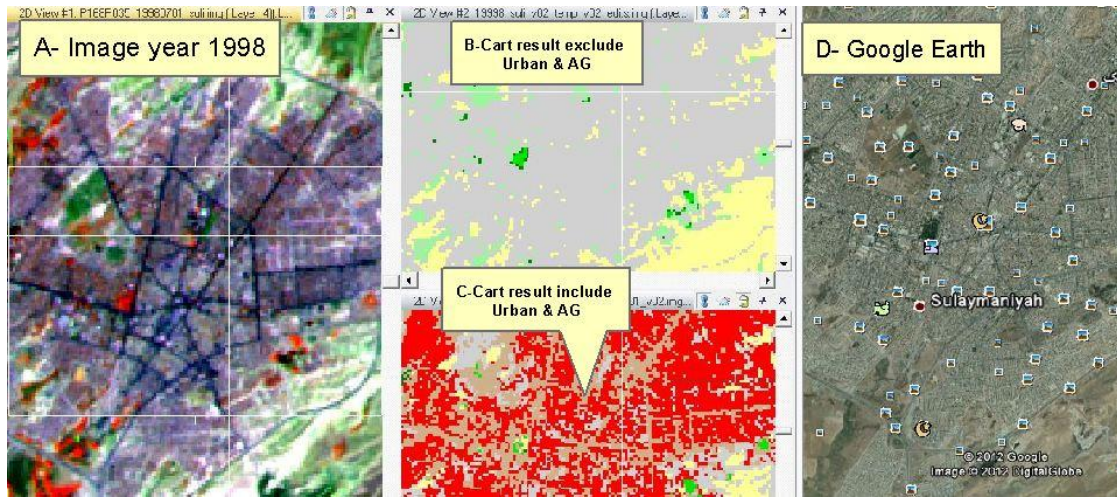
Figure 39 example of misclassification. A- is image of 1998, B- is CART outcome excluded AG and urban, C- is CART outcome included AG and Urban, D- Is a Google Earth view for that spot. This spot is over the main city of Sulaimanyia.

As result of these misclassification and in order to extract and classify most accurate number of all classes (in particular AG and Urban), the outcome with the exclusion of AG and urban were used for LULC of the AOS and these two classes been extracted and mapped by region growing, which is explained in section(4.3.3.2).

Excluding AG and urban does not eliminate the misclassification; there are some

other error sources, for example cloud and shadow of clouds. However, the images used

for this classification contain only a small area of cloud, which is on overlap part (Figure

40). In some LULC studies clouds area not classified and they are classified as cloud

layer because classifying them may lead to misclassifications. However; there is a

possibility to classify the cloud area to LULC classes if the cloud areas are small, and this

could be done based on the feature extents or based on the features around the cloud (for

example if the area above and bottom of cloud is forest evergreen it is possible to classify

the cloud area to forest evergreen after verification from another source.

Figure 40 (left) shows cloud and cloud shadows and, Figure 40 (middle) shows a

classification result of a cloud area and the shadow of cloud; the cloud itself was

classified to evergreen (which is wrong) and the shadow of cloud been classified to

water. CART classifies all shadows including terrain shadows and cloud shadows to

water as they are dark pixels. Figure 41 shows the terrain shadow which was classified

incorrectly. These errors were assigned the correct classes after a manual verification

using another source (e.g., Google Earth) and based on the features and classes around

them.
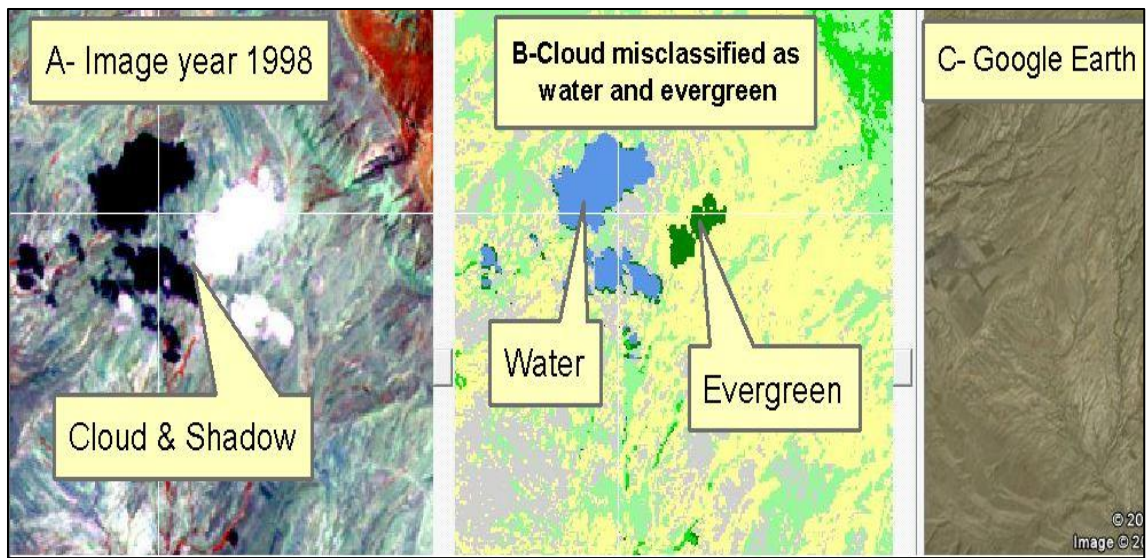
Figure 40 Example of wrong classification of cloud area; A: Image of 1998, B- CART result cloud classified as evergreen and shadow of cloud classified as water, C-Google Earth.
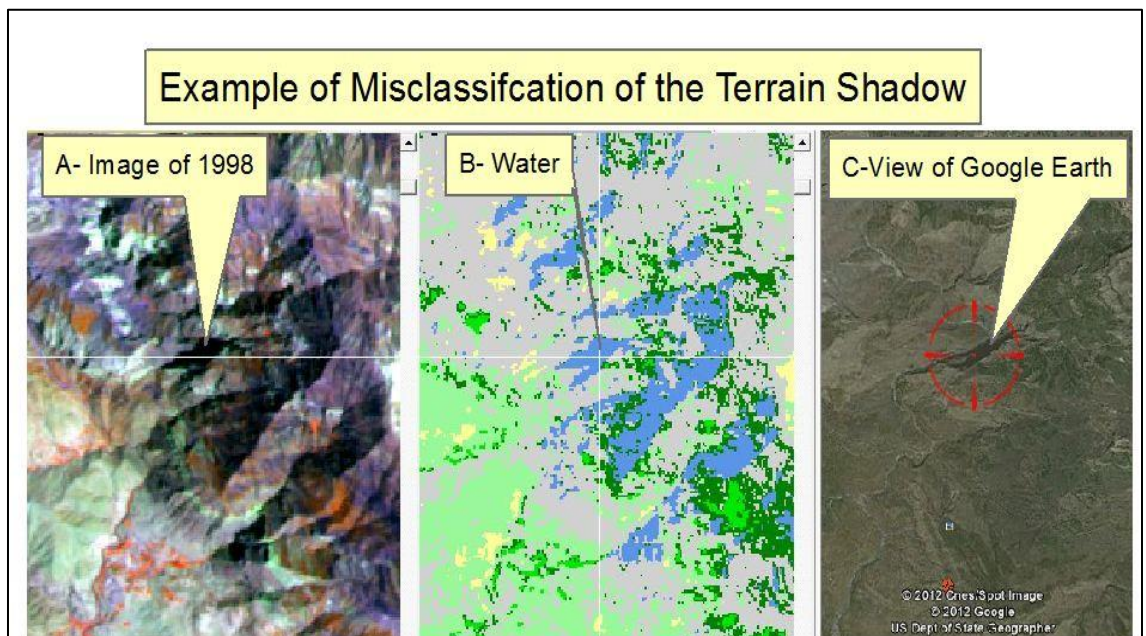
Figure 41 A- Image of 1998, B- Classification, C- View of same spot from Google Earth.

4.4.3.2 Region Growing

Region growing was used to extract the AG and urban based on the image 1998. Several factors were considered to identify these classes: shape, pattern, texture. Also for small areas of AG and urban Google Earth was used to delineate the exact area of AG and urban. Small urban areas are not visible in the Landsat images; however, roads, linear features, irrigation areas and pasture land sometime indicate small urban areas in rural areas. For capturing urban areas the maximum zoom level was used. Also, band 1, 3, and 5 were useful for identify the urban areas (Figures 42 and 43); all urban areas were extracted and mapped by region growing. The AG areas appeared as different tones within the area of study based on the stage of growth. Using band 3, 4, 5, AG was visible as dark gray, light gray, and orange to red tone; however, the geometric pattern and location were useful to identify the agricultural area (Figure 42, 43). All urban ad AG areas have been collected by region growing and they were merged with the first outcome in order to map the area to all LULC classes as a thematic map layer (Figure 44).
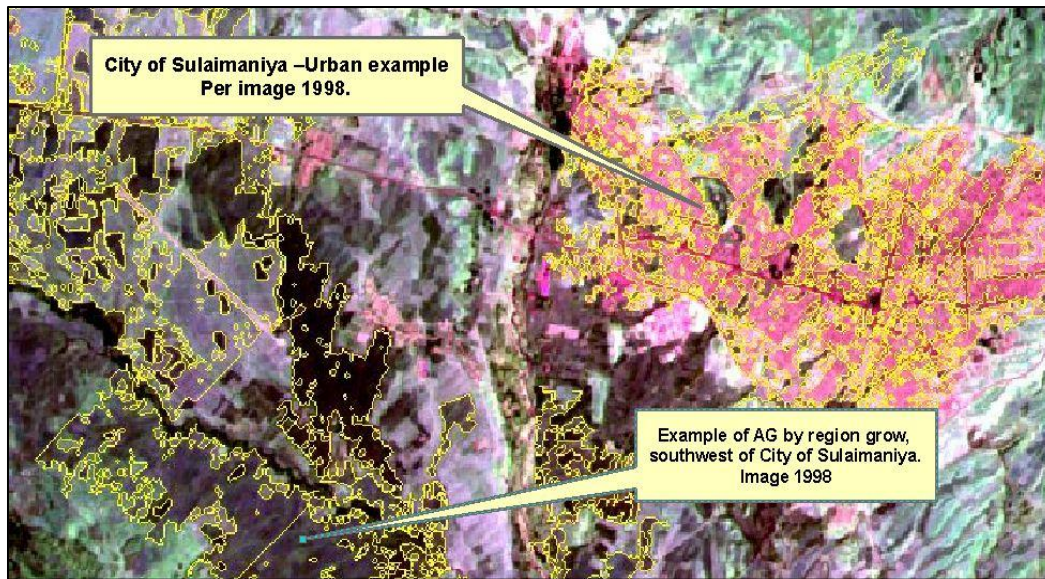
Figure 42 Example of AG and Urban by Region Grow near City of Sulaimaniya
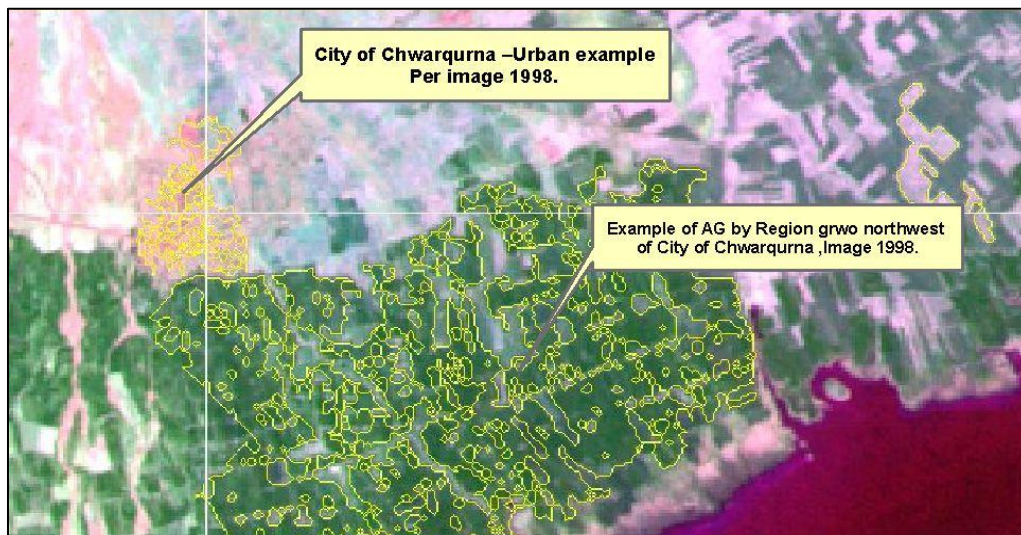
Figure 43 Example of AG and Urban near city of Chwarqurna per image 1998
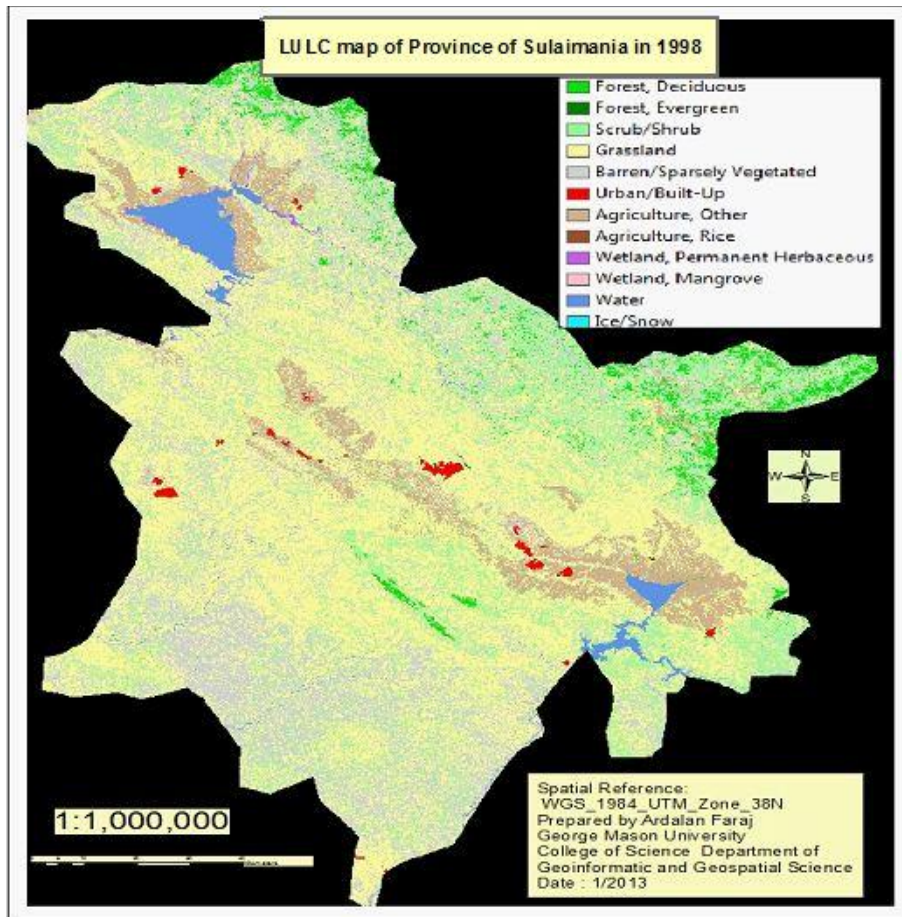
Figure 44 LULC map of AOS per images of 1998

4.5 LULCC

In order to identify differences in land cover between the late- and early-date era images from the same path/row, a semi-automated change detection algorithm (CCA) was applied. In order to deploy CCA both spectral images (1998 and 2010) should be partitioned by applying an unsupervised classification method, in this study IOSDATA method was used for clustering both images to 1000 clusters. Lower numbers of clusters (200, 300, and 700) were applied but they lead to speckles within the change layer.

The CCA compared the spectral image of 1998 with ISODAT layer of 2010, as well as spectral image of 2010 with Isodata layer of image 1998. CCA estimates the likelihood of change values, or measures, between the early- and late-date imagery. This analysis was performed on the individual scenes.

The likelihood of change layers were produced were manually threshold, to include areas of actual change and exclude areas of non-change. The outcome of this process was a binary file identifying both areas of change and non-change for the entire study area. The final step of the change detection is classifying the change area to an exact class (Figure 45) which was created by running CART; the LULC layer of 1998 was used as the dependent variable and 2010 spectral image was used as independent variable with a mask of changed area only, so only the change area is classified. The spatial distribution of the change layer represents a significant change around Dokan and Darbandikhan lakes., Significant changes within the urban area and around the cities including the main City of Sualimania, and around the burned areas (e.g., near the Tasluja Cement Factory) was also noted.

After a review of the result of the change detection it was noted that the CCA did not extract all urban changes, in particular near the cities (Figures 45, 46, and 47), therefore the region growing method was applied to map all urban areas. Figure 49 is final outcome of this process which was produced by overly a change layer (Figure 45) over a LULC map of 1998 (Figure 44).
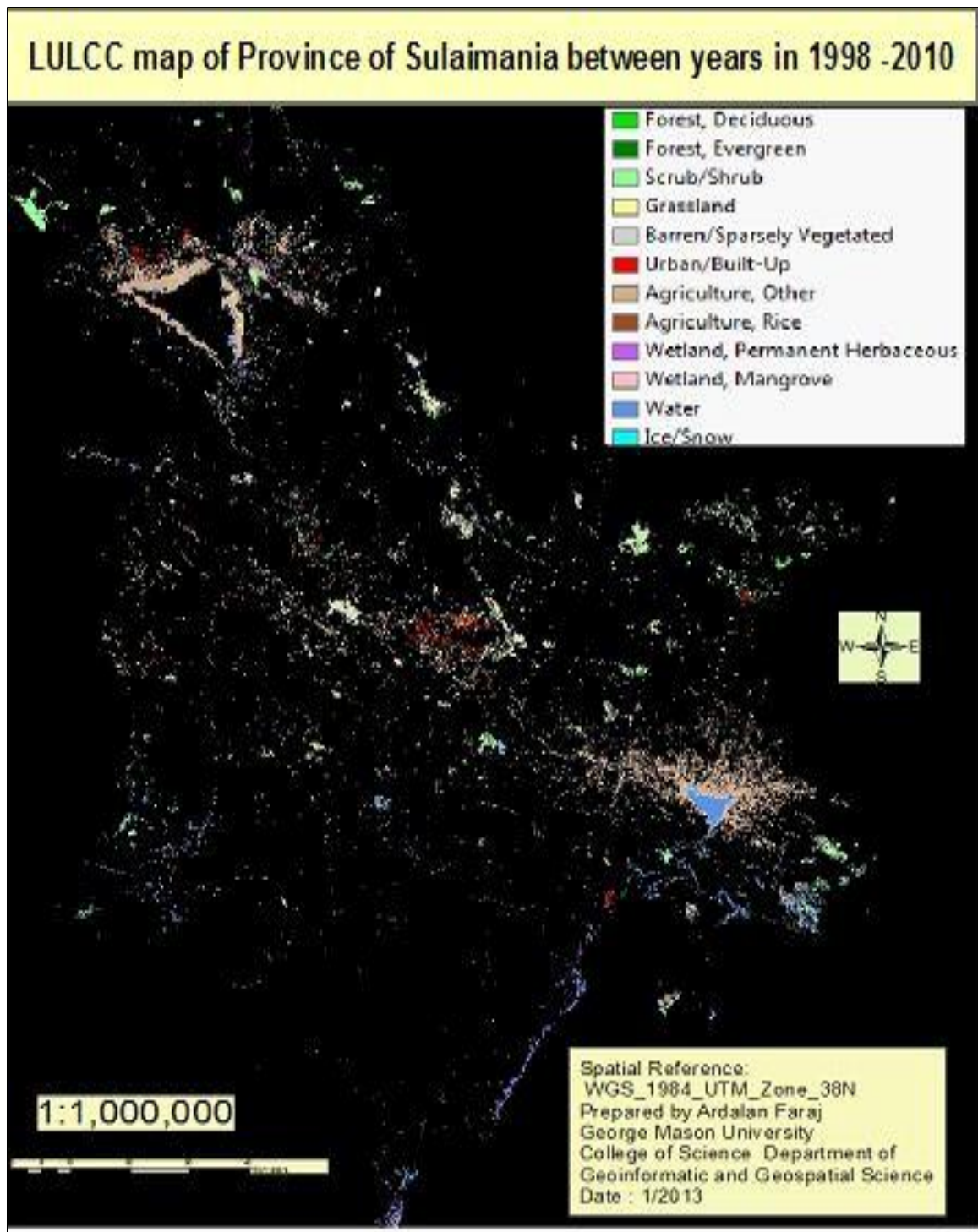
Figure 45 LULCC map of the area of study between years 1998 and 2010; this only the change layer.
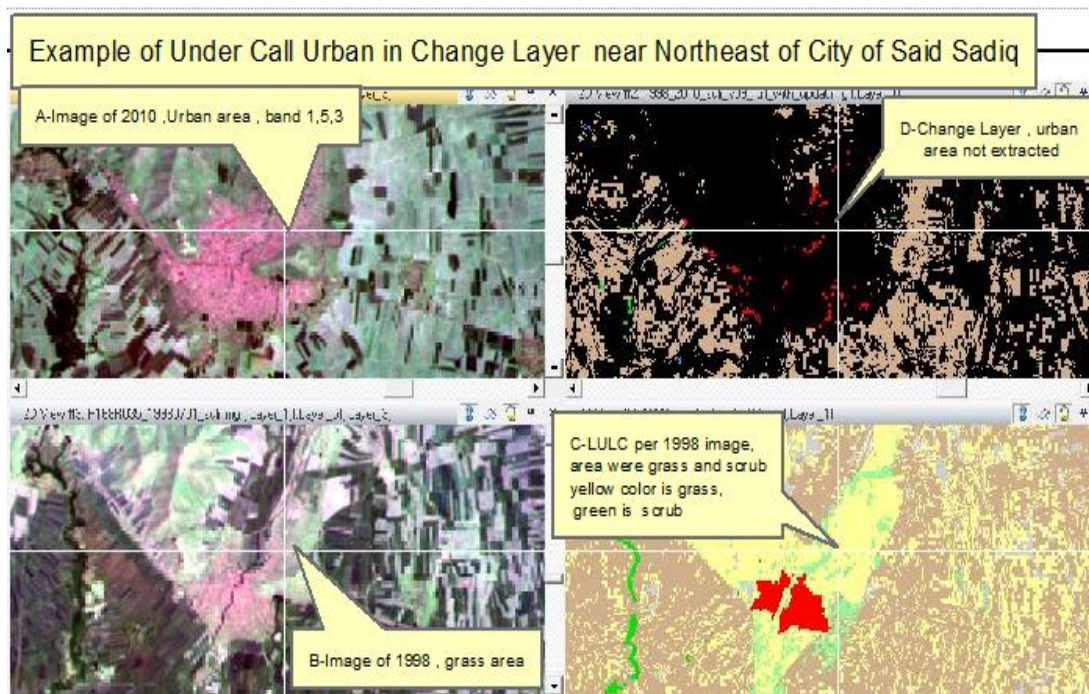
Figure 46 Example of under call urban in change layer near Northeast of City of Said Sadiq
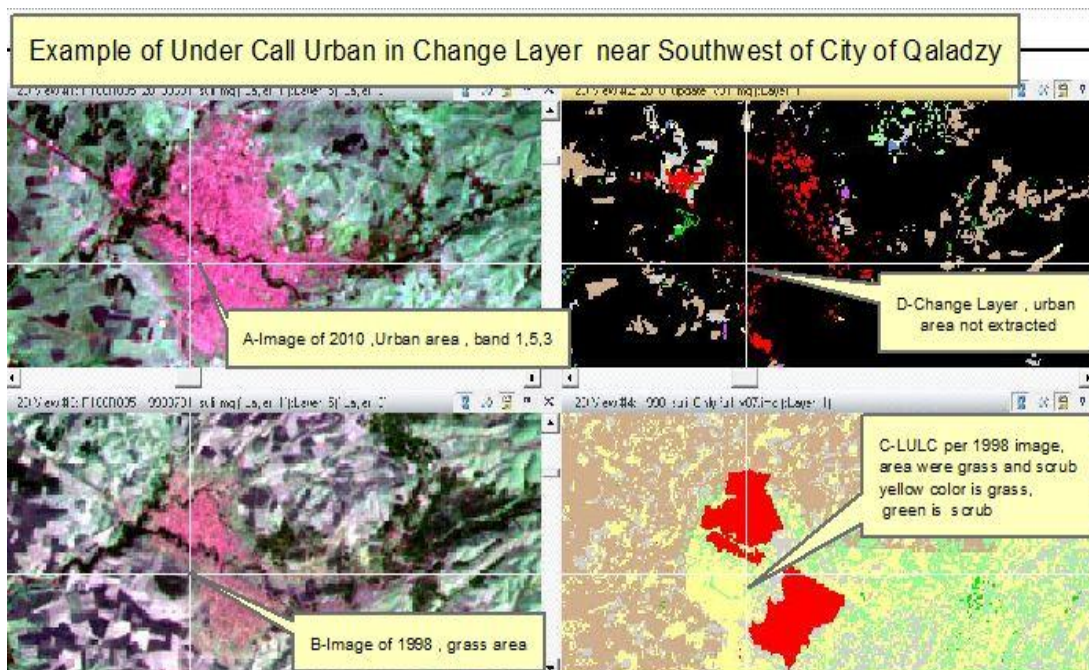
Figure 47 Example of under call urban in change layer near southwest of city of Qaladze
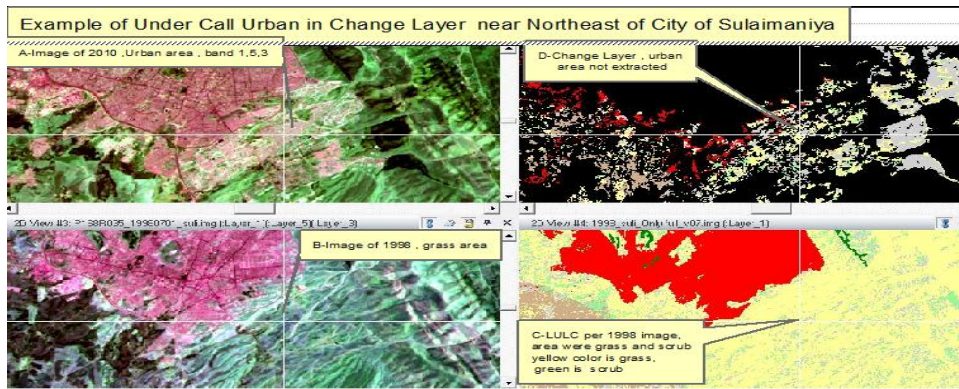
Figure 48 Example of urban under call near Northeast of City of Sulaimaniya
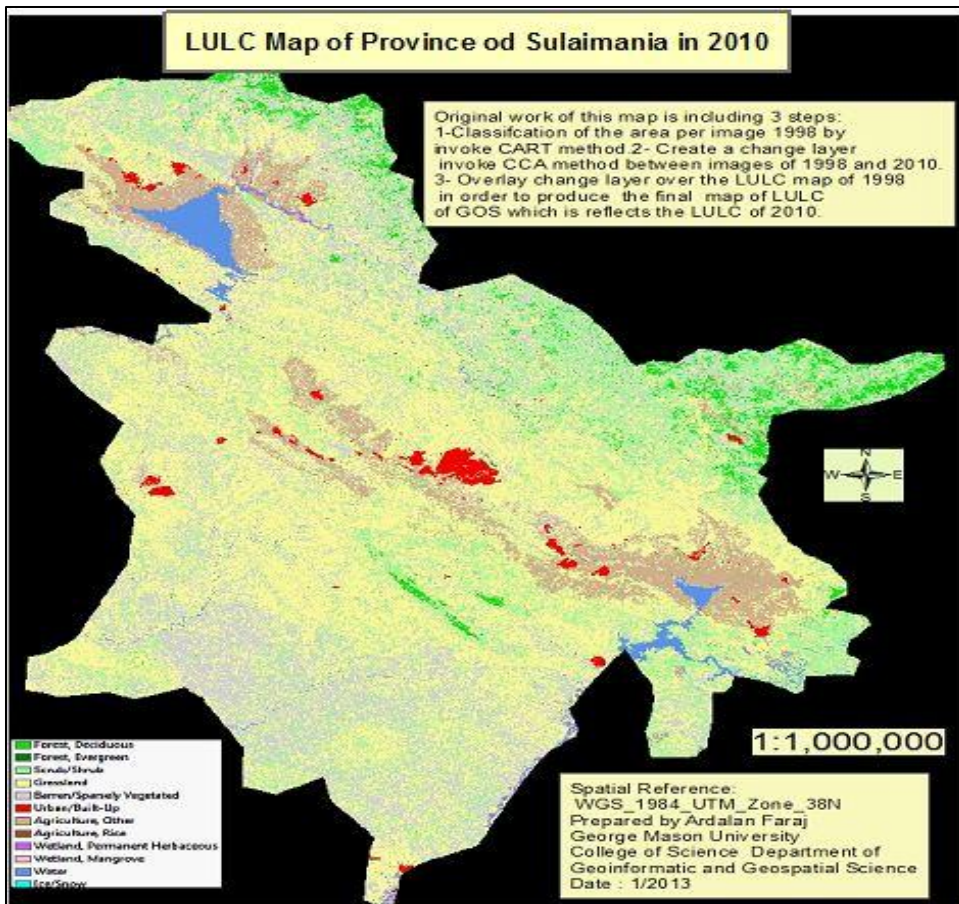
Figure 49 Final LULC map of the AOS

4.6 Validation (Accuracy Assessment)

Unfortunately, even after careful preprocessing, residual geometric and radiometric errors may exist (Jensen, 2005). For example, residual geometric error may cause pixels still to be in an incorrect geographic location. Similarly, carful atmospheric correction will not result in perfect relation between percent reflectance measured on the ground and percent measured by an optical remote sensing system for the same geographic area. As result, a validation process required.The validation process in this study involves several steps, namely:

- Identifying nature of the thematic accuracy assessment problem

- Identifying method of thematic accuracy assessment

- Computing total number of observation required in the sample

- Identifying sampling schema (design).

- Obtaining ground truth for the observation locations.

- Error matrix creation and analysis.

4.6.1 Nature of the thematic accuracy assessment problem:

The accuracy assessment problem in this study amounts to validating the LULC classes with in the AOS. Per the final thematic layer of this study based on image 2010, there are ten LULC classes (Table 7). The accuracy assessment process is dependent upon two types of sampling unit's points and areal (Stedman and Czaplewski, 1998).

Points sampling units have no areal extent .When conducting remote sensing-related accuracy assessment, analysts typically select one of three types of areal units: individual pixels (e.g. Landsat TM 30 x 40m pixels), Polygon, and fixed area plots (Jensen 2005); there is no consensus on the ideal type of sampling units, therefore my chosen sampling in unit is an aerial polygon. My chosen methods use sample polygons within the area of study (Figure 17). The sample size is based on multinomial distribution, and the sample distribution based on stratified random sampling. This is usually done by a random process stratified by classes and validated against reference data such as Rapid Eye or Google Earth (Campbell 2007, 392-403).

4.6.2 Thematic accuracy assessment:

Two methods that may be used to validate the accuracy of a remote sensing – derived thematic map:

- **Qualitative confidence** -**building assessment** which involves the visual examination of the thematic map associated with overall area by domain experts to identify any visible errors, such as urban areas in water bodies or unrealistic classes on the top of mountains. This method has been applied to LULC thematic map per the 1998 image (Figure 44), change layer map between images of 1998 and 2010 (Figure 45), and final LULC thematic map from 1998 to 2010 (Figure 49), to find visible errors. As was mentioned in section 4.3, issues such as cloud areas were classified as

77

water, and terrain shadows were classified as water, were corrected based on other open source data, and my knowledge of the AOS.

This method was specifically applied to wetland areas and snow areas were not cover by any of the validation polygons. Per (Jensen, 2005) if the thematic map seems reasonable, then the analyst may proceed to statistical confidence measurement to conduct final validation. In this study major issues ere not been identified, therefore the statistical confidence measurement has been applied to validate all the LULC classes within the AOS.

- **Statistical measurement method** is subdivided in to two types (Stehman, 2001): The first type is model -based inference, which is concerned with the estimation of errors of the remotes sensing classification process that generate thematic map. The second one is Design-based inference which is based on statistical characteristic of a finite population based on sampling frame. Some common statistical measurements include producer's error, consumer's errors, overall accuracy, and kappa coefficient of agreement. This type of statistical measurement has been applied to the validation of LULC classes with in the AOS.

4.6.3 Computing the observation required in the sample

This step is involves the number of observation per class. While the final thematic map of the AOS contains multiple classes, a multinomial distribution method is invoked

to determine the number and size of the validation sample to assess the classification

accuracy. The Sample size (N) derived from a multinomial distribution is based on

equation (Equation 2), (Tortora, 1978, Congalton and Green, 1999):

Equation 2 Sample size for validation

$$N = \frac{B\ \text{II}_i(\ 1 -\ \ \text{II}_i)}{b_i{}^2}$$

Where II*i* is the proportion of population in the ith class out of class K, b is the

desired precision, B is the upper (*a/k*) x100th percentile of the chi square (x^2) distribution

with one degree of freedom and k is number of classes and *a* is precision.

For the validation of this study the desire precision is 15% and the level of

confidence is 85% which is stander for many LULC mapping product; therefore the

value of B which is determine from x^2 table with one degree of confidence and 1- (*a/k*) i

= 5.695 (Jensen, 2005). Based on equation (2), the proportion of each class and the

sample size of each class have been determined; the total of the sample size and

observation number is a proximately 177 samples (Table 8),

Table 8 shows a summary of the observation samples result as follows:

Column A is represent LULC classes; column B represent value of pixels of

each class, column C represent proportion of each class , column D is represent number

of each sample for each class, and the Value of Chi2 in the table is = (1-B16)/B14. For example:

The proportion of class 1 is given by B3/B13,

The N value of class 1 is given by B18*C3*(1-C3)/B16^2.

This calculation is applied to all classes in order to gain the final N value (177).

Table 8 Number of Polygon samples for validation within the AOS

	A	B	C	D
1				
2	Class	Total Pixels	Proportion	N
3	1 Tree deciduous	455258	0.02367568	5.850699
4	2 Tree Evergreen	2100	0.00010921	0.027639
5	3 Scrub	3647809	0.189704211	38.90736
6	4 Grass	8717505	0.453353619	62.72704
7	5 Barren	4390354	0.228320245	44.59567
8	6 Urban	211869	0.011018242	2.758111
9	7 Agriculture	1419690	0.073830941	17.30772
10	9 Wetland	40031	0.002081811	0.525833
11	11 Water	344153	0.017897668	4.44902
12	12 Snow	161	8.3728E-06	0.002119
13	Total	19228930	1	177.1512
14	number of classes (k)	10		
15	Level of confidence	0.85		
16	Precision	0.15		
17	chi2 value	0.085		
18	B	5.695		

4.6.4 Identifying sampling schema (design).

It is impossible for analysts and scientist to visit every pixel or polygon in the remote sensing-derived classification map to assess its accuracy assessment (Jensen 2005), therefore the total sample size (N) and the number of samples is required per class (strata) were computed in the previous section (4.5.3). Following Jensen, the location of

the sample must be selected randomly without bias, because any bias may affect the statistical analysis of the error matrix and may result in an error or under-estimation of the true accuracy of the thematic map. There are five types of sampling designs used to collect ground reference test data for assessing the validation of remote sensing-derived thematic map (Congalton and Green, 1999), namely: random sampling, systematic sampling, stratified random sampling, stratified systematic unaligned sampling, and cluster sampling.

For this study Stratifies Random Sampling was invoked because many remote sensing analysts prefer this method (Jensen, 2005). A strata is create by extracting only polygons (or pixels) associated with a specific class. Sample locations are then randomly distributed throughout the geographic strata. ERDAS 2011 was used to created sample size and sample location (Figure 17). After determining the real world location (x, y) of the samples and after identifying the source of ground truth (ground reference) for each sample, validation is conducted for each sample.

4.6.5 Obtaining ground truth for the observation locations.

For the ground reference of the sampling or to determine label (e.g., scrub, grass, etc.) of each sample Google earth, Bing Map and ESRI base map of the world, and Rapid Eye Imagery were used during the validating. All sample polygons in this step were labeled based on the most recent open sources by using Arc Map. During processing each

of each sample two calls are considered: "truth" and "accept". Truth is the represents the most accurate classification of the area contained within the sampling polygon; typically this means the class that is observed to cover greater than 50% of the polygon area. Accept call is the class that is most likely to have been called if the true class was not available.

4.6.6 Error matrix creation and analysis:

In order to correctly perform a classification accuracy assessment, it is necessary to systematically compare two source of information, the first one is pixels or polygon in remote sensing-derived classification map and the second one is ground reference test information. The relation between these two sets of data is usually summarized in an error matrix. The error matrix compares, on a category-by-category basis, the relation between known reference data and the corresponding results of an automated classification (Lillesand et al., 2004).

There are two ways to evaluate error matrix of validation first one is descriptive statistical and the second one multivariate analytical statistical methods (Jensen, 2005).

4.6.6.1 Descriptive Evaluation of error matrix

This method evaluates the overall accuracy of the classification map and it is determined by dividing the total correct pixels (sum of the major diagonal) by total number of pixels in the error matrix. The columns of this matrix represent the ground test reference information, the rows correspond to the classification that are generated from the analysis of remote sensing data, and diagonal cells represent the correct pixels or polygons that is assigned to correct class (Table 9). This statistic indicates the probability of reference pixel being correctly classified and is a measure of omission error, per (Story and Congalton, 1986) this is called producer's accuracy because the producer of the classification is interested in how well a certain area can be classified.

Table 9 Overall Accuracy

Class name	Dec. For	Shrub/S	Grasslan	Barren	Urban	General	Water	Class'n Totals	Comm. Totals
Dec. Forest	2	2	0	0	0	1	0	5	40%
Shrub/Scrub	1	27	9	0	0	1	0	38	71%
Grassland	0	0	60	5	0	2	0	67	90%
Barren	0	4	0	38	0	2	0	44	86%
Urban	0	0	1	0	2	0	0	3	67%
General Ag.	0	1	3	1	0	12	0	17	71%
Water	0	0	0	1	0	0	2	3	67%
Validation Totals	3	34	73	45	2	18	2		
Omission Totals	67%	79%	82%	84%	100%	67%	100%		81%

Overall Accuracy of the LULC map (2010)of POS — Ground Reference

LCLU Classes of POS

Total Observations: 177
Overall Accuracy: 81%
Cohen's Kappa: 0.7364

4.6.6.2 Multivariate analytical statistical methods:

These methods have been used to statistically evaluate the accuracy of remote sensing-derived classification maps and error matrix. (Congalton and mead, 1983; Hudson and Ramm, 1987; Foody 2002). These methods are appropriate for analyzing remote sensing data because such data are discrete rather than continuous, and also binomially or multinomial distributed. These methods include K Coefficient of Agreement also called *Kappa Analysis* and *Kappa Analysis*.

Kappa Analyze was introduced to the remote sensing community in 1981 and was first published in remote sensing journal in 1983 (Congalton, 1981; Congalton et al., 1983). It measures accuracy between the remote sensing-derived classification map (in this study LULC map of the AOS) and the ground thrust data by the major diagonal of the error matrix, and the chance agreement, which is indicated by the row and column total refer to as marginal (Rosenfiled and Fitzpartick-Lins, 1986 ; Congalton 1996). The original expression of Rosenfiled and Fitzpatric-Lins was invoked to conduct Kappa Analysis of both Overall Accuracy curacy and the Fuzzy Accuracy. Equation 3 is representing Kappa value.

Equation 3: Kappa equation which based on original equation of Rosenfiled and Fitzpatric-Lins

$$k = \frac{N \sum_{i=1}^{k} x_{ii} - \sum_{1=1}^{k} (x_{i^+} \times x_{\cdot i})}{N^2 - \sum_{1=1}^{k} (x_{i^+} \times x_{\cdot i})}$$

where:

k is the Kappa value

k is the number of raw (e.g., land-cover classes) in the matrix

x_{ii} is number of observations in row $_i$ and column $_i$

x_i+ and $x+_i$ are the marginal totals for row $_i$ and cloumn $_i$

N is the total number of observations.

According to Landis and Koch (1997) a Kappa value > 0.80 represent a strong agreement or accuracy between the classification map and the ground reference, a Kappa value between 0.40 and 0.80 is considered moderate, and a Kappa value < 0.40 represent a poor agreement.

Fuzzy analysis is another method of **Multivariate analytical statistical techniques** accuracy assessment methods based on fuzzy sets which allow consideration of the magnitude of errors and assessment of the frequency of ambiguity in map classes. The concept of fuzzy sets was introduced by Zadeh (1965) to describe imprecision that is characteristic of much of human reasoning. Gopal and Weedcokc (1994) were the first to suggest the fuzzy logic be used to introduce real world fuzziness into the classification. Fuzzy sets provide a quantitative approach for dealing with vagueness in complex systems. A primary difference between fuzzy set theory and classical set theory concerns membership functions. In classical set theory, each object or element is either a member

of a set or it is not (Woodcock, 1999). Accuracy assessment methods based on fuzzy sets

allow consideration of the magnitude of errors and assessment of the frequency of

ambiguity in map classes. In fuzzy accuracy map labeled to five category scale instead of

wrong or right. However, Congalton and Green (1999) introduced methods to incorporate

fuzzy logic into an error assessment using fuzzified error matrix, the first method

involves accepting $\pm$ class along diagonal in the error matrix, this assumes that the data

represent a continuum or range; the second method by Conglaton is using the fuzzy logic

during the phase when the ground reference information is obtained and compared with

the remote sensing-derived classified map result (LULC map). The second method of

Conglton been used in this study. As been mentioned it is impossible to visit all locations

in the real world, therefore high-resolution images, Google earth and other open source

imager been used to verify the classes. Table (10) represents the Fuzzy accuracy of the

LULC classes of the AOS. The result of the Fuzzy Analysis is 86%. The Kappa based on

Fuzzy analyze is 0.8071 indication of (Landis and Koch, 1977).

Table 10 Fuzzy Accuracy of the LULC map of the AOS

	Class name	Dec. For	Shrub/S	Grasslan	Barren	Urban	General	Water	Class'n Totals	Comm. Totals
	Fuzzy Accuracy of the LULC map (2010) of the POS						Ground Reference			
	Dec. Forest	3	0	1	1	0	0	0	5	60%
	Shrub/Scrub	0	34	4	0	0	0	0	38	89%
	Grassland	0	6	58	2	0	1	0	67	87%
LULC classes of the POS	Barren	0	0	0	41	1	2	0	44	93%
	Urban	0	0	1	0	2	0	0	3	67%
	General Ag.	0	1	3	0	0	13	0	17	76%
	Water	0	0	1	1	0	0	1	3	33%
	Validation Totals	3	41	68	45	3	16	1		
	Omission Totals	100%	83%	85%	91%	67%	81%	100%		86%

Total Observations: 177
Fuzzy Accuracy: 86%
Cohen's Kappa: 0.8071

CHAPTER FIVE

Result, Discussions and Evaluation, Summary and Conclusion

5.1 Result

5.1.1 Result of LULC classification

The LULC classes used in this study are based on Anderson Classification System (USGS Schema) Level I and II, which is designed for remote sensing data. In addition the classification is based on the elements of image interpretation namely: image tone, image texture, shadow, pattern, association, shape, size, and site. Based on these elements, the image of 1998 was used to distinguish and introduce the most accurate classes, and as a result ten LULC categories were identified. These categories include evergreen forest, tree deciduous, scrub\shrub, grass\herbaceous\range land, barren, urban, water, agricultural\crop, wetland\herbaceous and ice\snow (Figures 44 and 49). The description of these categories was presented previously in (Table, 7). Also, Table 11 shows the area of each class within the AOS per image 1998. Based on this result, the grassland is a main class in the AOS which extends over 8017.5 2 km^2, and the second class is a barren land which extends 3899.4 km^2, and total vegetation (evergreen, tree deciduous, scrub, and agricultural land) extends over 4906.06 km^2. The total area of the AOS based on the result of this study is 17305.9 km^2 which is more than the original total

area by 282 km^2. This is less than 2% of the original area of AOS, and is probably as result of the shape file of the boundary of the area. This error dose not affects the result of LULC type and the change detection (more likely additional areas have been classified).

Table 11 Result of LULC per image 1998

Class Code	LULC Class	Area_Sq_Km
1	Forest, Deciduous	441.437711
2	Forest, Evergreen	1.177200829
3	Scrub/Shrub	3284.774614
4	Grassland	8017.532348
5	Barren/Sparsely Vegetated	3899.423747
6	Urban/Built-Up	78.42155525
7	Agriculture, Other	1178.67053
9	Wetland, Permanent Herbaceous	25.73641813
11	Water	378.5276667
12	Ice/Snow	0.202500143
	Totall of Area	17305.90429

5.1.2 Result of LULCC (change between 1998 and 2010)

The results of the CCA showed that the areas subjected to change were only 656.415 km^2. These areas have been classified by using CART between the 2010 image as independent variable and the LULC of 1998 as dependent variable. Also the change layer was used as mask so that only the change area to be classified. The classification of the change area is seen in Figure 45 and Table 12. Based on this result, agricultural, urban and barren land increased significantly.

Table 12 Result of classification of the change area only

Value	Class Name	Area_sq.km
1	Forest, Deciduous	20.76663299
2	Forest, Evergreen	0.88740141
3	Scrub/Shrub	68.56930893
4	Grassland	41.93826662
5	Barren/Sparsely Vegetated	85.71523616
6	Urban	115.7329838
7	Agriculture, Other	272.3890327
9	Wetland, Permanent Herbaceous	18.5733295
11	Water	31.69805035
12	Ice/Snow	0.14490023
	Total	656.4151428

The classification of the change layer has was merged and overlaid on LULC result of 1998 in order to derive a final LULC map that reflects the situation in 2010 (Figure 49, Table 13).

Table 13 Classification result of 2010 after being overlaid on a change layer from the 1998 results

Class Code	Class_Name	Area_sq.km
1	Forest, Deciduous	409.73
2	Forest, Evergreen	1.89
3	Scrub/Shrub	3283.03
4	Grassland	7845.76
5	Barren/Sparsely Vegetated	3951.32
6	Urban/Built-Up	190.68
7	Agriculture, Other	1277.72
9	Wetland, Permanent Herbaceous	36.02
11	Water	309.73
12	Ice/Snow	0.0034
		17305.8834

For in-depth detailed analysis, both LULC maps of 1998 and 2010 were compared by conducting Bivariate Analysis which involves the analysis of two or more variables in order to find the relation between them. In this work, the variables are the ten

LULC classes and the relation aims to find which class changes to which class in a twelve-year period. For this purpose and based on Bivariate Analysis Model was run. In this model area of all classes of LULC map in 1998 were compared with area of all LULC classes of map in 2010. The result of this model was a layer with an attribute table containing ninety cases of change between all classes. Some of these cases were small local changes which are as a result of errors, and they have been deleted from the attribute table of the changes. Table 15 within Appendix 2 shows the full result of changes with the ninety cases of change. Each case represents a specific change from class to another class. This table describes the original classes of new urban and so on for all other changes. All these changes are related to either natural factors or human factors which are explained in the discussion section within this chapter

5.1.3 Result of Accuracy assessment of LULC map of the AOS

Generally, classification accuracy could be affected by lack of fine details, and the resolutions of images used due to the need of making generalizations. To insure the right usage of land cover maps and any statistics derived from such analysis, errors must be quantitatively explained (Hussein, 2009). A common method used by researchers to assess classification accuracy is the use of an error matrix (Lilesand et al, 2004). The standard form for reporting site specific error is an error matrix (Campbell, 2007).

In this study, first the *Qualitative Confidence Accuracy* method was applied to result of each step. Then, accuracy assessment was carried out and a statistical confidence

measure calculated to conduct final validation. The overall accuracy was 81% and Cohen's Kappa was 0. 73 (Table 9), and the result of the Fuzzy Accuracy analysis was 86% with Cohen's Kappa of 0.80 (Table 10)

5.2 Discussions, Analysis and Evaluation

5.2.1 Evaluation LULC schema used in this study

The result of the LULC classification of image 1998 was based on dry-season imagery and the Anderson classification schema level I and II. Based on that schema, the AOS was classified to ten classes (Figure 44, Table 11), and the number of resulting classes is comparable to other studies. For example, the LULC map prepared by UN (Chapter 2, Section 5) has only six LULC classes (Figure 9). Another example, the map created by GLCF/UMD (Figure 10) lacks urban space and more open shrub land is seen around the lake of Dokan, for this area should be mostly crop land (AG) in different stages of growth as seen in this study. Also, according to GLCF/UMD the dominant LULC classes along the Iranian border are grass and GA, but it should be deciduous trees and scrub. According to the result of this study all these areas along the Iranian border have more appropriate LULC classes.

The classification result from this study could be used as a tool to conduct further more in-depth studies. For example, identifying, types of orchards and vineyards among the vegetated areas, identifying types of crops within AG areas, and identifying types of urban land such as residential or commercial. In addition, this research is could be further

expanded by applying level III and IV of Anderson classification system if high-resolution imagery is available.

5.2.2 Evaluation CART Result

Despite of CART advantages which have been explained in (chapter 2, section 8) there are some issues regarding to the performance of CART, including:

- Classifying terrain shadow as water and evergreen, which require manual analysis editing. This issue occurred in this study within small segment of the mountainous areas, and has been reclassified to the correct class. Time and seasons have a role in increasing the importance of this issue.

- Classifying cloud and cloud shadow to other classes which occurred in the south of Darbandikhan city. The issue of cloud coverage is always editable by creating a mask and classifying it based on different images or open-sources data if the cloud coverage is not extension.

- Classifying scan lines area to different classes. LANDSAT 7 images have a scan line, but it was not used in the classification of the 1998 image.

As was stated in the previous chapters, CART may not be the best method for classifying urban and agricultural lands because of the similarity of urban pixels with barren land, and the similarity of AG pixels with pixels of other vegetation classes. Therefore, in order to avoid misclassification in this study, both urban and AG lands have been extracted by a region-growing method

5.2.3 Evaluation CCA

The advantage of using CCA was explained in chapter 2 of this study. However, there is a concern regarding the number classes in ISODATA (unsupervised classification), which was applied to all images (1998 and 2010) as part of CCA. It has been noted that the ISODTA with 100, 200, 300, 400 clusters led to some speckle areas which do not reflect actual change. It was also noted that 1000 cluster of ISODAT limited the speckle area. In addition, cloud and scan lines are two other factors which CCA identifies as change while no actual change occurred. In this study the 2010 image does not contain any clouds, but a small segment on north west of the AOS covered by LANDSAT 7 which contains a scan line, these scan lines caused some misclassification (Appendix3, Figure 57).

5.2.4 Bivariate Analysis

Bivariate analysis was conducted to compare the LULC map of 1998 and the LULC map of 2010 in order to identify the type of change that occurred. The Bivariate model identified specific types of change that happened between classes. The result was a change matrix and a heat map image with conditional color was created based on the result of bivariate analyze (Appendix 2, table 16). The red color within the heat map represents high value of change. Yellow represents medium value of change and blue represents zero (no) change. Some factors of these changes are seasonal and some others

are as a result of population explosion and economic growth. All types of change and possible causes of change are explained as follows:

- The AG class increased by 272.33 km^2, the classes which changed to AG namely are:

  1. Grassland changed by 98.93 km^2, this occurred mostly among pervious AG areas as a result of seasonally and near the new rural community which was destroyed by the former Saddam Hussein regime in 1988, and it was rebuilt mainly after 2003(Appendix 3 , figures 58 and 59).

  2. Water changed by 81.59 km^2 to AG, and this change occurred near and around the lakes of Dokan and Drabandikhan as result a decrease in water level, as was shown from rainfall records (Appendix 3, figure 60).

  3. Barren land changed to AG by 57.66 km^2, scrub changed by 35.77 km^2, (Appendix 3, figure 61).

  4. A small amount of evergreen and deciduous tree changed to AG as a result of new urbanization, which at the same time leads to deforestation

- The urban class increased by 115.71 km^2; this is the result of population increase and economic growth in the region after 1998. Also, rebuilding of destroyed cities and villages, which were destroyed during Former regime in 1988, led to re-urbanization. Urbanization and re-urbanization in the AOS led to deforestation in some scrub and tree areas (Appendix 3, figure 62).

- 85.97 km^2 of scrub area changed to other classes, all of these changes led to deforestation. For instance, 35.77 km^2 of scrub changed to AG, and some other to

barren and as a result of fire. At same time some other areas are changed to scrub 68.55 km^2, mostly within grassland and barren, which way lead to reforestation in the future. A small segment of evergreen changed to scrub; this may be a result of deforestation.

- Barren areas have increased by 85.69 km^2, mostly grassland changed to the barren which is acceptable as a result of seasonality and the dry season. However, as a result of fire significant portion of grass area changed to barren area. This occurred in the west of a Taslujah Cement Factory (Appendix 3 Figure 63), as well as in the Goizha Mountain Range in the north of the city of Sulaimainya. Some of the scrub area was changed to barren and this led to deforestation of some of these scrub areas which were within the burn area. Additional deforestation was identified near Iranian border. In addition, some AG was changed to barren, possibly because of the early growth stage of AG. Finally some water areas changed to barren near around lake Dokan and lake Darbandikhan.

- In general, grass area decreased within the AOS as result of new urbanization, new AG, and some other changes to barren. Areas around all the cities within the AOS are typical examples of grass areas changing to urban. Also the change in the west of Ranya city is an example of change of grass to AG. More grass to AG change occurs near the both lakes of Dokan and Darbandikhan as a result of different stages of AG growth and seasonality. Finally, other grass areas were changed to barren in the burn area.

- All changes within the snow areas are false changes, and they occurred as a result of melting of snow in previous years and new snow areas in recent years. The change in snow areas depends on the month of the new snow and the melting snow. The areas where snow melt contain old classes which covered by snow, and CART classified these areas based on the training data

- Water class is decreased as the result of the low-rainfall between 1998 and 2010. The majority of water changes were around the Dokan and Darbandikhan lakes where water level decreased.

- Change from wetland to other classes was not significant, and was estimated at 8.2 km^2. It occurred only within the stream and river beds and also near the lakes. As the result of a dry season, the scrub, grass and AG were visible among the wetland area. Meanwhile, some other classes changed to wetland, for example, change from barren to wetland and grassland to wetland in the south of Bestansur village within the bed of the Tanjaro stream (45°42'18.76"E 35°20'24.808"N) ,(Appendix 3, figure 65).

- The deciduas forest class is increased by 20.76 km^2. This change occurred mostly in the grassland, scrub, and barren areas, which led to reforestation mostly in the northeast of Qaladze city, near Iranian border. In some other areas, deciduous tree changed to other classes mostly to scrub by 8.4 km^2. Given the smooth texture of this change area (Appendix 3, figure 66) in new image, the area may still be deciduas, but the trees affected due to lack of leaves or for any reasons the tree did not have enough leaves in this season.

- The evergreen class change within the area was very limited among small segments of grass, scrub and barren areas. Mostly, these are not actual change as a result of dark tone CART classified as evergreen. Evergreen in the AOS is very limited, and mostly seen in the Goizhah Mountain, and also in parks as tree line in the north of Sulaimaniya city.

5.3 Summary and Conclusion

The basis of this research comprises the multitemporal classification of Landsat TM and ETM+ satellite imagery to classify, detect, delineate, and map LULC classes in Province of Sulaimania between 1998-2010, in order to understand the nature of LULCC, to identify the factors that caused the change, as well as to explore and evaluate the potential and performance of remote-sensing data and remote-sensing methods for understanding the impact of political factors on LULC. Thus, the aim of this research was to produce both recent and past LULC maps of AOS from recent and historic satellite imagery across the period of study, and to detect and map any land change. The applications and software which have been used to perform the data analysis are ERDAS imagine (version 11) and ArcGIS (version 11). The origin for the mapping LULC of the AOS was the classification of the 1998 images, which result in a base LULC dataset. This data set was used to perform change detection in relation to images from later dates (e.g. image from 2010).

Several key steps were taken to complete this research, namely identifying the LULC classification scheme, image data acquisition, scene processing, data analysis, other post processing, and validation. These steps are outlined below:

- *LULC Classification scheme*: the USGS Classification Schema also known as the Anderson Schema level I and II was selected and employed to identify the most accurate land classes (for example, scrub, urban, etc.) within the area of study (Campbell, 2007, p.559-81 ; Anderson, 1976, p.2-22).

- *Image data acquisition*: Images of the study were downloaded from the USGS website. The study area is covered by three Landsat path rows (p169r035, p168r036, p168r035) for the years 1998 and 2010(USGS, 2011). The amount of colud and scan line have been considered in the selection of the images.

- *Scene processing*: this step involved geo-reference the images, staging the single band images to a single six band image, and generating and organizing the data required for classification and change detection, namely, NDSI (Lin et al., 2010, p.2-3), NDMI(Goodwin, 2009, p.1-3), NDVI, TCAP(Campbell, 2007, p.478-477), and a training layer.

- *Data analysis*: in this work CART was utilized to perform image classification based on the 1998 imagery. Also, CCA was explored to identify the change between the 1998 and 2010 images.

Ten LULC classes were identified in this area, namely: urban, water, general agricultural, grass land, barren, forest evergreen, forest deciduous, snow and

98

wetland. Temporal variations (such as season) played an important role in the classification of LCULC, and in LULCC. Classes can be identified by the difference in the spectral wavelength in dry season image of dry and wet seasons; an example are wetland areas near stream beds in some areas of image of 1998 were wetland ,but due to more dry condition in the same season, the same area become a barren or grass. However, for the same reason, some grass land in these areas was changed to wetland. In addition, the definition of the LULC classes used is another important factor in LULC classification which can make a difference in the classification. Process, often depends on the knowledge and skill set of the analyst. In this study, the definition of grass land and barren class were close to each other and similar. In some areas, there is a possibility of transition from barren to grass; therefore and depending of the density of these two classes, the definition has been considered during collection of training data, classification, and change detection.

The result showed that the urbanization, re-urbanization, deforestation, reforestation, and farming –new agricultural land, burned scar, seasonality change from one class to another have occurred in this area. All of these have important role in understanding the ecological system of the area and have an impact on natural balance in the area. The results of this study provided important information in support of developing a deeper understanding of the nature of LULC and LULCC in the AOS. Furthermore, it is hoped that they will serve as a

valuable tool for decision making and for managing lands in the AOS. Results

from this study may also assist in understanding where public services will be

most needed (for example, which areas of the Province have schools, hospitals,

and well-developed infrastructure), and in understanding other sociodemographic

factors. Finally, the results and methods used in this study could be generalized to

other regions in Iraq or the Middle East, providing an important tool for

measuring and monitoring the relationships between political changes and

LULCC.

CART trails, after running CART the See5 classifier tool creates ten decision trees for each trails. Each trails include a decision tree which explain how the decision been made to classify specific pixel to a specific LULC class in another world based on the dependent and independent variables.

```
See5 [Release 2.05]        Tue Feb 28 20:28:48 2012
-------------------
    Options:
        10 boosting trials
        Probability thresholds
Class specified by attribute `dep'
Read 1336 cases (15 attributes) from 19980701_suly_clip_cart_v01.data

-----  Trial 0:  -----

Decision tree:

band04 <= 19 (50): 11 (1154)
band04 >= 81 (50):
:...band05 >= 124 (122): 4 (19)
    band05 <= 120 (122):
    :...band07 >= 127 (126.5):
        :...band11 <= 97 (102.5): 2 (7)
        :   band11 >= 108 (102.5): 1 (16)
        band07 <= 126 (126.5):
        :...band09 <= 13 (13.5): 5 (57/1)
            band09 >= 14 (13.5):
            :...band01 >= 51 (50.5): 3 (46)
                band01 <= 50 (50.5):
                :...band08 >= 135 (134.5): 3 (19)
                    band08 <= 134 (134.5):
                    :...band04 <= 83 (85): 3 (3/1)
                        band04 >= 87 (85):
                        :...band03 <= 54 (54.5): 3 (2)
                            band03 >= 55 (54.5): 5 (13)

-----  Trial 1:  -----

Decision tree:

band04 <= 19 (50): 11 (1010)
band04 >= 83 (50):
:...band08 <= 133 (134.5):
    :...band04 <= 108 (115.5): 5 (156.9/19.3)
    :   band04 >= 127 (115.5): 4 (11.4)
    band08 >= 135 (134.5):
    :...band07 >= 141 (126.5): 1 (20.1/6.1)
        band07 <= 124 (126.5):
        :...band05 <= 116 (121): 3 (132.4/7)
            band05 >= 127 (121): 4 (5.3)
```

Figure 50 CART result include trial 0, and 1 of Sees classifier result

```
-----   Trial 2:  -----

Decision tree:

band04 <= 19 (50): 11 (904)
band04 >= 81 (50):
:...band07 >= 127 (126.5): 2 (48.9/12.5)
    band07 <= 124 (126.5):
    :...band05 <= 93 (93.5):
        :...band09 <= 24 (24.5): 5 (110.8)
        :    band09 >= 25 (24.5): 3 (13.8)
        band05 >= 94 (93.5):
        :...band11 <= 60 (64): 5 (47/10.2)
            band11 >= 67 (64): 3 (211.4/10.2)

-----   Trial 3:  -----

Decision tree:

band04 <= 19 (50): 11 (823.7)
band04 >= 82 (50):
:...band07 >= 129 (126.5): 1 (102.2/28.3)
    band07 <= 124 (126.5):
    :...band05 >= 124 (122): 4 (87.7)
        band05 <= 119 (122):
        :...band12 >= 81 (80.5): 5 (42.4/5.7)
            band12 <= 77 (80.5):
            :...band11 <= 60 (64): 5 (33.5)
                band11 >= 67 (64):
                :...band01 <= 46 (48.5): 5 (95.1/13.8)
                    band01 >= 49 (48.5): 3 (151.3)
```

Figure 51 Trial 2, and 3 of the See5 classifier result.

```
-----   Trial 4:   -----

Decision tree:

band04 <= 19 (50): 11 (765.5)
band04 >= 81 (50):
:...band07 >= 127 (126.5):
    :...band11 <= 97 (102.5): 2 (70.1)
    :   band11 >= 108 (102.5): 1 (58.3)
    band07 <= 124 (126.5):
    :...band05 >= 124 (122): 4 (69.3)
        band05 <= 119 (122):
        :...band01 <= 45 (45.5): 5 (48/6.7)
            band01 >= 46 (45.5):
            :...band09 >= 21 (20.5): 3 (138.8)
                band09 <= 20 (20.5):
                :...band12 >= 81 (77.5): 5 (29.7)
                    band12 <= 74 (77.5):
                    :...band09 >= 20 (19.5): 5 (21.9)
                        band09 <= 19 (19.5):
                        :...band11 <= 61 (64): 5 (31.2)
                            band11 >= 67 (64): 3 (103.3)

-----   Trial 5:   -----

Decision tree:

band04 <= 19 (50): 11 (718.8)
band04 >= 81 (50):
:...band07 >= 127 (126.5): 2 (99.5/45.9)
    band07 <= 124 (126.5):
    :...band05 >= 124 (122): 4 (54.5)
        band05 <= 113 (122):
        :...band09 >= 25 (24.5): 3 (277.3/2.9)
            band09 <= 21 (24.5):
            :...band05 <= 93 (93.5): 5 (52.6)
                band05 >= 98 (93.5): 3 (133.3/46.5)
```

Figure 52 Trial 4, 5 of the See5 classifier result

```
-----    Trial 6:   -----

Decision tree:

band07 >= 127 (126.5):
:...band04 <= 19 (50): 11 (687.3)
:    band04 >= 81 (50):
:    :...band11 <= 97 (102.5): 2 (42.5)
:        band11 >= 108 (102.5): 1 (75.2)
band07 <= 124 (126.5):
:...band03 >= 85 (74.5):
    :...band04 <= 110 (115.5): 5 (93.3)
    :    band04 >= 121 (115.5): 4 (46.3/1.8)
    band03 <= 74 (74.5):
    :...band09 >= 25 (24.5):
        :...band01 <= 44 (44.5): 5 (4.7)
        :    band01 >= 45 (44.5): 3 (216.2)
        band09 <= 21 (24.5):
        :...band01 <= 48 (48.5): 5 (50.6)
            band01 >= 49 (48.5):
            :...band09 <= 12 (12.5): 5 (30.4)
                band09 >= 13 (12.5): 3 (89.5/11.9)

-----    Trial 7:   -----

Decision tree:

band07 >= 129 (126.5):
:...band04 <= 19 (50): 11 (660)
:    band04 >= 91 (50): 1 (91.4/32.8)
band07 <= 124 (126.5):
:...band09 >= 23 (22): 3 (212.4/4.2)
    band09 <= 21 (22):
    :...band04 >= 121 (115.5): 4 (35.8)
        band04 <= 110 (115.5):
        :...band05 <= 93 (93.5): 5 (160.9)
            band05 >= 100 (93.5):
            :...band11 <= 61 (64): 5 (92.7)
                band11 >= 67 (64): 3 (82.7/22)
```

Figure 53 Trial 6, and 7 of the See5 classifier result

```
-----    Trial 8:   -----

Decision tree:

band07 >= 127 (126.5):
:...band04 <= 19 (50): 11 (641.3)
:    band04 >= 81 (50):
:    :...band11 <= 97 (102.5): 2 (86.1)
:        band11 >= 108 (102.5): 1 (47.2)
band07 <= 124 (126.5):
:...band05 >= 124 (122): 4 (29.9)
    band05 <= 120 (122):
    :...band11 >= 89 (87.5): 3 (145.6)
        band11 <= 87 (87.5):
        :...band10 <= 89 (89.5): 3 (54.7/21.1)
            band10 >= 90 (89.5):
            :...band12 >= 81 (78.5): 5 (113.4)
                band12 <= 74 (78.5):
                :...band12 >= 74 (73): 3 (18.5)
                    band12 <= 72 (73):
                    :...band08 <= 134 (134.5): 5 (180.2/24.2)
                        band08 >= 135 (134.5): 3 (19.1)

-----    Trial 9:   -----

Decision tree:

band07 >= 127 (126.5):
:...band04 <= 19 (50): 11 (626.1)
:    band04 >= 81 (50):
:    :...band11 <= 97 (102.5): 2 (66.6)
:        band11 >= 108 (102.5): 1 (38)
band07 <= 124 (126.5):
:...band05 >= 124 (122): 4 (25.1)
    band05 <= 120 (122):
    :...band11 >= 89 (87.5): 3 (114.8)
        band11 <= 87 (87.5):
        :...band07 >= 110 (95.5):
            :...band03 <= 52 (53): 3 (9.3)
            :    band03 >= 54 (53): 5 (236/30.2)
            band07 <= 95 (95.5):
            :...band09 <= 11 (13): 5 (27.4)
                band09 >= 15 (13):
                :...band01 <= 46 (47.5): 5 (17.5)
                    band01 >= 49 (47.5): 3 (175.2)
```

Figure 54 Trial 8 and last which is nine of the See5 Classifier results

```
Evaluation on training data (1336 cases):

Trial        Decision Tree
-----     ----------------
          Size        Errors

   0        10        2( 0.1%)
   1         6       37( 2.8%)
   2         6       42( 3.1%)
   3         7       25( 1.9%)
   4        10        1( 0.1%)
   5         6       73( 5.5%)
   6        10       13( 1.0%)
   7         7       18( 1.3%)
   8        10       19( 1.4%)
   9        10       15( 1.1%)
boost                 0( 0.0%)    <<


        (a)    (b)    (c)    (d)    (e)    (f)      <-classified as
        ----   ----   ----   ----   ----   ----
        16                                          (a): class 1
                7                                   (b): class 2
                      70                            (c): class 3
                              19                    (d): class 4
                                     70             (e): class 5
                                            1154    (f): class 11
```

Figure 55 Evaluation training data in CART

```
Evaluation on test data (0 cases):

Trial        Decision Tree
-----     ----------------
          Size        Errors

   0        10        0( 0.0%)
   1         6        0( 0.0%)
   2         6        0( 0.0%)
   3         7        0( 0.0%)
   4        10        0( 0.0%)
   5         6        0( 0.0%)
   6        10        0( 0.0%)
   7         7        0( 0.0%)
   8        10        0( 0.0%)
   9        10        0( 0.0%)
boost                 0( 0.0%)    <<


        (a)    (b)    (c)    (d)    (e)    (f)      <-classified as
        ----   ----   ----   ----   ----   ----
                                                    (a): class 1
                                                    (b): class 2
                                                    (c): class 3
                                                    (d): class 4
                                                    (e): class 5
                                                    (f): class 11
```

Figure 56 Evaluation of test data

Table 14 Rainfall history of the POS from 1980 t0 2010; the original source is from University of Sulaimnauia , college of Science, Department of Geology by.Dyari Ali

	A	Jan	Feb	Mar	Apr	May	Jun	Jul	Aug	Sep	Oct	Nov	Dec	Sum Per year	Ave Per Year
2	1980	81	105.5	115.3	56.6	6.7	0	0	0.1	0.8	12.6	109.1	78.5	566.2	47.18333333
3	1981	174.5	157.7	141.7	71.5	28.3	4.2	0	0	0	48.7	99.4	57.7	781.7	65.14166667
4	1982	164.2	91.4	106.2	157.5	68	0	0	0	6.7	148.2	167.9	64.7	972.8	81.06666667
5	1983	113	104.4	63.9	43.9	59.7	0.2	0	0	0	0	34.9	64.4	484.4	40.36666667
6	1984	17.2	41	128.7	116.7	53.1	0	0	0	0	41.1	232.1	82.1	710	59.16666667
7	1985	114.1	155.3	83.2	85.4	38.6	0	0	0	0	4.9	101.3	137.7	720.5	60.04166667
8	1986	34	170.1	58.9	101	69.5	0	0	0	0.4	32.5	201.3	61.6	729.3	60.775
9	1987	38.4	67.9	167.9	18.6	65.5	0	0	0	0	102.5	18.3	289.8	748.9	62.40833333
10	1988	153.1	204.5	148.7	126	0.7	5.7	0	0	0	22.6	61.3	180.6	903.2	75.26666667
11	1989	35.2	53	165.8	1.1	1.2	0	0	0	0.1	10.5	145.2	86.4	498.5	41.54166667
12	1990	121	96.4	90.7	67	19.3	0	0	0	0	14.6	25.2	100	534.2	44.51666667
13	1991	193.4	193.4	193.4	193.4	193.4	0	0	0	0	54.2	172	354	1547.2	128.9333333
14	1992	159	224.9	122.2	85	74.5	6.4	0	0	0	18.7	160	156.8	1007.5	83.95833333
15	1993	79.9	67.8	81.8	223	89.9	0	0	0	0	55.5	196.1	79.7	873.7	72.80833333
16	1994	189.1	96.4	104	96.3	7.8	0	0	0	6.8	69.8	264.4	118.2	952.8	79.4
17	1995	64.1	111.7	138.8	196.3	71.2	18.6	0	0	12.1	0	12.7	33.6	659.1	54.925
18	1996	229.5	108.2	176.7	89	59.5	3	0	0	0.7	9.1	0	114.4	790.1	65.84166667
19	1997	138	47.5	191.5	68.1	47	0	0	0	0	51.5	164.1	147.1	854.8	71.23333333
20	1998	273.6	91.5	142.6	68.9	34.6	4.4	0	0	0	0	4.2	3.8	623.6	51.96666667
21	1999	87.9	97.8	18.7	17.2	0.5	0	0	0	0	6.7	51.2	59.4	339.4	28.28333333
22	2000	147.2	45.8	37.9	32.9	13.9	0	0	0	2.7	28.2	31.4	185.3	505.3	42.10833333
23	2001	82.6	83.9	81.9	35.3	12.6	0	0	0	3.7	21.8	42.9	148.1	512.8	42.73333333
24	2002	208.4	64.6	134.2	131.6	27.2	0	0	0	0	57	58.2	248.3	929.5	77.45833333
25	2003	127.3	173.8	131.5	65.6	18.7	0	0	0	0	2	130.8	161.2	810.9	67.575
26	2004	272	103	13.3	74	86.4	0	0	0	0	13.4	116.4		678.5	61.68181818
27	2005	143.8	123.3	141.5	55.8	20.2	0	0	0	0	0	0	0	484.6	40.38333333
28	2006	141.6	276	3	132.5	85.6	0	0	0	0	80.6	40.6	18.7	778.6	64.88333333
29	2007	52.4	146.1	82	161	22	0	0	0	0		4	118.6	586.1	53.28181818
30	2008	59	121.1	48.3	17.5	0.9	0	0	0.2	2.5	96.8	12.4	21.5	380.2	31.68333333
31	2009	39.5	67.2	87.1	97.6	2.9	2.6	0	0	10.1	72.9	136.4	98.3	614.6	51.21666667
32	2010	69	161.9	93.2	77.1	80.8	0	0	0	0	0.6	1	0	483.6	40.3

Biavriate Analyses

Bivariate studies measure the relationship between two variables. Neither of the variables being studied is an independent variable, so the procedure is not experimental. Correlations are common bivariate tools which are used to study how one variable influences the other. In this research, Bivariate Analyses used to deploy Bivariate Model between LULC in 1998 and 2010 in order to see the differences between the two layers in perspective of class change and to find the change relation between each class. The result of each change area stated in (Table 15).

Table 15 Result of Bivvariate Analyses between LULC map of 1998 and LULC map of 2010. The red color is maximum change and blue color is minmum change

|	Channge from to	Forest Deciduo	Forest, Evergre	Scrub/Shr	Grasslar	Barren/Sparsely Veget	Urban/Built-	Agriculture, Oth	Wetland, Permanent Herbac	Water10	Ice/Snov1
2	Forest, Deciduous to Fo	0.00000	0.00900	8.43302	0.69645	2.22253	0.11967	2.73272	0.02969	0.12687	0.06929
3	Forest, Evergreen	0.00270	0.00000	0.01440	0.02879	0.00630	0.11608	0.00630	0.00000	0.00000	0.00000
4	Scrub/Shrub	3.64243	0.16197	0.00000	11.77402	16.42244	9.24285	35.77105	0.80983	3.75131	0.02429
5	Grassland	11.94948	0.28704	33.30287	0.00000	47.69984	69.76138	98.93503	3.63793	13.36488	0.00180
6	Barren/Sparsely Vegeta	2.99457	0.18386	21.15814	17.91612	0.00000	20.89089	47.66654	7.21738	12.24912	0.04949
7	Urban/Built-Up	0.00090	0.00000	0.11248	0.27174	0.10348	0.00000	0.10438	0.03779	0.00630	0.00000
8	Agriculture, Other	1.82841	0.09178	4.94896	6.54612	9.73505	15.55952	0.00000	0.66316	0.87012	0.00000
9	Wetland, Permanent He	0.02429	0.00180	0.05759	0.66496	0.68656	0.00630	5.51854	0.00000	1.32002	0.00000
10	Water	0.28614	0.14487	0.51289	4.02125	8.68857	0.01170	81.59119	6.16730	0.00000	0.00000
11	Ice/Snow	0.03329	0.00090	0.01440	0.00990	0.13227	0.00540	0.00540	0.00630	0.00000	0.00000
12	Totall	20.76222	0.88721	68.55474	41.92935	85.69702	115.71379	272.33115	18.56938	31.68861	0.14487

APPENDIX 3
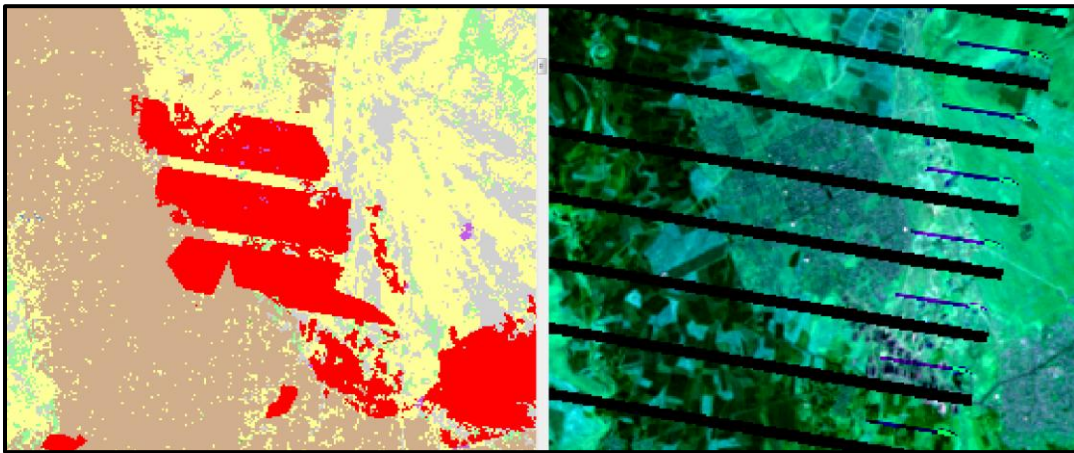
Figure 57 South of Hajy Awa City and it is an example of sscan line issue and example of change :
 right is image 2011 and left is t the classifcation of 2010 after the chanege layer merged to LULC
1998, and thi is befor final edit. The purpuse of this screen shot to show the sac line issue with Landsat7.
The areas classfied to dfrrent class, but this been fied to urban in filan copty to the map

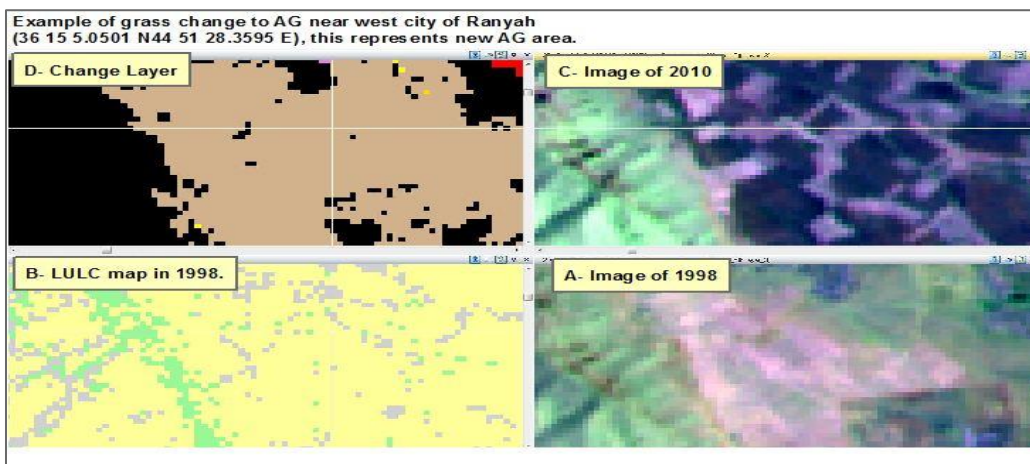**Figure 58 Example of grass change to AG**
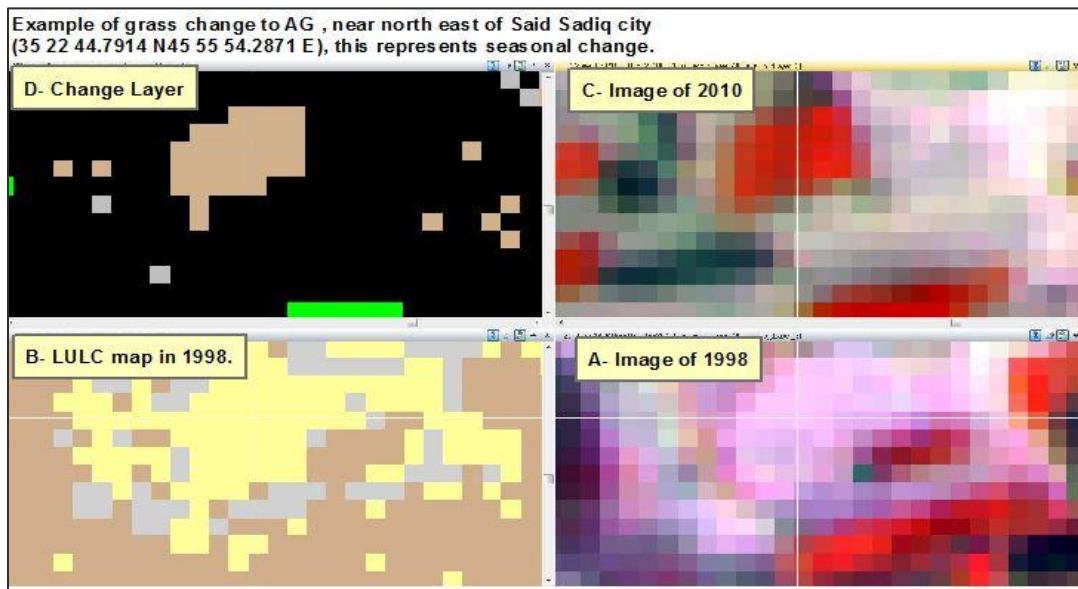
109

Figure 59 Example of grass change to AG
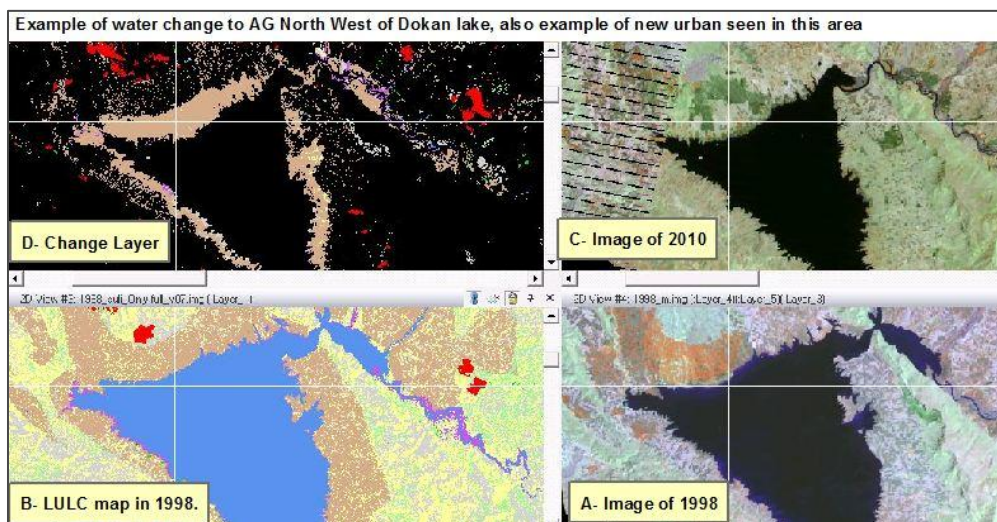

Figure 60 Example of water change to AG ,also new urbanization
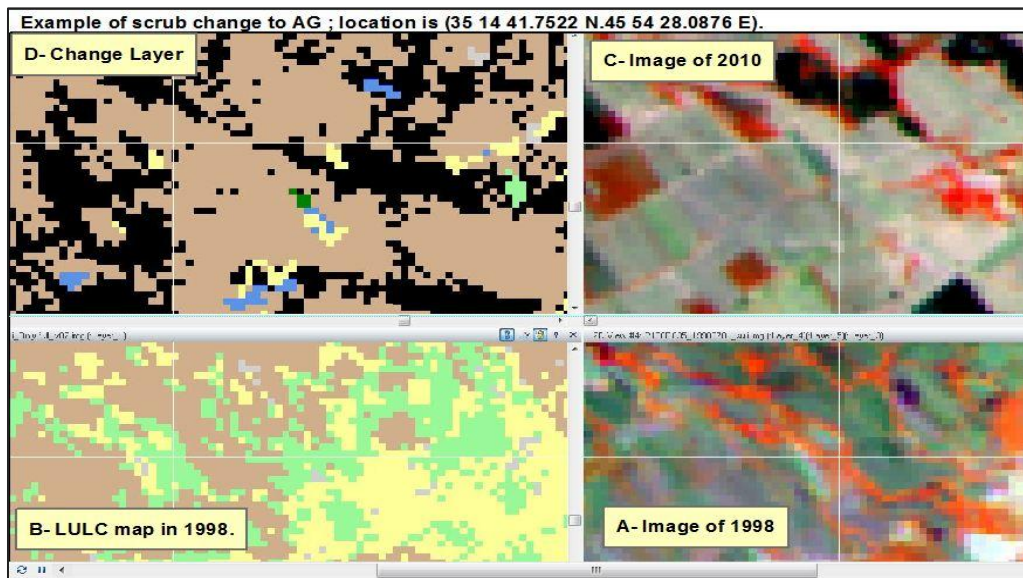
Figure 61 Example of scrub change to AG .

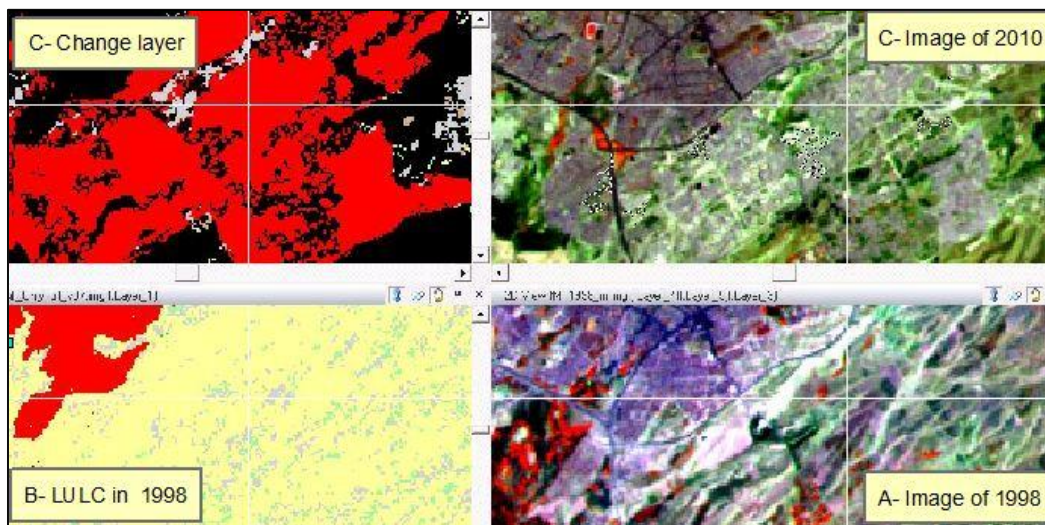**Figure 62 Example of urbanization, west of Sulaimaniya**
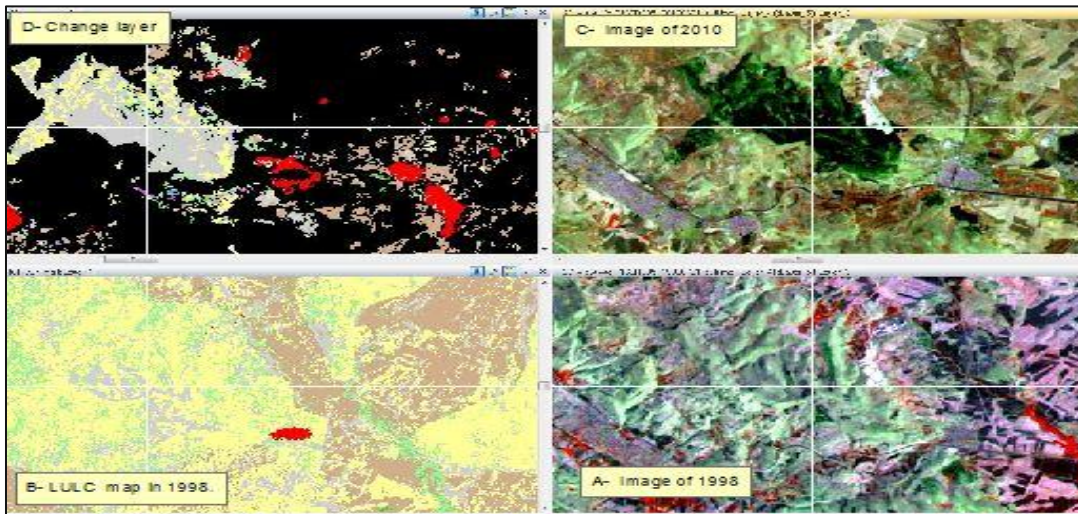
Figure 63 Example of burnscar, west of Tasluja Cement Factory, which led to change grass to barren.
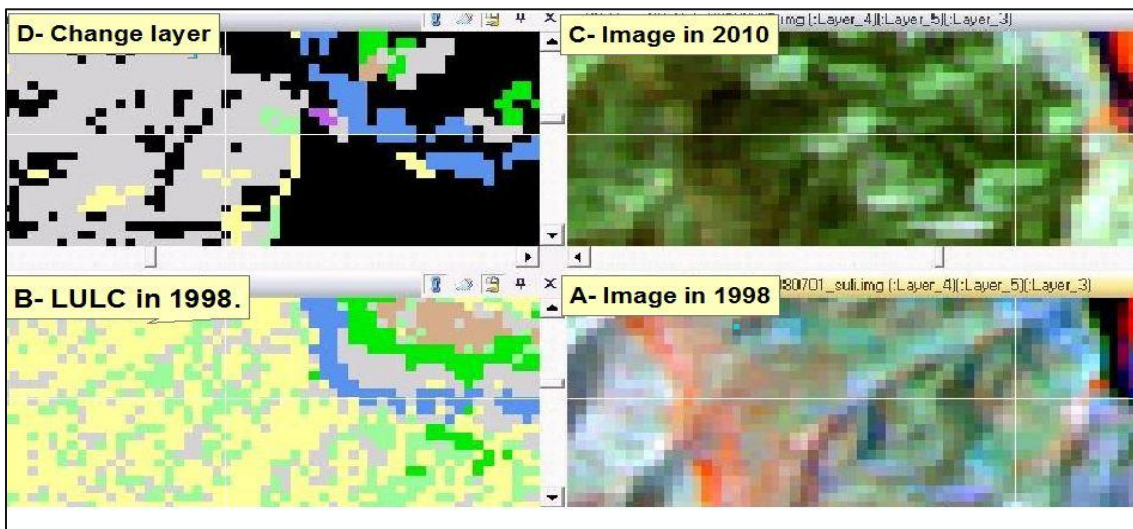
Figure 64 Example of scrub change to barren location is west of Mokaba (354627N 452513E)
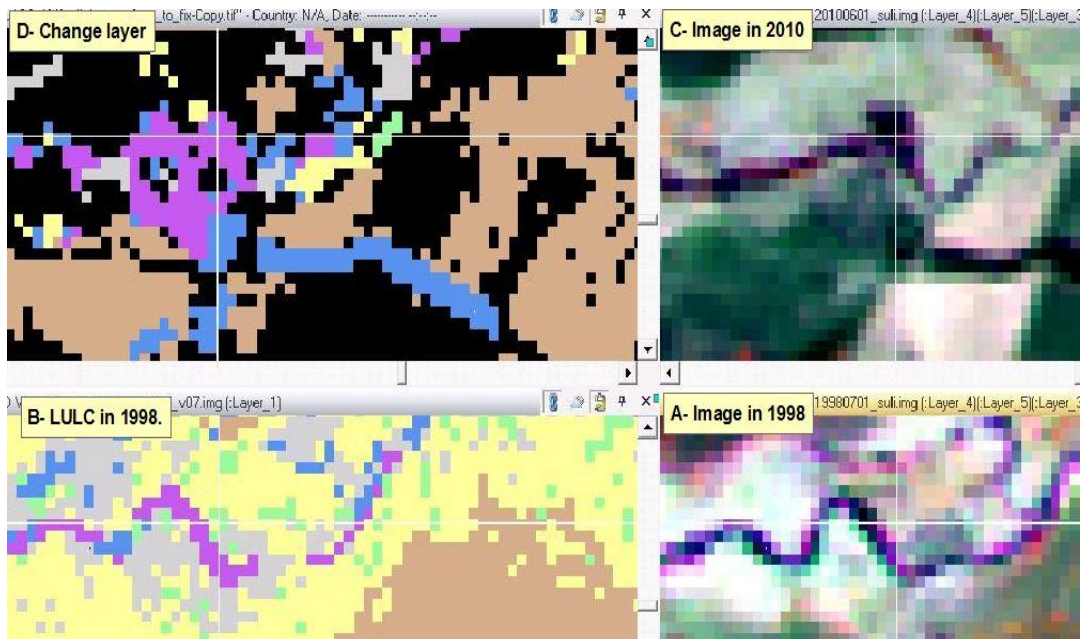
Figure 65 Example of grassland change and barren change to wetland.
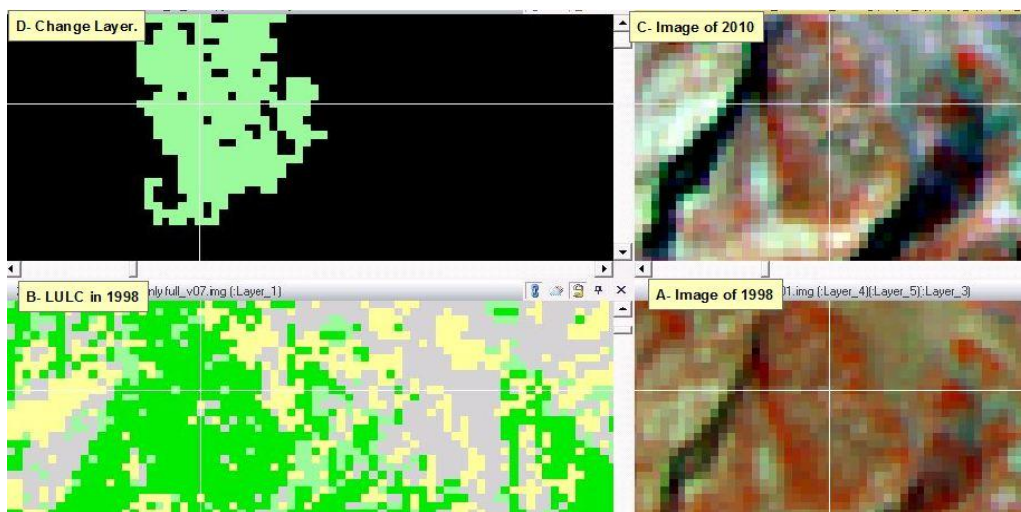
Figure 66 Example of tree deciduas change to scrub.
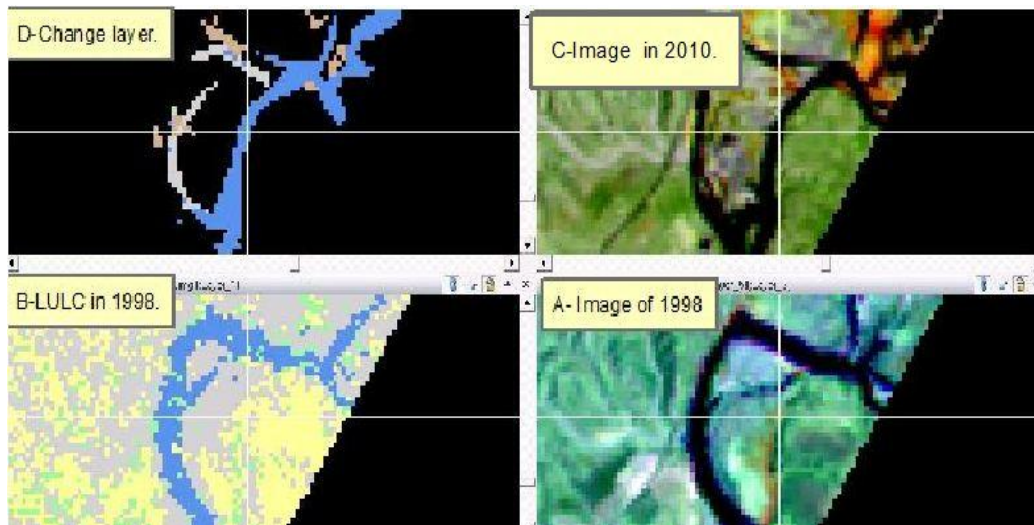
Figure 67 Example of water change, south of City of Maidan, near the border between Sulaimaniya and Dyala (34°54'1.04''N, 45°35'24.49''E)
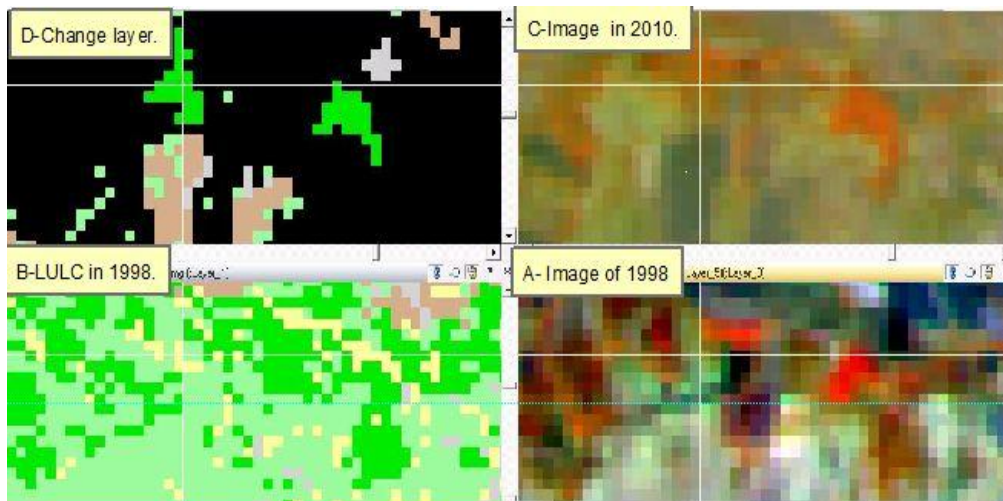
Figure 68 Example of reforestation near city of Penjwen- Northeast of   PROVINCE. The bright pixels in image 1998 were grass and have been changed to tree deciduous the orange pixels in image of 2010
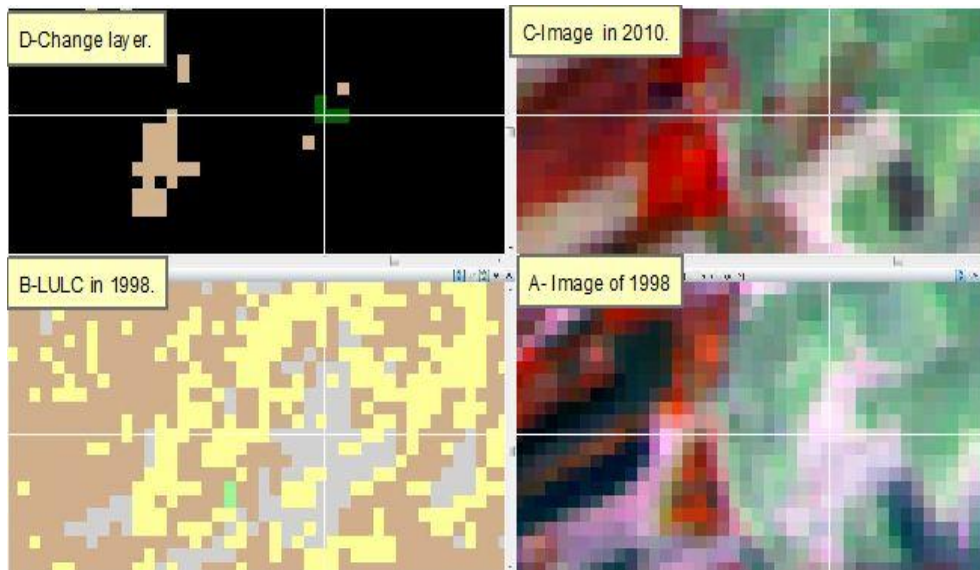
Figure 69: Example of reforestation, barren changed to evergreen tree near Qadefary Village at35 20 14.4302 N45 58 28.9184 E.
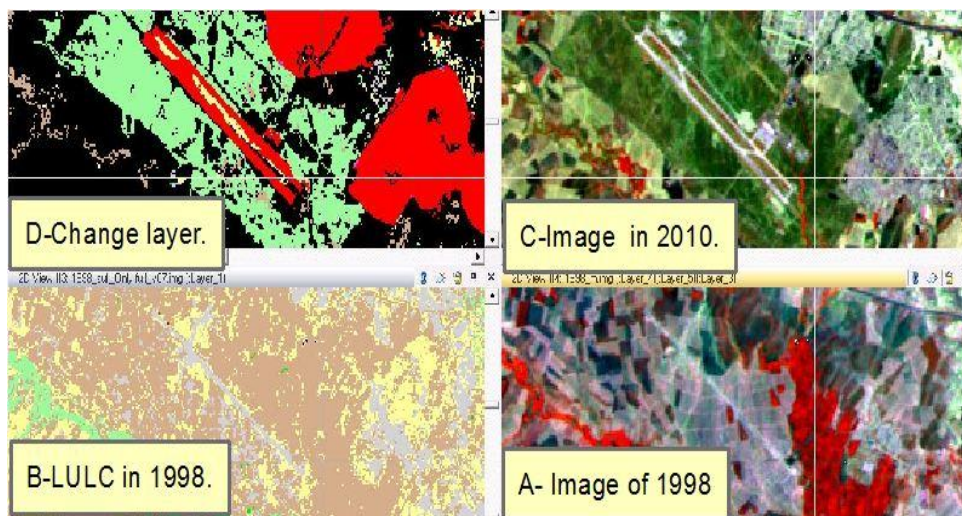
Figure 70 . Example of new urban area including an airport is on south west of city of As Sulaimanyia. Also, AG area have been change to the scrub area as result of new development on that area.

115

APPENDIX 4

4.1 ISODATA

ISODATA is one of the unsupervised classification methods; It is Iterative Self-Organizing Data Analysis Technique which is commonly used in remote sensing, don't need to know the number of clusters and the algorithm splits and merges clusters; also user defines threshold values for parameters and the computer runs algorithm through much iteration until threshold is reached (Ashley Vassilaros, 2010; Thomas Lillesand, Ralph Kiefer, and Jonathan Chipman, 2004; Tou, and Gonzalez, 1974). ISODTA algorithm is a modification of the *k*-means which includes a) merging clusters if their separation distance in multispectral feature space below a user specified threshold and b) rules for splitting a single cluster to into tow clusters (Jensen, 2005; Schowengerdt, 1997). This Algorithm permits number of clusters to change from one iteration to the next; the general process follows that described above the *K*-means (Thomas Lillesand, Ralph Kiefer, and Jonathan Chipman, 2004).

First an arbitrary cluster vector is assigned. Next each pixel is classified according to the closest cluster. Then new cluster mean vectors are created using the information from the pixels in each cluster. These two steps are repeated until the difference between iterations becomes small. This difference can be determined by calculating either the

116

change in distance of the mean cluster vector or the percentage of pixels that have

changed (www.yale.edu/ceo).

One advantage of the ISODATA algorithm is that it allows for further refinements

through the splitting and merging of clusters. Clusters are merged if either the number of

members (pixels) of a cluster is less than a certain threshold or if the centers of two

clusters are closer than a certain minimum distance. Clusters are divided if the cluster

standard deviation exceeds a predefined value and the number of pixels is twice the

minimum number of members (JENSEN, 1996). In this study the ISODATA algorithm

used as pre classification in change detection for CCA process (Figure).

4.2 Region Growing

Region growing is a method to segments an image to group of segments or

regions per their pixel similarity. Segmentation means the grouping of neighboring pixels

into regions (or segments) based on similarity criteria (digital number, texture). For

remotely sensed images, region growing segmentation is a widely-used technique for

object extraction and identification; however, the main negative aspect of region growing

segmentation is the threshold setting for stopping the growth of a region (Li-Yu Chang

and Chi-Farn Chen, 2001). Different type techniques in variety studies have been used to

control threshold setting.

There are different programs to conduct the segmentations and each of them work with a specific algorithm namely: eCognnition 2.1 and 3.0 , Data Dissection Tools, CAESAR 3.1 , InfoPack 1.0, Image Segmentation(for ERDAS Imagine), Minimum Entropy Approach , and Spring 4.0(Meinel and Nueburt 2004). In this study due to limited access to all these programs only the ERDAS Imagine 11 has been used to extract urban and agricultural by segmentation. The algorithm which been used for segmentation in ERDAS is region growing algorithm; to control the property of the region growing the minimum distance decision rule been invoke (also called spectral distance) which calculates the spectral distance between the measurement vector for the candidate pixel and the mean vector for each signature (Figure 72) ,(Nirupama, Slobodan P. Simonovic 2002, and Field Guide ERDAS 11).
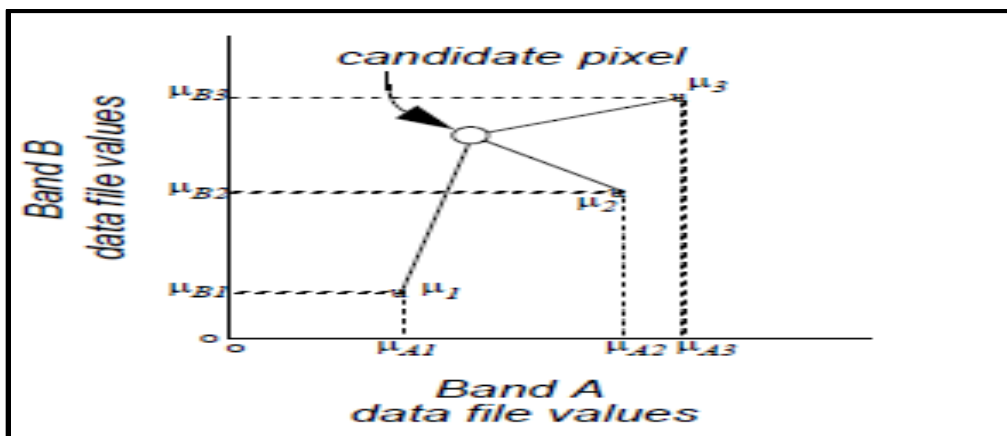

Figure 71 spectral distance is illustrated by the lines from the candidate pixel to the means of the three signatures. The candidate pixel is assigned to the class with the closest mean (Nirupama, Slobodan P. Simonovic 2002 and ,Field Guide ERDAS 11).

The equation for classifying by spectral distance is based on the Equation for

Euclidean distance which originally found by (Swain and Davis, 1978), (Equation 7):

Equation 4 Euclidean distance Swain and Davis, 1978

$$SDxyc = \sqrt{\sum_{i=1}^{n} (\mu ci - Xxyi)^2}$$

Where:

n = number of bands (dimensions)

i = a particular band

c = a particular class

$Xxyi$ = data file value of pixel x,y in band i

μci = mean of data file values in band i for the sample for class c

$SDxyc$ = spectral distance from pixel x,y to the mean of class c

Meinel and Nueburt (2004) in their study compared all segmentation programs (

which been mentioned in first paragraph of this section) to conduct segmentations in

order to compare the result from all programs; the segmentation result by ERDAS in

their study was well-contrasted boundaries between main land cover classes were

correctly presented; areas of low contrast were often not segmented. The quality of there

result been graded as good, even it leaded to some over and under segmentation , but this

was a minor issue and adjustable for the users. The property of the region growing tool in

ERDAS is controlled by users which is makes it flexible from the area to area within one

image for specific land classes.

(Li-Yu Chang and Chi-Farn Chen, 2001) proposed multi scale region growing, based on the maximization of the change of edge density segmentation in order to overcome the drawback of region growing . Improper threshold setting not only causes over-segmentation or under-segmentation, but also cannot create needed object regions for various targets. By invoke this method on IKONOS image with different scales the results were: over-segmented for the region growing with small threshold, under-segmented for the region growing with large threshold, and was average with purposed scale.

(G.M Espindola, G. Camara , I.A Reis, L.S. Bins , A.M. Monterio 2006) proposed an objective function for selecting suitable parameter for region growing algorithm to ensure best quality result. It conceders that segmentation has two desirable properties: each of the resulting segments should be internally homogenous and should be distinguishable from its neighborhood. The author of this method used two parameters; a similarity threshold and an area threshold. It starts by neighboring pixels and merging them into regions if they are similar. The algorithm then tries iteratively to merge the resulting regions.

4.3 Landsat Thematic Mapper Sensor:

Campbell (2007) provided a detailed history of the Landsat program and its renowned success. The landsat program has had a several impact in several application arenas. In addition the landsat program has also provided researchers and scientists with real-world data and access to valuable enhanced spatial and analytical tools. The principle of the Landsat program is that the Earth's objects, features, and landscapes can be identified, categorized, and mapped on the basis of their spectral reflectance and emissions. The Landsat World-Wide-Reference system catalogues the Earth's landmasses into 57,784 scenes, each 115 miles (185 kilometers) wide by 106 miles (170 kilometers) long (USGS, 1999). An example of the approximate coverage extent of a Landsat TM scene can be seen in (Figure 14). It requires 3 separate Landsat Scenes mosaic or tiled together in order to cover the entire Province. The study area considered for this project, Province of Sulaimaniya in red, is entirely contained in the Landsat scene Path/Row 168/35, Path/Row 168/36, Path/Row 169/35 and, Path/Row 169/36 (Figure 14)
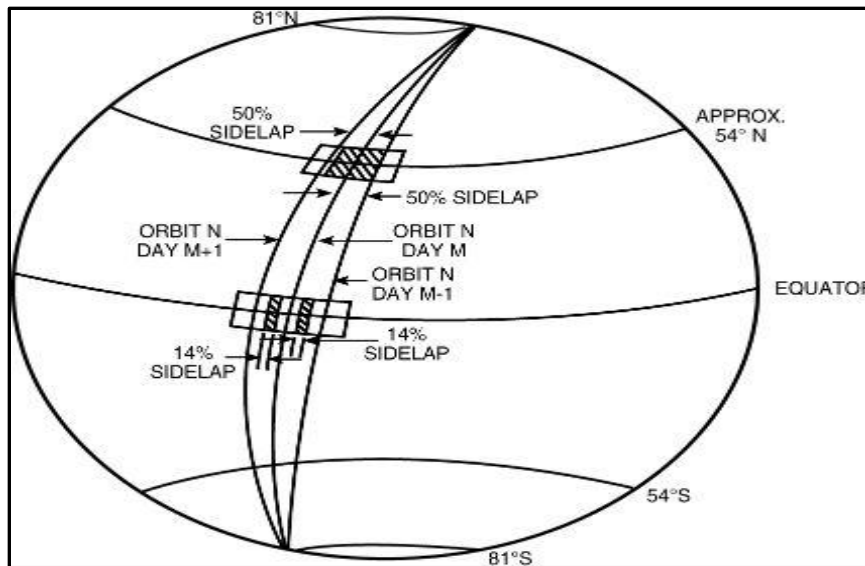
Figure 72 LANDAST-5 Orbit characteristics (NASA Homepage)

4.4 Landsat TM's Bands

The following list describes each of the seven TM bands which been used in this study (CAST 1999):

Band 1 – Visible Blue, 0.45 – 0.52 um Useful for mapping coastal water areas, differentiating between soil and vegetation, forest type mapping, and detecting cultural features.

Band 2 – Visible Green, 0.52 – 0.60 um corresponds to the green reflectance of healthy vegetation. Also, it is useful for identification of cultural feature.

Band 3 – Visible Red, 0.63 – 0.69 um Useful for discriminating between many plant species. It is also useful for determining soil boundary and geological boundary delineations as well as cultural features.

Band 4 – Reflective - infrared, 0.76 – 0.90 um this band is especially responsive the amount of vegetation biomass present in a scene. It is useful for crop identification and emphasizes soil/crop and land/water contacts.

Band 5 – Mid - infrared, 1.55 – 1.74 um this band is sensitive to the amount of water in plants, which is useful in crop drought studies and in plant health analyses. This is also one of the few bands that can be used to discriminate between clouds, snow, and ice.

Band 6 – Thermal - infrared, 10.40 – 12.50 um this band is useful for vegetation and crop stress detection, heat intensity, insecticide applications, and for locating thermal pollution. It can also be used to locate geothermal activity.

Band 7 – Mid - infrared, 2.08 – 2.35 um, this band is important for the discrimination of geologic rock type and soil boundaries, as well as soil and vegetation moisture content.

Different combinations of the TM bands can be displayed to create different composite effects. The following combinations are commonly used to display images:

Bands 3, 2, and 1 create a true color composite. True color means that objects look as though they would to the naked eye, similar to a photograph.

Bands 4, 3, and 2 create a false color composite. False color composites appear similar to an infrared photograph where objects do have the same colors or contrasts as they would naturally. For instance, in an infrared image, vegetation appears red, water appears navy or black.

Bands 5, 4, and 2 create a pseudo color composite. (A thematic image is also a pseudo color image.) In pseudo color, the colors do not reflect the features in natural colors. For instance, roads may be red, water yellow, and vegetation blue.

With the adequate knowledge of band properties and the appropriate combination of Landsat TM bands, the extraction of numerous themes, land use and land cover classes; can be achieved for various mapping applications.

APPENDIX 5

Vegetation Indices (VI)

Ray D. Jakson, Alfredo R. Huete, and Kevin P. Davie (1991) studied spectral indices related to remote sensing of vegetation. To successfully use these indices, analysts must know the input variable units and understand the manner in which the external environmental and the architectural aspects of the vegetation canopy influence and alter the index values. Although vegetation indices have been developed to extract plant signals only, the soil background, moisture conditions, solar zenith angle, view angle, and atmosphere all affect the index values in complex ways.

John R Jensen, 2005, stated that the vegetation indices have been used since 1960 by the scientists, and they have extracted and modeled various vegetation biophysical using remotely sensed data. A vegetation index should be:

(a) Maximize sensitivity to plant biophysical parameters; (b) Normalize or model external effects such as sun angle, viewing angle, and the atmosphere; (c) Normalize internal effects such as canopy background variations; and (D) be coupled with a specific, measurable biophysical parameter such as biomass.

Campbell 2007, stated that the VIs attempt to measur biomass or vegitation vigor; also a VI is formed from combination of several spectral vlaues that are added, divided , or multiplied in a manner to yield a single value that indicates the amont of vigor of vegitation. High values of VI inditify pixels covered by substantial proportions of healthy vegitation. Per Campbell 2007 , the applications of VIs can divide into two categories , first one applications of is to validate ; many of the first studies defined   Vis to vlaidate their usefulness by estabilshing values of the Vis are closely related to bilogicla prporties of plants. The objectiv of thus studies is to esatblish use of Vis as means of remote monitoring of the growth and productivivty of spsecifc crops. A second category of use of Vis application as a mapping devices, that is much more as a qualitative rather than qunatitative tool. Such applications use Vis to assist in image classifcation , to separate vegtatge from nonvegetated areas, to distinguish between different types and densities of vegitation.

There are many vegetation indices those which used in this study created in preprocessing and used as independent variable with in CART their role is to enhance and to identify the vegetation and moisture in the soil and vegetation areas. These are help the CART in classification by assigning pixels to correct classes as much as possible per the training points when collected; I have briefly expanded the indices those been used in this study below in the following subsections.

5.1 Normalized Difference Moisture Indices (NDMI):

126

The information about vegetation water has widespread helpfulness in agricultural (John Jensen, 2005). Hardisky et al. (1983), Gao (1996) ,Goodwin (2008) found that the NDMI based in Landsat TM near-infrared (NIR) band 4 content to the mid-infrared (MIR) band 5 (equation 3)

Equation 5 NDMI

$$NDMI = \frac{Band4 - Band5}{Band4 + Band5}$$

In 2005, Sader compared NDMI and tassels cap wetness transformation for detection forest disturbance. Also, it been used in 2006 by (Meng-Lung Lina, Yu Caob, Chung-Hsin Juanc, Cheng-Wu Chend, I-Chen Hsuehe, Qiu-Bing Wangf, Yung-Tan Leea) to monitoring drought dynamics in the Ejin Oasis using drought indices from MODIS data

Goodwin (2008) used NDMI to track Mountain Pine Beetle (MPB) attack in forest stands across the Province of British Columbia, by use Landsat satellite imagery to monitor moisture changes on a year-by-year basis. Also, NDMI have used to characterize the environmental thermal effects due to different land use types in Taoyuan, north Taiwan with the application of remote sensing techniques and indices. (NDMI) were calculated in each pixel of the image and linearly regressed with the surface temperature in order to find the surface temperature (Chia-Kai Yanga, Chih-Hung Tanb, Chung-Hsin Juanc, Meng-Lung Lind, 2008)

5.2 Normalized Difference Vegetation Indices (NDVI)

Per (Ray D. Jakson and Alfredo R. Huete), (Deering 1978) found the low dynamic range of the NIR/Red ration over sparse vegetation could be enhanced by rationing the difference between the NIR and the red bounds to sum of the two bands , this VI was subsequently called normalized difference vegetation index (NDVI). Also, per (Randy R. Price and Kevin Price 2009) the NDVI was first presented in the late of 1970s and it is strongly influenced by green plant productivity and leaf chlorophyll concentration, and has ability to normalize data to a certain degree. Scientists and researchers can use NDVI for different type of studies and different type of projects. In addition, (Campbell 2007, 465-477) pointed in his book that the NDVI ratio is calculated by dividing the difference in the NIR (Band 4) and red color (Band 3) bands by the sum of the NIR and red color (Equation 4)

Equation 6 NDVI

$$NDVI = \frac{NIR - Band3}{NIR + Band3}$$

The upper value of the NDVI approaches to one, while the lower bounds is usually close to zero. The lower value may be slightly positive or slightly negative, depending on sensor characteristics and the units of the input variables (volts, radiances ,reflectance, digital numbers. Etc.).

5.3 Normalized Difference Soil Indices (NDSI)

Soil water content or soil moisture is one of key parameter in the ecological process to understand the below-ground biomass or soil carbon. The NDSI is established to enhance the vegetation information and soil information. It is calculated by dividing NIR and SWIR by the sum of NIR and SWEIR (Equation 5) (Lin, Zha, and Quanfang 2010, 2-3).

Equation 7 NDIS

$$NDSI = \frac{NIR - SWIR}{NIR + SWIR}$$

The NDSI have been used in different studies; recently, it has been used to find soil water contains estimation in Mongolia in 2009 by (Supannika Potithep, Reiichiro Ishii, Rikie Suzuki). The relationship between soil water content and normalized soil index (NDSI) that was calculated from shortwave infrared and near infrared wavelength was investigated. Also, another study to find to evaluate rice yield and protein estimation methods based on various vegetation indices (VIs), NDSI and PLS using an hyperspectral sensor AISA in Shonai plane, northeast Japan by (Shinya Odagawa*1, Kuniaki Uto 2, Yukio Kosugi 2, Genya Saito 2, Yuka Sasaki 3, Kunio Oda 4 and Masatane Kato *5*)

5.4 Tasseled Cap Transformation (TCT)

Per (Jensen 2005) TCT first adapted by Kauth and Thomas in (1976) produced an orthogonal transformation of original Landsat MSS data space to a new four-dimensional

feature space, It was called tasseled cap. It created four new axes: the soil brightness

index (B), greenness vegetation (G), yellow stuff index (Y), and non-such (N). Later in

(1986) has been improved by derived the visible, near-infrared. And middle-infrared for

transformation of Landsat TM imagery into brightness, greenness, and wetness variables:

In addition, (Campbell 2007, 476) discrbed TCT as a linear transformation of

Landsat MSS and has been extended to Landsat TM, projecting soil and vegetation into a

single plane in multispectral data and thematic data.

TCT produces three components: brightness, greenness, and wetness for Landsat

TM. The names of three components reflect their content. The brightness is the

responses to physical properties that affect total reflection . The greenness is the

responses to the combintion of high absorption of chlorophyll in visisble bands and the

high reflection of leaf structures in the near-infrared, which is characteristic of healthy

vegitation. The wetness is responsive to the amount of moisture being held by the

vegetation or soil (Qingsheng Gaohuna 2010, 1).

The TCT has been used in many studies in RS felid, including a study in 2005,

by Sader which compared NDMI and tassels cap wetness transformation for detection

forest disturbance. Also, (Qingsheng LIU, Gaohuan LIU , 2009) combined TCT and

Finite Gaussian Mixture Model (FGMM) for Landsat TM imagery data is proposed in

this paper to employ an unsupervised classification method on Landsat TM imagery data.

The spectral dimensionality of the imagery data is firstly reduced by TCT into the Brightness Component (TCTB) and Greenness Component (TCTG) and Wetness Component (TCTW), then the transformed data is modeled by FGMM, the parameters of the model are estimated using the Expectation-Maximization (EM) algorithm. Finally the data after TCT is classified according to the mixture model. The results from the present study suggest that the TCTB is enough to classify the Landsat TM image to water, vegetation and town or bare land, and the combination of TCTB and TCTG is better to classify the image to water, wetland, shrub and grass land, farmland and town or bare land than the combinations of TCTG and TCTW, TCTB and TCTW, and the combinations of TCTB, TCTG and TCTW is the most reasonable and delicate method for the classification of Landsat TM imagery data.

In addition, a study which conducted by (Qingsheng LIU Gauguin LIU, 2010) they combined TCT with support vector machine to Classify Landsat TM Imagery Data. The spectral dimensionality of the imagery data is firstly reduced by TCT into the Brightness Component (TCTB) and Greenness Component (TCTG) and Wetness Component (TCTW), and then the transformed data is inputted into Support Vector Machine and classified into water, wetland, shrub and grass land, farmland and town or bare land. The present results show that compared to SVM classification of the original six bands of Landsat TM imagery data, the classification method of combining TCT with SVM has a high accuracy.

REFERENCES

Agarwal, C., Green, G. M., Grove, J. M., Evans, T. P., and Schweik, C. M, (2002). A Review and Assessment of Land-use Change Models: Dynamics of Space, Time and Human Choice. http://www.nrs.fs.fed.us/pubs/gtr/gtr_ne297.pdf, [accessed February 1, 2013].

Vassilaros, A., (2010).Isodata – Lecture notes. http://web.pdx.edu/~jduh/courses/Archive/geog481w07/Students/Vassilaros_ISODATA.pdf
, [accessed January 23, 2013].

Campbell, J. B. (2007). In Itroduction to Remote Sensing (4th Ed.). New York: The Guilford Publications Press.

Tan, C., Juan, C.H., Lin, M.L., (2008). Characterizing the Meso-Scale Environmental Thermal Effects Due to Different Landuse Types Using Remo. http://ieeexplore.ieee.org.mutex.gmu
,[accessed October 20, 2012]

Zubair, A. Opeyemei, (2006). Change Detection in Land-use and Land-cover Using Remote Sensing Data and GIS. http://www.geospatialworld.net/uploads/thesis/OpeyemiZubair_ThesisDOC.doc, [accessed April 14, 2013].

COSIT, (2012), Central Organization for Statistics and Information Technology (COSIT), Iraqi Population (1997- 2011). http://cosit.gov.iq/english/AAS2012/section_2/5.htm, [Retrieved May 21, 2012].

Lewis M. C., Virginia C., Francis C. G., and Edward T. L., (1979).Classification of Wetland and Deepwater Habitats of the United States. U.S. Department of the Interior. http://www.charttiff.com/pub/WetlandMaps/Cowardin.pdf, [accessed November, 21, 2013].

Curtis W. W., (1999). "Fuzzy set theory and thematic maps: accuracy assessment and areaestimation."http://www.colorado.edu/geography/leyk/geog_5113/readings/woodcock_gopal_2000_IJGIS.pdf, [accessed November 26, 2012].

Diary A. ,[2008]. "Water Resources Management in Ranyia Area Sulaimaniya NE-Iraq. Thesis of Degree of Doctor of Philosophy of Science, Iraq-Baghdad: University of Baghdad. http://www.kurdistangeology.com, [accessed October 13, 2012].

Erb K.H. , Gaube V., Krausmann F., Plutzar C., Bondeau A. and Haberl H. (2007). "A Comprehensive Global 5 Min Resolution Land-use Dataset for the Year 2000 Consistent with National Census Data - IGBP". http://www.igbp.net/publications/publishedarticlesandbooks, [accessed January 18, 2013].

ERDAS Field Guide, (2011). Earth Resources Data Analysis System. ERDAS Inc. Atlanta, Georgia. 628 pages.

Giri, C. P. (2012). Remote Sensing of Land Use and Land Cover. http://www.crcnetbase.com.mutex.gmu.edu/doi/pdfplus/10.1201/b11964-18, [accessed May 23, 2012].

Meinel G., Neubert M., (2004). A Comparison of Segmentation Programs for High Resolution Remote Sensing Data. Leibniz Institute of Ecological and Regional Development (IOER), http://www.isprs.org/proceedings/XXXV/congress/comm4/papers/506.pdf, [accessed November 28, 2012].

Goodwin, N.R . , (2009). Ministry of Forests, Lands and Natural Resource Oparations (MoLNRO). http://www.for.gov.bc.ca/hts/rs/mpb_impact/documents/YOD-NDMI_rev2.pdf, [accessed May 20, 2012].

Gregorg, K. (2000). Cross-correlation analysis: mapping landcover . Rockville, MD, US. www.glc.org/wetlands/docs/CCA_Paper.doc, [accessed May 23, 2012].

Espindola G.M., Camarai A. R., Bins A. M., (2006).Parameter Selection for Region-Growing Image Segmentation Algorithms Using Spatial Autocorrelation. International Journal of Remote Sensing, 515(122201-001). http://www.dpi.inpe.br/gilberto/papers/espindola_camara_ijrs.pdf, [accessed November 28, 2012].

Hansen, M., DeFries R., Townshend J.R.G, and Sohlberg R., (2009).Global Land Cover Classification (GLCF),UMD Global Land Cover Classification, 1 Kilometer. http://glcf.umd.edu/data/landcover/, [accessed February 20, 2013].

Hussien A, Oumer, (2009). Land-use and Land-cover Change, Drivers and Its Impacts: A Comparative Study from Kuhar Michael and Lenche Dima of Blue Nile and Awash Basin of Ethiopia.http://soilandwater.bee.cornell.edu/Research/international/docs/Thesis%20Hussien%20Ali_Formatted2.pdf, [accessed February 2, 2013].

Joint Analysis Policy Unit, (2011). Sulaymaniya Governorate Profile. NGO. www.iauiraq.or. http://www.iauiraq.org/documents/463/GP-Sulaymaniyah.pdf, [accessed May 1, 2012].

Erb K. , Gaube V., Krausmann .F, Plutzar C., Bondeau A. and Haberl H., (2009) .International Geosphere and Biosphere Programs, Land Cover Institute (LCI). http://landcover.usgs.gov/globallandcover.php, [accessed September 24, 2012].

John R J., (2005). Introduction Digital Image Processing a Remote Sensing Perspective (3rd Ed.), Pearson Education, Inc. (pp 495-511).

Kamal H. K., (2009).Basic Principle of Geology of Iraq. http://kurdistan-geology.com/wp-content/uploads/2011/11/Geology-of-kurdistan-3-20111.pdf,[accessed October 13, 2012].

Lillesand, T.M., and Kiefer, R.W. (1987). Remote Sensing and Image Interpretation. John Wiley & Sons. New York. (p 599).

Center for Advanced Spatial Technologies (CAST), (1997). LULC Change in Carroll County Areas. http://www.cast.uark.edu/home/research.html, [accessed December 20, 2012].

Lin, W., Zha, S., & Quanfang, W. (2010). Construction and application of characteristic bands of typical land cover based on spectrum-photometric method. Geoinformatics, 2010 18th International Conference on 18-20 June2010 (pp. 1-6) http://ieeexplore.ieee.org.mutex.gmu.edu/Xplore/home.jsp, [accessd March 20, 2012]

Li Y. C. and Chi F. Ch., (2001).A Multi-Scale Region Growing Segmentation for High Resolution Remotely Sensed Images. http://www.a-a-r-s.org/acrs/proceeding/ACRS2007/Papers/PS3.G5.10.pdf, [accessed November 28, 2012].

Meng L., Yu C., Chung J., Cheng Ch., Chen H., Qiu W., Yung L., (2006).Monitoring Drought Dynamics in the Ejin Oasis Using Drought Indices from MODIS Data http://ieeexplore.ieee.org.mutex.gmu.edu, [accessed October 20, 2012].

Meyer, W.B, (1995). Past and Present Land Use and Land Cover in the USA. *Consequences* 1(1). http://www.gcrio.org/CONSEQUENCES/spring95/Land.html, [accessed January 26, 2013]

Michaelson, J. , Davis F., and Borchert M., (1987). Non-parametric methods for analyzing hierarchical relationships in ecological data. *Conenoses*, 1: 97-106, [accessed October20, 2012]

Nirupama P., Slobodan P. Simonovic,2002. Role of Remote Sensing in Disaster Management. ICLR Paper Series – No. 2. http://www.scribd.com/doc/34798503/Role-of-Remote-Sensing-in-Disaster-Management, [accessed January 10, 2013].

Ojima, D.S., Galvin K.A., Turner II B.L.,(1994). The Global Impact of Land-use Change. *BioScience*, Vol. 44, No. 5, Global Impact of Land-Cover Change (May, 1994), pp. 300-304

Qingsheng G., (2010). Combining Tasseled Cap Transformation with Support Vector Machine to Classify Landsat TM Imagery Data. In Proc. of Sixth International Conference on Natural Computing (ICNC`2010). Volume 7, p. 3570 – 3572.

Salahadding S. A., (2007). Geology and Hydrology of Sharazoor- Piramagrun Basin in Sulaimani Area, Northeastern Iraq. Ph.D. Degree Thesis, Belgrade University. http://www.kurdistangeology.com, [accessed October 13, 2012].

Odagawa, S., Uto, K., Kosugi, Y., Saito, G., Sasaki, Y., Oda, K., and Kato, M. (2011). Evaluation of paddy yield and protein estimation methods based on various vegetation indices, NDSI and PLS using an airborne hyperspectral sensor AISA in Shonai Plain, Yamagata, Japan. In Proc. *IEEE International Symposium* of *Geoscience and Remote Sensing Symposium (IGARSS), 2011* (pp. 1926-1929).

Smith, F.G.F., Herold, N., Derry, D., Nichols, C., the Classification of Early-Date Imagery Based on Late-Date Training Data. ASPRS conference, Denver, (May 2004), http://www.asprs.org/ASPRS-Past-Events/Denver-2004.html, accesses [July 10 2012].

Supannika P. , Reiichiro I., Rikie S., (2009).The Potential of Normalized Difference Soil Index (NDSI) for Soil Water Content Estimation in Mongolia. Japan Agency for Marine-Earth Science and Technology Research Institute for Global Change. http://www.a-a-r-s.org/acrs/proceeding/ACRS2009/Papers/Oral%20Presentation/TS16-05.pdf, accessed October 20, 2012.

Tso, B. and Mather, P. M. (2009). Classification Methods for Remotely Senses data. http://www.crcnetbase.com.mutex.gmu.edu/isbn/978-1-4200-9072-7, [accessed May 22, 2012]

Terri R. and Raid Al-T., (2000). Modeling Land Use and Land Cover Dynamics to Assess Sustainability in Trinidad and Tobago. http://www.gsdi.org/gsdiconf/gsdi10/papers/TS48.1paper.pdf, [accessed April 14, 2013].

Turner, B.L. II, & Butzer, K.W., (1992). The Colombian Encounter and Land-Use Change. Environment. http://www.clarku.edu/faculty/facultybio.cfm?id=338, Vol. 34. p. 16, [accesses May, 25, 2012]

USGS. (n.d.). U.S. Geological Survey, (2011). USGS: http://earthexplorer.usgs.gov/ [accessed July 2011].

United Nation Organization. Iraq Land Cover Map. USGS. http://unosat-maps.web.cern.ch/unosat-maps/IQ/land_cover.pdf, [accessed September 22, 2012].

Ray D. J. and Alfredo R. H. (1991). Interpreting Vegetation Indices. http://www.uprm.edu/biology/profs/chinea/gis/lectesc/intvegindx.pdf, [accessed May 10, 2012].

"Unsupervised Classification Algorithms." (2013). http://www.yale.edu/ceo/Projects/swap/landcover/Unsupervised_classification.htm, [Accessed January 23, 2013].

Villarreal, M. L., Norman L.M. and Wallace III, (2011). A Multi-temporal (1979-2009) Land Use/Land Cover Data Set of the Binational Santa Cruz Watershed, U.S. | School of Natural Resources and the Environment. USGS. http://www.snr.arizona.edu/node/1707, [accessed April 14, 2013].

Wilkie, D.S., and Finn, J.T. (1996). Remote Sensing Imagery for Natural Resources Monitoring. Columbia University Press, New York. [accessed August 11, 201012].

CURRICULUM VITAE

Ardalan Faraj graduated from Halkaut High School, Sulaimaniya, Iraq, in 1985. He received his Bachelor of Science from Baghdad University in 1989. He received his Master of Science in GEOINT from George Mason University in 2013.